



National Library
of Canada

Acquisitions and
Bibliographic Services Branch

395 Wellington Street
Ottawa, Ontario
K1A 0N4

Bibliothèque nationale
du Canada

Direction des acquisitions et
des services bibliographiques

395, rue Wellington
Ottawa (Ontario)
K1A 0N4

Your file - Votre référence

Our file - Notre référence

NOTICE

The quality of this microform is heavily dependent upon the quality of the original thesis submitted for microfilming. Every effort has been made to ensure the highest quality of reproduction possible.

If pages are missing, contact the university which granted the degree.

Some pages may have indistinct print especially if the original pages were typed with a poor typewriter ribbon or if the university sent us an inferior photocopy.

Reproduction in full or in part of this microform is governed by the Canadian Copyright Act, R.S.C. 1970, c. C-30, and subsequent amendments.

La qualité de cette microforme dépend grandement de la qualité de la thèse soumise au microfilmage. Nous avons tout fait pour assurer une qualité supérieure de reproduction.

S'il manque des pages, veuillez communiquer avec l'université qui a conféré le grade.

La qualité d'impression de certaines pages peut laisser à désirer, surtout si les pages originales ont été dactylographiées à l'aide d'un ruban usé ou si l'université nous a fait parvenir une photocopie de qualité inférieure.

La reproduction, même partielle, de cette microforme est soumise à la Loi canadienne sur le droit d'auteur, SRC 1970, c. C-30, et ses amendements subséquents.

Canadä

University of Alberta

**The Bayonet Tube: A Numerical Analysis of
Laminar Frictional Characteristics**

by

Harpal S. Minhas



**A thesis
submitted to the Faculty of Graduate Studies and Research
in partial fulfilment of the requirements for the degree of**

Master of Science

Department of Mechanical Engineering

Edmonton, Alberta

Fall, 1993



National Library
of Canada

Acquisitions and
Bibliographic Services Branch

395 Wellington Street
Ottawa, Ontario
K1A 0N4

Bibliothèque nationale
du Canada

Direction des acquisitions et
des services bibliographiques

395, rue Wellington
Ottawa (Ontario)
K1A 0N4

Your file - Votre référence

Our file - Notre référence

The author has granted an irrevocable non-exclusive licence allowing the National Library of Canada to reproduce, loan, distribute or sell copies of his/her thesis by any means and in any form or format, making this thesis available to interested persons.

L'auteur a accordé une licence irrévocabile et non exclusive permettant à la Bibliothèque nationale du Canada de reproduire, prêter, distribuer ou vendre des copies de sa thèse de quelque manière et sous quelque forme que ce soit pour mettre des exemplaires de cette thèse à la disposition des personnes intéressées.

The author retains ownership of the copyright in his/her thesis. Neither the thesis nor substantial extracts from it may be printed or otherwise reproduced without his/her permission.

L'auteur conserve la propriété du droit d'auteur qui protège sa thèse. Ni la thèse ni des extraits substantiels de celle-ci ne doivent être imprimés ou autrement reproduits sans son autorisation.

ISBN 0-315-88074-0

Canada

TO WHOM IT MAY CONCERN

I hereby grant permission to Mr. Harpal S. Minhas for the use of the photographs, Figures 4.10, 4.16 and 4.17, pp 63, 71 and 72 respectively, in his thesis, "The Bayonet Tube: A Numerical Analysis of Laminar Frictional Characteristics", originally published in "Laminar Frictional Behaviour of a Bayonet Tube", Proc. 3 rd Sym. on Cold Regions Heat Transfer, Fairbanks, pp 425-40.



(Dr. G.S.H. Lock)

University of Alberta

Release Form

Name of Author:

Harpal S. Minhas

Title of Thesis:

**The Bayonet Tube: A Numerical Analysis
of Laminar Frictional Characteristics**

Degree:

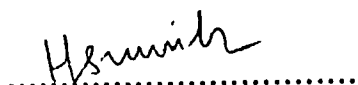
Master of Science

Year this degree granted:

1993

**Permission is hereby granted to The University of Alberta Library to
reproduce single copies of this thesis and to lend or sell such copies for private,
scholarly, or scientific research purposes only.**

**The author reserves other publication rights, and neither the thesis nor
extensive tracts from it may be printed or otherwise reproduced without the
author's written consent.**


.....

(Student's signature)

Harpal S. Minhas

#305, 5020, Riverbend Rd.

Edmonton, Alberta

T6H 5J8

Date: Sept. 1, 1993

UNIVERSITY OF ALBERTA

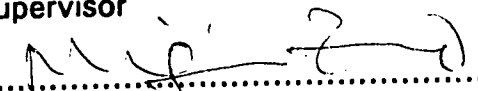
FACULTY OF GRADUATE STUDIES AND RESEARCH

The undersigned certify that they have read, and recommend to the Faculty of Graduate Studies and Research for acceptance, a thesis entitled **The Bayonet Tube: A Numerical Analysis of Laminar Frictional Characteristics** submitted by **Harpal S. Minhas** in partial fulfilment of the requirements for the degree of **Master of Science**.

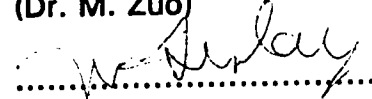


(Dr. G.S.H. Lock)

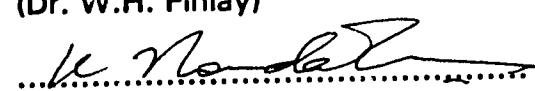
Supervisor



(Dr. M. Zuo)



(Dr. W.H. Finlay)



(Dr. K. Nandakumar)

Date Aug 31, 1993

To My Wife and To My Mother

Abstract

The results of a numerical analysis of laminar flow in a bayonet tube under steady conditions are provided. Using the SIMPLE-C algorithm, data has been obtained on the influence of the principal variables ; namely, flow rate, outer tube length, outer tube diameter, inner tube diameter and inner tube length on the pressure drop. The results are presented in nondimensionalized form using the Reynolds number, Re, length to diameter ratio, L/D, area ratio, F_i/F_a and end clearance ratio, H/D. The study includes the effect of these parameters on pressure drop for both central and annular admission of the fluid.

For central admission, the effect of Reynolds number and length-diameter ratio was as expected. The pressure drop decreased with Re and increased with L/D. A characteristic minimum was noted in the effect of area ratio at values lower than expected. The flow pattern revealed a stable ring vortex, in axisymmetric form, accounting for the minimum. For F_i/F_a less than the minimum a secondary vortex accounted for higher frictional losses. For F_i/F_a more than the minimum, three dimensional effects produced higher pressure drops. A diminishing secondary vortex accounted for a local minimum in the effect of clearance ratio, while a local maximum at a higher value of H/D corresponded to a ring of separation. The formation of a stable ring vortex in

axisymmetric form marked an asymptotic value.

The pressure drops for annular admission were, as expected, higher than the central admission due to increased entrance area. The effects of Reynolds number and clearance ratios were qualitatively similar to those found in central admission. A different flow pattern in the clearance space accounted for a minimum value of area ratio greater than expected. More organised flow at higher clearance ratios resulted in a decreased pressure drop.

Acknowledgements

The author would like to express his sincere appreciation to Dr. G.S.H. Lock, who supervised the preparation of this thesis. His thoughtful guidance, encouragement, and advise are greatly appreciated.

A Research Assistantship from the Natural Sciences and Research Council of Canada is greatly appreciated.

Finally, the author is most thankful to his wife and family for their immeasurable support and encouragement during his study at the University of Alberta.

Contents

Nomenclature

Chapter 1

Introduction	1
1.1 The concept and use of the bayonet tube	1
1.2 Previous work	4
1.3 Scope and outline of the thesis	6

Chapter 2

Mathematical Formulation	9
2.1 Governing equations and boundary conditions	9
2.2 Non-dimensionalization	14
2.3 Parameters	19

Chapter 3

Numerical Technique	23
3.1 Introduction	23
3.2 Finite difference equations	25
3.2.1 Grid and control volume definitions	25

3.2.2 Discretization	25
3.3 The Algorithm	34
3.4 Program validation	40

Chapter 4

Frictional Characteristics With Central Admission	46
4.1 Introduction	46
4.2 Effect of Reynolds number	48
4.3 Effect of length-diameter ratio	50
4.4 Effect of area ratio	54
4.5 Effect of clearance ratio	64

Chapter 5

Frictional Characteristics With Annular Admission	73
5.1 Introduction	73
5.2 Effect of Reynolds number	74
5.3 Effect of length-diameter ratio	76
5.4 Effect of area ratio	76
5.5 Effect of clearance ratio	79

Chapter 6	
Conclusions and Recommendations	86
References	89
Appendix A	
Listing of Computer Program	93

List of Figures

1.1 Sketch of the bayonet tube	3
2.1 The cylindrical coordinates	10
3.1 Control volume and notation in the staggered grid (x-r plane)	26
3.2 Grid nomenclature (X-R plane)	27
3.3 Comparison of friction factor data for a circular tube	43
4.1 Effect of Reynolds number on Euler number	49
4.2 Velocity profile for $Re = 1000$ and 200	51
4.3 Effect of length-diameter ratio on Euler number	52
4.4 Velocity profile for $L/D = 20$ and 10	55
4.5 Velocity profile for $L/D = 20$ and 40	56
4.6 Effect of area ratio on Euler number	57
4.7 Velocity profile for $F_i/F_a = 0.47$ and 0.2	59
4.8 Velocity profile in three dimensions for $F_i/F_a = 1.5$	60
4.9 Velocity profile in R- Θ plane for $F_i/F_a = 1.5$	61
4.10 Velocity profile in X-R plane for $F_i/F_a = 2.26$	63
4.11 Effect of clearance ratio on Euler number	65
4.12 Velocity profile for $H/D = 1.0$ and 0.2	66
4.13 Velocity profile for $H/D = 1.0$ and 0.4	67

4.14 Velocity profile for H/D = 1.0 and 0.8	68
4.15 Velocity profile for H/D = 1.0 and 2.0	69
4.16 Velocity profile for H/D = 0.5	71
4.17 Velocity profile for H/D = 1.0	72
5.1 Effect of Reynolds number on Euler number	75
5.2 Effect of length-diameter ratio on Euler number	77
5.3 Effect of area ratio on Euler number	78
5.4 Velocity profile for $F_i/F_a = 0.8$	80
5.5 Effect of clearance ratio on Euler number	81
5.6 Velocity profile for H/D = 0.2	83
5.7 Velocity profile for H/D = 0.8	84
5.8 Velocity profile for H/D = 3	85

Nomenclature

a	coefficient in the discretization equation
b	constant term in the discretization equation
C	coefficient
D	outer tube diameter; also used to denote diffusion conductances
d	coefficient in the pressure-difference equation; also inner tube diameter
e	unit vector
Eu	Euler number
F	flow rate through a control volume; also cross sectional area
H	clearance length
J	total (convective + diffusion flux)
K	length-diameter ratio
KM	number of circumferential nodal points
L	length of outer tube
I	length of inner tube
M	number of axial nodal points
m	mass

N	number of radial nodal points
P,p	pressure; P is also used to denote cell Peclet number
p'	pressure correction
Pe	Peclet number
R,r	radial coordinate
Re	Reynolds number
Δr	r-direction width of a control volume
δr	r-distance between two adjacent grid points
U,u	axial velocity
U_m	characteristic velocity
u'	axial velocity correction
u^*	axial velocity based on guessed pressure p^*
V,v	radial velocity
W,w	circumferential velocity
X,x	axial distance
$\Delta x, \delta x$	similar to $\Delta r, \delta r$

Greek

α	relaxation
ρ	mass density
μ	fluid dynamic viscosity
ν	momentum diffusivity

Θ, θ circumferential distance

Subscripts

a	annulus
A	annulus; also area
B,T	neighbour grid points on the bottom and top respectively
b,t	control volume face on the bottom and top respectively
E,w	neighbour grid point on the east and west respectively
e,w	control volume face on the east and west respectively
i	inlet; also inner tube
N,S	neighbour grid points on the north and south respectively
n,s	control volume face on the north and south respectively
nb	general neighbour grid point
P	central grid point under consideration

Superscripts

- . per unit time
- * previous iteration value of a variable
- c characteristic

Chapter 1

Introduction

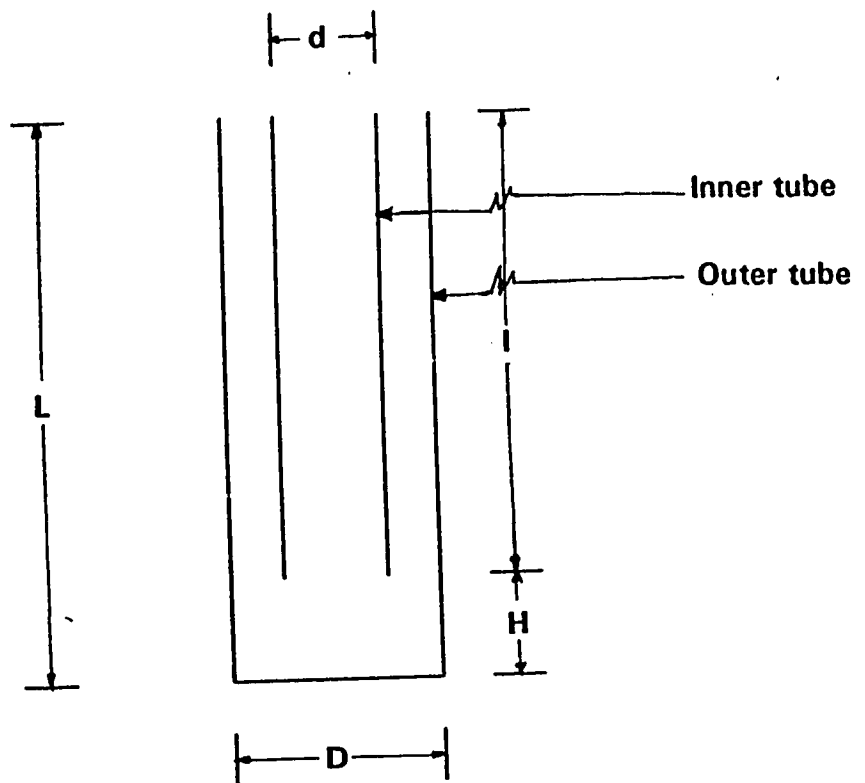
1.1 The concept and use of the bayonet tube

The design of industrial heat exchangers is often constrained by such factors as tube stress, access, system dimension and ease of maintenance. High tube stresses may cause early wear and tear and hence high financial penalty. Also, there are situations when the system to be heated (or cooled) is accessible from one side only thus making the use of conventional heat exchangers impractical. In the process industries, a heat exchanger breakdown may lead to complete system shutdown until repairs are made. The need for a heat transfer device free from the above shortcomings is self evident.

The bayonet tube is a simple refluent heat exchanger. It is constructed from two concentric tubes as shown in Figure 1.1. The outer tube is sealed at one end. One end of the inner tube reaches close to the sealed end of the outer tube. The fluid flowing inside the inner tube is constrained to return along the annular gap between the two tubes, or vice versa. The pressure difference between the inlet and the outlet drives the flow. Forced convection may thus be superimposed on natural convection or boiling (and condensation). The device is therefore suitable for both single and two phase operations.

Bayonet tubes are particularly suitable for situations where the medium to be heated or cooled is either too large to be treated in its entirety or is readily accessible from one side only. The tubes can also be fitted into any process equipment, since they only require penetration through one wall. Also since one end of the tube is free, the system is free from any bending and axial compressive stresses. The use of bayonet tubes may thus be advantageous in highly corrosive environments where stress related tubing failures are a concern [1].

The use of bayonet tubes in the process industry was cited as early as 1946 [2]. The tubes, then called "Field tubes", were used in vacuum condensers, suction tank heaters and alkylation contactors. Recent industrial uses include : a potassium condenser boiler in a binary cycle power plant [3],



d = inner tube diameter
D = outer tube diameter
l = inner tube length
L = outer tube length
H = clearance length

FIGURE 1.1 SKETCH OF THE BAYONET TUBE

a counterflow heat exchanger in a chemical processing plant [4], a water tube reformed gas boiler in an ammonia plant [5] and a high temperature burner duct recuperator in a steel mill soaking pit [6].

In a geophysical context, bayonet tubes may be used for geothermal heat extraction in steam generation above the ground surface [7]. Another application is found in the penetration of the earth's surface by bayonet tubes in northern regions [8]. The internal circulation of cold winter air maintains the ground in a frozen state thus enabling it to support towers, buildings and roads. Bayonet tubes inserted through the cold winter ice on a river may be used to create a submerged wall of ice, hence facilitating the control of spring runoff [9].

Biomedical applications include cryosurgery. The technique utilises bayonet tubes as a cryoprobe for producing very low localised temperatures [10]. This phenomenon is used for selective destruction of damaged tissues. The method has been found to be safe and effective.

1.2 Previous work

The mean effective temperature difference in a bayonet tube with unheated walls for four different arrangements of flow direction on the shell

and tube side was studied by Hurd in 1946 [2]. It was found that large temperature differences occur when the flow direction in the annulus was counter to the flow direction of the circulating medium on the shell side.

Tests on a bayonet tube were conducted by Jahns, Miller, Power, Rickey, Taylor and Wheeler in 1973 [8]. Results were compared with an open pile without tube insert. Bayonet tube heat removal rates were higher. Laboratory tests conducted by Haynes and Zarling in 1982 to assess the heat performance characteristics of bayonet tube suggested that the heat removal rates depended directly on the volume of air forced through the annulus [11].

An analytical solution of the governing equations was performed by Baum in 1978 [1]. It was shown that the inner tube should have three quarters of the diameter of the outer tube and should be somewhat thicker. The effect of wind and the insert tube length on the thermal performance of the tube was studied by Lock and Kirchner in 1988 [12]. It was suggested that at high speeds an increased length leads to an increase in the heat transfer rate, while at low speeds the opposite was true. The effect of the length to diameter ratio of the outer tube on heat transfer rate of the tube was found to be monotonic by Lock and Kirchner in 1990 [13].

A numerical study of flow in a bayonet tube with spherical end geometry was conducted by Yang and Hsieh in 1988 [14]. An axisymmetric flow condition was assumed. A vortex at the end clearance zone was detected. Experiments were conducted to study the effect of main tube parameters on the pressure drop in the tube by Lock and Wu in 1991 [15]. Visual studies were also conducted. The presence of an end vortex in the vicinity of the end clearance zone was confirmed. Later in 1992, Lock and Wu [16] studied the effects of mass flow rate and tube geometry on the heat performance of the tube.

1.3 Scope and outline of the thesis

As seen in the previous section, work on the study of the bayonet tube is limited. Though the work lays a foundation for an advanced study on the topic, it is by itself insufficient to give much useful information to a designer. The analytical work does not consider the formation of an end vortex in the end clearance zone. The numerical work assumes an axisymmetric flow. The experimental work indicates the effect of the tube parameters on the frictional performance, but the results are limited in accuracy. Also no information on the local velocity profiles is provided. None of the above studies provides information on the frictional behaviour for annular entry of the fluid.

In this study a numerical analysis has been performed for steady, laminar flow of constant property fluids to examine hydraulic behaviour and compare it with experimental data. The study discusses the importance of various tube parameters on the overall pressure drop thus providing the designer with information on the conditions for a minimum pressure drop. As well, it studies the effects of these parameters on the local velocity profiles. It explains the importance of the flow behaviour on the overall pressure drop for laminar flow. In particular, three dimensional effects are studied. Lastly, the effect of annular admission of the fluid is also studied.

In chapter 2, the governing differential equations and the boundary conditions are described. The principal parameters are then defined. Chapter 3 deals with the numerical formulation of the problem. The finite difference equations and main steps in the algorithm are outlined. The accuracy of the developed computer program is then established using a grid size test and by comparison with the solution of a standard problem : axisymmetric flow in a straight pipe.

In chapter 4, the frictional characteristics of a bayonet tube with central admission of the fluid are studied : this includes the effect of mass flow rate and tube geometry. In chapter 5, the frictional performance is investigated

again considering the effect of the principal parameters listed above, but this time annular admission of the fluid is considered.

Finally, conclusions and recommendations for further study are developed in chapter 6.

Chapter 2

Mathematical Formulation

2.1 Governing equations and boundary conditions

In cylindrical coordinates (see Figure 2.1), the continuity and momentum equations for steady, laminar, constant property flow are :

Continuity :

$$\frac{\partial U}{\partial X} + \frac{1}{R} \frac{\partial}{\partial R} (RV) + \frac{1}{R} \frac{\partial W}{\partial \Theta} = 0 \quad (2.1)$$

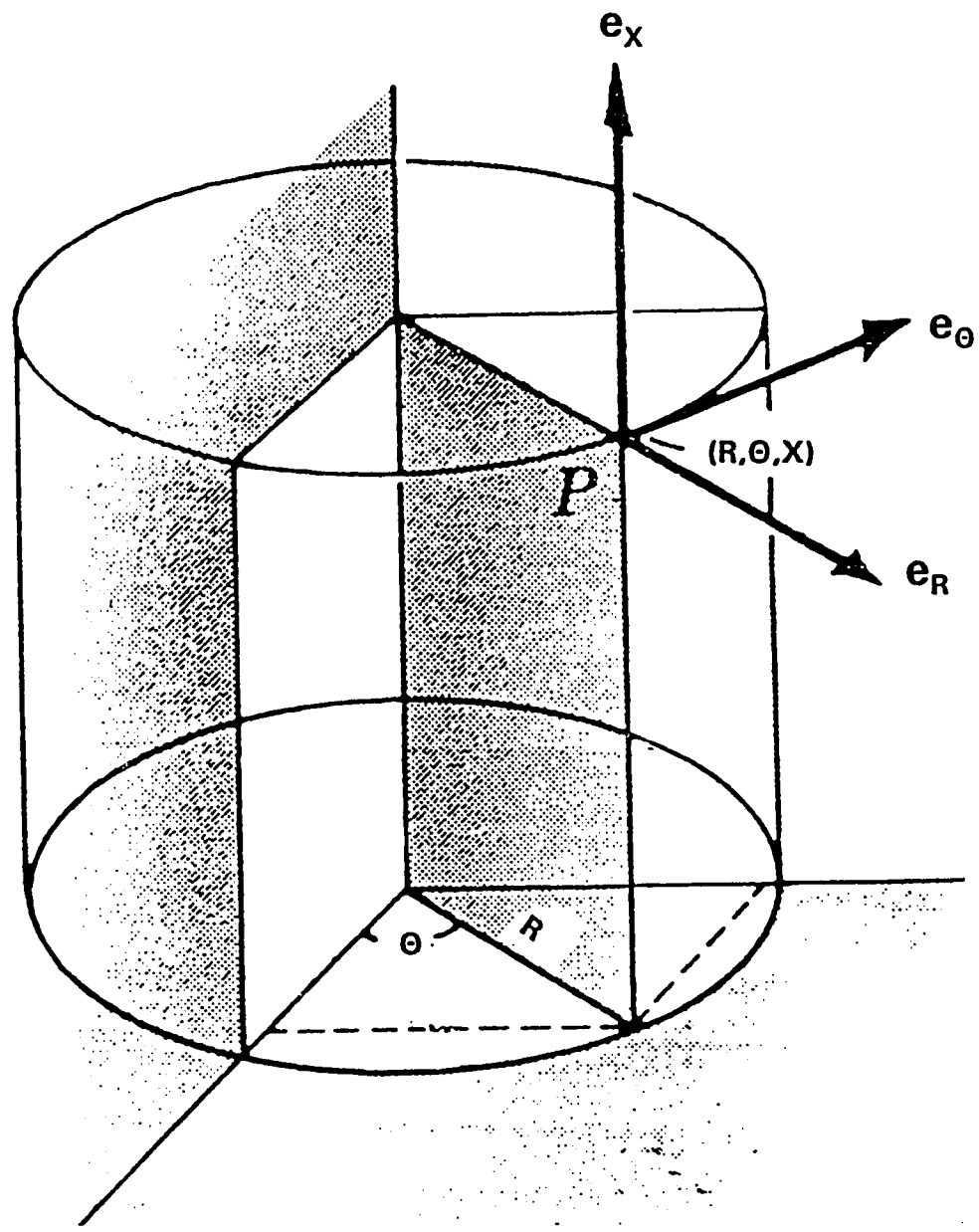


FIGURE 2.1 THE CYLINDRICAL COORDINATES

Axial momentum :

$$\rho \left(U \frac{\partial U}{\partial X} + V \frac{\partial U}{\partial R} + \frac{W}{R} \frac{\partial U}{\partial \Theta} \right) = - \frac{\partial P}{\partial X} \\ + \mu \left(\frac{\partial^2 U}{\partial X^2} + \frac{1}{R} \frac{\partial}{\partial R} \left(R \frac{\partial U}{\partial R} \right) + \frac{1}{R^2} \frac{\partial^2 U}{\partial \Theta^2} \right) \quad (2.2)$$

Radial momentum :

$$\rho \left(U \frac{\partial V}{\partial X} + V \frac{\partial V}{\partial R} + \frac{W}{R} \frac{\partial V}{\partial \Theta} - \frac{W^2}{R} \right) = - \frac{\partial P}{\partial R} \\ + \mu \left(\frac{\partial^2 V}{\partial X^2} + \frac{1}{R} \frac{\partial}{\partial R} \left(R \frac{\partial V}{\partial R} \right) + \frac{1}{R^2} \frac{\partial^2 V}{\partial \Theta^2} - \frac{V}{R^2} - \frac{2}{R^2} \frac{\partial W}{\partial \Theta} \right) \quad (2.3)$$

Circumferential momentum :

$$\rho \left(U \frac{\partial W}{\partial X} + V \frac{\partial W}{\partial R} + \frac{W}{R} \frac{\partial W}{\partial \Theta} + \frac{VW}{R} \right) = - \frac{1}{R} \frac{\partial P}{\partial \Theta} \\ + \mu \left(\frac{\partial^2 W}{\partial X^2} + \frac{1}{R} \frac{\partial}{\partial R} \left(R \frac{\partial W}{\partial R} \right) + \frac{1}{R^2} \frac{\partial^2 W}{\partial \Theta^2} - \frac{W}{R^2} + \frac{2}{R^2} \frac{\partial V}{\partial \Theta} \right) \quad (2.4)$$

where

X = axial distance

R = radial distance

Θ = circumferential distance

U = axial velocity

V = radial velocity

W = circumferential velocity

The above equations are subject to the following initial and boundary conditions:

Inlet ($X=0$, $R=0$ to $d/2$, $\Theta=0$ to 2π)

$$U = 2U_i \left[1 - \left(\frac{2R}{d} \right)^2 \right], \quad V = 0, \quad W = 0 \quad (2.5)$$

where U_i and d are the average inlet velocity and the inner tube diameter, respectively.

Outlet ($X=0$, $R=d/2$ to $D/2$, $\Theta=0$ to 2π)

$$\frac{\partial U}{\partial X} = 0, \quad \frac{\partial V}{\partial X} = 0, \quad \frac{\partial W}{\partial X} = 0 \quad (2.6)$$

Assuming the inner tube to have no thickness, the boundary conditions at the walls are :

Wall boundaries

Inner tube, inside and outside ($X=0$ to L , $R=d/2$, $\Theta=0$ to 2π)

$$U = 0, V = 0, W = 0 \quad (2.7)$$

Outer tube, inside ($X=0$ to L , $R=D/2$, $\Theta=0$ to 2π and; $X=L$, $R=0$ to $D/2$, $\Theta=0$ to 2π)

$$U = 0, V = 0, W = 0 \quad (2.8)$$

Axis of symmetry ($X=0$ to L , $R=0$, $\Theta=0$ to 2π)

$$\frac{\partial U}{\partial R} = 0, V = 0, W = 0 \quad (2.9)$$

Plane of symmetry ($X=0$ to L , $R=0$ to $D/2$, $\Theta=0$ and 2π)

$$U_{\Theta=2\pi} = U_{\Theta=0}, \quad V_{\Theta=2\pi} = V_{\Theta=0}, \quad W_{\Theta=2\pi} = W_{\Theta=0} \quad (2.10)$$

The conditions at the inlet, stated by equation (2.5), represent hydrodynamically developed flow entry. Alternatively, $U = U_i$ may be used.

2.2 Non-dimensionalization

The following dimensionless parameters are introduced to non-dimensionalize the governing equations and boundary conditions.

Displacement

$$x = \frac{X}{L}, \quad r = \frac{R}{R_0}, \quad \theta = \frac{\Theta}{\Theta^c} \quad (2.11)$$

Velocity

$$u = \frac{U}{U_m}, \quad v = \frac{V}{\left(\frac{R_0 U_m}{L}\right)}, \quad w = \frac{W}{\left(\frac{\Theta^c R_0 U_m}{L}\right)} \quad (2.12)$$

Pressure

$$p = \frac{P - P_L}{\rho U_m^2} \quad (2.13)$$

where

L = outer tube length

R_0 = outer tube radius = $D/2$

Θ^c = maximum circumferential distance = 2π

U_m = characteristic velocity = $4Kv/D$

P_L = reference pressure at entry and exit

Substitution of the above parameters into equations (2.1) to (2.4) yields the following non-dimensional equations

$$\frac{\partial u}{\partial x} + \frac{1}{r} \frac{\partial}{\partial r} (rv) + \frac{1}{r} \frac{\partial w}{\partial \theta} = 0 \quad (2.14)$$

$$\begin{aligned} u \frac{\partial u}{\partial x} + v \frac{\partial u}{\partial r} + \frac{w}{r} \frac{\partial u}{\partial \theta} &= - \frac{\partial p}{\partial x} + \frac{1}{ReK} \frac{\partial^2 u}{\partial x^2} \\ &+ \frac{4K}{Re} \frac{1}{r} \frac{\partial}{\partial r} \left(r \frac{\partial u}{\partial r} \right) + \frac{4K}{Re(\Theta^c)^2} \frac{1}{r^2} \frac{\partial^2 u}{\partial \theta^2} \end{aligned} \quad (2.15)$$

$$\begin{aligned} u \frac{\partial v}{\partial x} + v \frac{\partial v}{\partial r} + \frac{w}{r} \frac{\partial v}{\partial \theta} &= -4K^2 \frac{\partial p}{\partial r} + \frac{1}{ReK} \frac{\partial^2 v}{\partial x^2} \\ &+ \frac{4K}{Re} \frac{1}{r} \frac{\partial}{\partial r} \left(r \frac{\partial v}{\partial r} \right) + \frac{4K}{Re(\Theta^c)^2} \frac{1}{r^2} \frac{\partial^2 v}{\partial \theta^2} \\ &- \frac{4K}{Re} \frac{v}{r^2} - \frac{8K}{Re} \frac{1}{r^2} \frac{\partial w}{\partial \theta} + (\Theta^c)^2 \frac{w^2}{r} \end{aligned} \quad (2.16)$$

$$\begin{aligned} u \frac{\partial w}{\partial x} + v \frac{\partial w}{\partial r} + \frac{w}{r} \frac{\partial w}{\partial \theta} &= - \frac{4K^2}{(\Theta^c)^2} \left(\frac{1}{r} \frac{\partial p}{\partial \theta} \right) \\ &+ \frac{1}{ReK} \frac{\partial^2 w}{\partial x^2} + \frac{4K}{Re} \frac{1}{r} \frac{\partial}{\partial r} \left(r \frac{\partial w}{\partial r} \right) \\ &+ \frac{4K}{Re(\Theta^c)^2} \frac{1}{r^2} \frac{\partial^2 w}{\partial \theta^2} - \frac{4K}{Re} \frac{w}{r^2} \\ &+ \frac{8K}{Re(\Theta^c)^2} \frac{1}{r^2} \frac{\partial v}{\partial \theta} - \left(\frac{vw}{r} \right) \end{aligned} \quad (2.17)$$

where

$$Re = \frac{\rho U_m D}{\mu} \quad (2.18)$$

$$K = \frac{L}{D} \quad (2.19)$$

The above represent the Reynolds number and the length-diameter ratio, respectively. Note that the tube diameter ratio d/D does not appear. This is because the above equations are written considering a single tube. However, the ratio d/D appears later when the tube characteristic velocity is defined considering both tubes (see equation (2.32)).

The initial and boundary conditions expressed in non-dimensionalized form are:

Inlet ($x=0, r=0$ to $d/D, \theta=0$ to 1)

$$u = 2u_i(1-r^2), \quad v = 0, \quad w = 0 \quad (2.20)$$

where u_i is the non-dimensionalized average inlet velocity.

Outlet ($x=0, r=d/D$ to 1, $\theta=0$ to 1)

$$\frac{\partial u}{\partial x} = 0, \quad \frac{\partial v}{\partial x} = 0, \quad \frac{\partial w}{\partial x} = 0 \quad (2.21)$$

Wall boundaries

Inner tube, inside and outside ($x=0$ to l/L , $r=d/D$, $\theta=0$ to 1)

$$u = 0, \quad v = 0, \quad w = 0 \quad (2.22)$$

Outer tube, inside ($x=0$ to 1, $r=1$, $\theta=0$ to 1; and $x=1$, $r=0$ to 1, $\theta=0$ to 1)

$$u = 0, \quad v = 0, \quad w = 0 \quad (2.23)$$

Axis of symmetry ($x=0$ to 1, $r=0$, $\theta=0$ to 1)

$$\frac{\partial u}{\partial r} = 0, \quad v = 0, \quad w = 0 \quad (2.24)$$

Plane of symmetry ($x=0$ to 1 , $r=0$ to 1 , $\theta=0$ and 1)

$$u_{\theta=1} = u_{\theta=0}, \quad v_{\theta=1} = v_{\theta=0}, \quad w_{\theta=1} = w_{\theta=0} \quad (2.25)$$

2.3 Parameters

The results are expressed in terms of the following parameters, divided into two categories.

A. Geometry

1. Length-diameter ratio: L/D , where L and D are the length and diameter, respectively, of the outer tube
2. Area ratio: F_i/F_a , where

$$F_i = \frac{\pi}{4} d^2, \quad F_a = \frac{\pi}{4} (D^2 - d^2) \quad (2.26)$$

3. Clearance ratio: H/D , where H is the end clearance of the inner tube

B. Flow rate :

1. Reynolds number: In general the Reynolds number may be defined in terms of the mass flow rate m by taking

$$Re = \frac{\dot{m}}{\rho v} \left(\frac{X}{A} \right) \quad (2.27)$$

where X and A are the appropriate length and cross sectional area, respectively.

For an annulus,

$$\left(\frac{X}{A} \right)_a = \frac{4}{\pi (D+d)} \quad (2.28)$$

whereas for the inner tube

$$\left(\frac{X}{A} \right)_i = \frac{4}{\pi d} \quad (2.29)$$

Hence by defining

$$Re = \frac{4\dot{m}D}{\rho \pi v (D+d) d} = Re_a \frac{D}{d} \quad (2.30)$$

the appropriate limiting forms when $d \rightarrow D$ and $d \ll D$ may be recovered.

Equation (2.30) thus provides a simple and convenient definition that covers the full range of F_i/F_a .

The above will be considered as independent variables which influence the overall system performance, as measured by the Euler number in which the pressure drop incorporates two main effects, viscous and inertial. The structure given in equation (2.30) is equivalent to taking the characteristic "diameter" as:

$$D^c = \frac{d(D-d)}{D} \quad (2.31)$$

and the characteristic velocity as

$$U^c = \frac{4\dot{m}D^2}{\rho \pi (D^2-d^2) d^2} = U_a \left(\frac{D}{d} \right)^2 \quad (2.32)$$

This permits an Euler number to be defined by

$$Eu = \frac{2\Delta P}{\rho (U^c)^2} \quad (2.33)$$

where, using the energy equation between the inlet and outlet,

$$\Delta P = \Delta P_t + \rho U_i^2 \left[1 - \frac{3}{4} \left(\frac{F_i}{F_a} \right)^2 \right] \quad (2.34)$$

Chapter 3

Numerical Technique

3.1 Introduction

The non-dimensional governing equations formulated in the previous chapter, equations (2.14) to (2.17), are non-linear partial differential equations, which cannot be solved analytically. Therefore a numerical technique is used for their solution.

The problem may be stated as that of solving the Navier-Stokes equations governing the fluid velocity field. Since the Navier-Stokes equations contain a pressure gradient term, a knowledge of the pressure field is

necessary. However, there is no explicit equation for obtaining pressure. Therefore, the pressure field is specified indirectly through the continuity equation. When correct pressure field is substituted into the momentum equation, the resulting velocity field satisfies the continuity equation.

Patankar and Spalding [17] have suggested a method for the numerical solution of the Navier-Stokes equations. The method called SIMPLE (Semi-Implicit Method for the Pressure Linked Equations) utilizes the approach of transforming the continuity equation into an equation for obtaining the pressure, understanding that pressure is only an agent to enforce continuity. The method was developed in 1972 and has since been used to solve incompressible flow problems. To date, some modifications in the SIMPLE algorithm have been proposed for better convergence. Examples are the SIMPLE-R (SIMPLE Revised) algorithm of Patankar[18] and SIMPLE-C (SIMPLE Consistent) algorithm of Van Doormaal and Raithby [19]. The SIMPLE-C algorithm has been shown to posses better convergence and improved economy, and is thus used in this study.

3.2 Finite Difference equations

3.2.1 Grid and Control Volume Definitions

A finite difference grid with orthogonally intersecting grid lines for the x-, r- and θ -coordinates is used. The grid is staggered (see Figure 3.1) so that the velocities are located at the cell faces and the pressure at the nodal points. The advantages of using a staggered grid are described in the original reference [18]. In this study, a M x N x KM (see Figure 3.2) unequally spaced grid is used.

3.2.2 Discretization

The non-dimensional governing equations (2.14) to (2.17) are integrated over the cell control volume to get the finite difference equations. The complete detail of the method is given in references [18,19]. A brief description is given below.

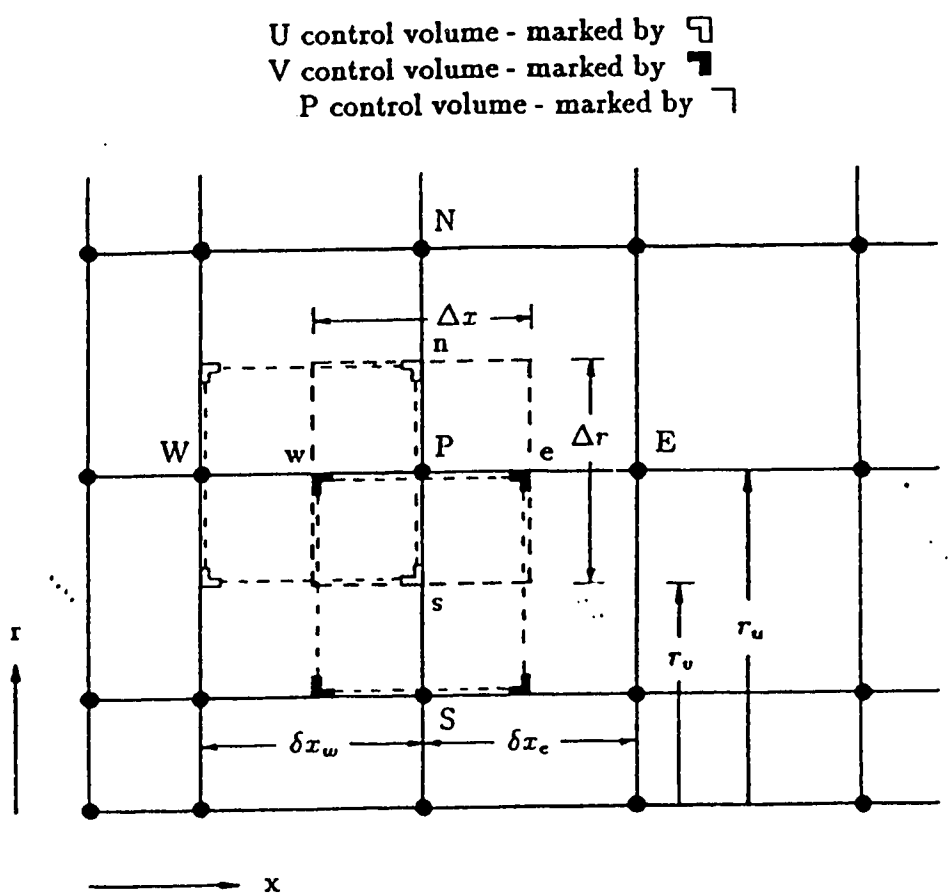
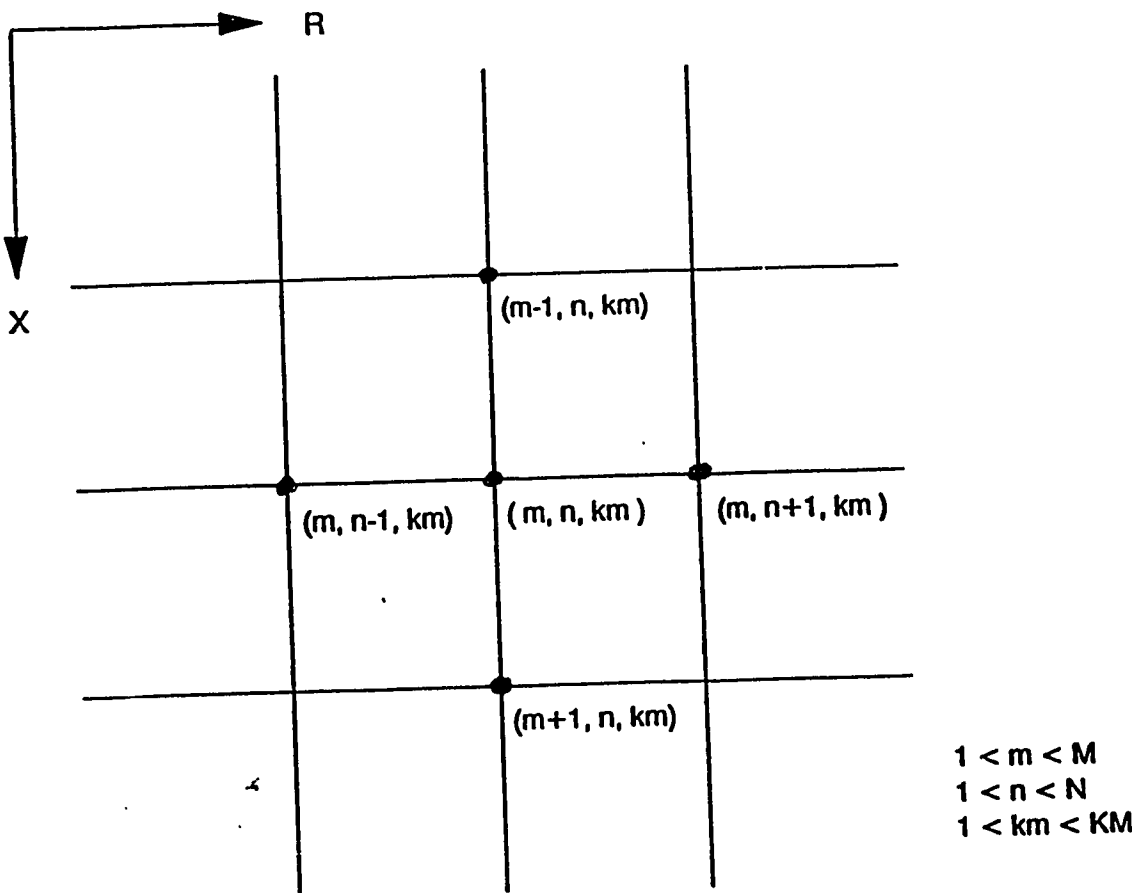


**FIGURE 3.1 CONTROL VOLUME AND NOTATION
IN STAGGERED GRID (x - r plane)**



M = no. of grid lines in X-direction
 N = no. of grid lines in R-direction
 KM = no. of grid lines in Θ -direction

FIGURE 3.2 GRID NOMENCLATURE (X-R plane)

The axial momentum equation (2.15) can be written as

$$\frac{1}{r} \frac{\partial J_x}{\partial x} + \frac{1}{r} \frac{\partial J_r}{\partial r} + \frac{1}{r^2} \frac{\partial J_\theta}{\partial \theta} = - \frac{\partial p}{\partial x} \quad (3.1)$$

where J_x , J_r and J_θ are the total (convective plus diffusion) fluxes given by

$$J_x = r u u - \left(\frac{1}{Re K} \right) r \frac{\partial u}{\partial x} \quad (3.2)$$

$$J_r = r v u - \left(\frac{4 K}{Re} \right) r \frac{\partial u}{\partial r} \quad (3.3)$$

$$J_\theta = r w u - \left(\frac{4 K}{Re (\Theta^c)^2} \right) \frac{\partial u}{\partial \theta} \quad (3.4)$$

The integration of equation (3.1) over the cell control volume gives

$$J_e r \Delta \theta \Delta r - J_w r \Delta \theta \Delta r + J_n r \Delta \theta \Delta x - J_s r \Delta \theta \Delta x + J_t \Delta x \Delta r - J_b \Delta x \Delta r = (p_w - p_e) r^2 \Delta r \Delta \theta \quad (3.5)$$

To evaluate the flux terms at the control volume face, an interpolation scheme is required. A second order accurate central difference approximation, using a piecewise-linear profile, may lead to non-convergent solutions for cell Peclet numbers (P) > 2 . An alternative is an upwind scheme [20,21]. However, this scheme may lead to inaccurate converged solutions at small Peclet numbers. Thus, for a successful scheme, a compromise must be made between the accuracy and the numerical stability. In this study the power difference scheme recommended by Patankar is used. For cell Peclet numbers greater than 10 in magnitude, the power scheme reverts to the upwind scheme: otherwise an approximation of the locally exact profile is obtained using a fifth power curve.

The application of the power difference scheme to equation (3.5) leads to a discretized equation of the following form :

$$a_p u_p = a_E u_E + a_W u_W + a_N u_N + a_S u_S + a_T u_T + a_B u_B + b \quad (3.6)$$

or simply

$$a_p u_p = \sum a_{nb} u_{nb} + b \quad (3.7)$$

where the coefficients are given as

$$a_E = D_e A(|P_e|) + \text{MAX}(-F_e, 0) \quad (3.8)$$

$$a_W = D_w A(|P_w|) + \text{MAX}(F_w, 0) \quad (3.9)$$

$$a_N = D_n A(|P_n|) + \text{MAX}(-F_n, 0) \quad (3.10)$$

$$a_S = D_s A(|P_s|) + \text{MAX}(F_s, 0) \quad (3.11)$$

$$a_T = D_t A(|P_t|) + \text{MAX}(-F_t, 0) \quad (3.12)$$

$$a_B = D_b A(|P_b|) + \text{MAX}(F_b, 0) \quad (3.13)$$

$$a_p = a_E + a_W + a_N + a_S + a_T + a_B \quad (3.14)$$

$$b = (P_w - P_e) r^2 \Delta r \Delta \theta \quad (3.15)$$

The cell flow rates in the above equations are :

$$F_e = (\varphi_e)^2 u_e \Delta x \Delta \theta \quad (3.16)$$

$$F_w = (\varphi_w)^2 u_w \Delta x \Delta \theta \quad (3.17)$$

$$F_n = (\varphi_n)^2 v_n \Delta x \Delta \theta \quad (3.18)$$

$$F_s = (\varphi_s)^2 v_s \Delta x \Delta \theta \quad (3.19)$$

$$F_t = \varphi_t w_t \Delta x \Delta \vartheta \quad (3.20)$$

$$F_b = \varphi_b w_b \Delta x \Delta \vartheta \quad (3.21)$$

and cell conductances are :

$$D_e = \frac{1}{ReK} \frac{(\varphi_e)^2}{(\delta x)_e} \Delta x \Delta \theta \quad (3.22)$$

$$D_w = \frac{1}{ReK} \frac{(x_w)^2}{(\delta x)_w} \Delta x \Delta \theta \quad (3.23)$$

$$D_n = \frac{4K}{Re} \frac{(x_n)^2}{(\delta x)_n} \Delta x \Delta \theta \quad (3.24)$$

$$D_s = \frac{4K}{Re} \frac{(x_s)^2}{(\delta x)_s} \Delta x \Delta \theta \quad (3.25)$$

$$D_t = \frac{4K}{Re (\Theta^c)^2} \frac{\Delta x \Delta r}{(\delta \theta)_t} \quad (3.26)$$

$$D_b = \frac{4K}{Re (\Theta^c)^2} \frac{\Delta x \Delta r}{(\delta \theta)_b} \quad (3.27)$$

The cell Peclet number is the ratio of F and D ; thus $P_e = F_e/D_e$ and so on. The function A(|P|) is given as

$$A(|P|) = MAX[0, (1-0.1|P|)^5] \quad (3.28)$$

The function MAX chooses the larger of the two arguments in the bracket.

The radial and the circumferential momentum equations are similarly discretized, resulting in the same form as equation (3.6) except with minor differences in the coefficients. For the radial momentum equation,

$$a_p = \Sigma a_{nb} + \frac{4K}{Re} \Delta x \Delta r \Delta \theta \quad (3.29)$$

$$b = 4K^2 (p_s - p_n) r^2 \Delta x \Delta \theta + \frac{8K}{Re} (w_b - w_t) \Delta x \Delta r \quad (3.30)$$

$$+ (\Theta^c)^2 w^2 r \Delta x \Delta r \Delta \theta$$

and for the circumferential momentum equation,

$$a_p = \Sigma a_{nb} + \frac{4K}{Re} \Delta x \Delta r \Delta \theta + vr \Delta x \Delta \theta \Delta r \quad (3.31)$$

$$b = \frac{4K^2}{(\Theta^c)^2} (p_b - p_t) r \Delta x \Delta r \quad (3.32)$$

$$+ \frac{8K}{Re (\Theta^c)^2} (v_t - v_b) \Delta x \Delta r$$

The solution of the discretized equation (e.g. equation (3.6)) depends on the solution of other dependent variables (e.g. v and w). An iterative solution procedure is used to handle the resulting inter-equation linkages and nonlinearities. At the beginning of each cycle, the coefficients are evaluated using u, v and w values evaluated in the previous cycle. However, the cycle to cycle change in coefficients may lead to large changes in the u, v and w values. This can cause slow convergence or even divergence. To moderate the changes in consecutive solutions, under-relaxation is introduced through α as:

$$\frac{a_p}{\alpha} u_p = \sum a_{nb} u_{nb} + r^2 \Delta x \Delta \theta (p_w - p_e) + \frac{1-\alpha}{\alpha} a_p u^* p \quad (3.33)$$

$$= \sum a_{nb} u_{nb} + A_p (p_w - p_e) + b_p \quad (3.34)$$

where $u^* p$ is the u_p value from the previous cycle.

3.3 The Algorithm

The continuity equation is converted into a pressure correction equation. The finite difference equations for the velocities u,v and w have the form of

equation (3.34). The u-momentum equation for the control volume centred at e, can be written as

$$a_e u_e = \sum a_{nb} u_{nb} + A_e (p_p - p_E) + b_e \quad (3.35)$$

where a_e is now $\sum a_{nb}/a$. For a guessed pressure field p^* , the velocity field u^* satisfies

$$a_e u^*_e = \sum a_{nb} u^*_{nb} + A_e (p^*_{\bar{p}} - p^*_{\bar{E}}) + b_e \quad (3.36)$$

Subtraction of equation (3.36) from (3.35), gives

$$a_e \dot{u}_e = \sum a_{nb} \dot{u}_{nb} + A_e (\dot{p}_{\bar{p}} - \dot{p}_{\bar{E}}) \quad (3.37)$$

where

$$u = \dot{u} + u^* \quad (3.38)$$

$$p = \dot{p} + p^* \quad (3.39)$$

In the SIMPLE algorithm, the first right hand term in equation (3.37) is neglected for economic calculation. In SIMPLE-C algorithm, however, the velocity correction equations are obtained by subtracting $\sum a_{nb} u'_e$ from both sides of the equation. This gives

$$(a_e - \sum a_{nb}) \dot{u}_e = \sum a_{nb} \dot{u}_{nb} - \dot{u}_e + A_e (\dot{p}_p - \dot{p}_E) \quad (3.40)$$

The term $\sum a_{nb} u'_{nb} - u'_e$ is now neglected, resulting in

$$u_e = u_e^* + d_e (\dot{p}_p - \dot{p}_E) \quad (3.41)$$

where

$$d_e = \frac{A_e}{a_e - \sum a_{nb}} \quad (3.42)$$

Pressure correction equation is now obtained by substituting equations like (3.41) for u , v and w into the discretized continuity equation for the control volume around the main grid point, that is,

$$u_e r_e \Delta r \Delta \theta - u_w r_w \Delta r \Delta \theta + v_n r_n \Delta x \Delta \theta - v_s r_s \Delta x \Delta \theta + w_t \Delta x \Delta r - w_b \Delta x \Delta r = 0 \quad (3.43)$$

The resulting pressure correction equation is

$$a_p \delta_p = a_E \delta_E + a_W \delta_W + a_N \delta_N + a_S \delta_S + a_T \delta_T + a_B \delta_B + b \quad (3.44)$$

where

$$a_E = A_e d_e \quad (3.45)$$

$$a_W = A_w d_w \quad (3.46)$$

$$a_N = 4K^2 A_n d_n \quad (3.47)$$

$$a_S = 4K^2 A_s d_s \quad (3.48)$$

$$a_T = \frac{4K^2}{(\Theta^c)^2} A_t d_t \quad (3.49)$$

$$a_B = \frac{4K^2}{(\Theta^c)^2} A_b d_b \quad (3.50)$$

$$b = A_w u^*_w - A_e u^*_e + A_s v^*_s - A_n v^*_n \\ + A_b w^*_b - A_t w^*_t \quad (3.51)$$

$$A_e = (\tau_e)^2 \Delta x \Delta \theta \quad (3.52)$$

$$A_w = (\tau_w)^2 \Delta x \Delta \theta \quad (3.53)$$

$$A_n = (\tau_n)^2 \Delta x \Delta \theta \quad (3.54)$$

$$A_s = (\tau_s)^2 \Delta x \Delta \theta \quad (3.55)$$

$$A_t = I_t \Delta x \Delta I \quad (3.56)$$

$$A_b = I_b \Delta x \Delta I \quad (3.57)$$

The TDMA (Tri-Diagonal Matrix Algorithm) procedure is used to solve for the dependent variables. Each algebraic equation along a constant line is written as

$$a_p \phi_p = a_N \phi_N + a_S \phi_S + S \quad (3.58)$$

The other neighbouring coefficients are incorporated in S and assumed to be temporarily known. This formulation, equation (3.58), allows a line by line iteration method.

Boundary conditions for velocity are imposed by specifying the function or the function gradient. The boundary treatment of p' is implicit and depends on the velocity boundary condition. For velocity normal to the boundary $\partial p' / \partial x$ is ~~specified~~: when pressure is specified, $p = p^*$ and $p' = 0$ at the boundary. For the outlet boundary condition of $\partial u / \partial x$, $\partial v / \partial x$ and $\partial w / \partial x$, $p = 0$ is set at the exit ($x = 0, r = d/2$ to $D/2, \theta = 0$ to 2π).

The details of the numerical method are given in the original references [18,19].

The main steps in the algorithm are :

1. Guess the pressure field, p^* .
2. Solve the momentum equations for u , v and w using line by line iterations based on TDMA procedure. The obtained velocities, u^* , v^* and w^* , do not in general satisfy continuity.
3. Solve pressure correction equation for p' .
4. Apply the pressure corrections to correct pressure, thus eliminating continuity errors in the current iteration.
5. Using the p found in step 4 as the new p'' , return to step 2. Repeat this iteration cycle until convergence is reached to a specified tolerance on changes in velocities and pressure over two successive iterations.

3.4 Program validation

A computer program, for steady, laminar, constant property and axisymmetric flow in a straight pipe, was written in FORTRAN 77 using the Algorithm described in section (3.3). A fully developed velocity profile was assumed at the inlet boundary.

Convergence criteria are listed in Table 1.

TABLE 1

Function	Nodal average change over two successive iterations (%)
u	10^{-4}
v	10^{-3}
p	10^{-4}
Source	10^{-7}

Effect of grid size on mass flow rate error is illustrated below.

TABLE 2

Grid	Mass error (%)
8 X 8	6.83
12 X 12	2.48
16 X 16	1.27
20 X 20	0.76
* 24 X 24	0.52
30 X 30	0.32

* selected grid

The calculations are made for a Reynolds number of 100 and a length to diameter ratio of 20. An optimal relaxation factor of 0.72 was used. From Table 2 it is clear that the percentage mass error between the inlet and the outlet decreases with grid size. A 24 X 24 grid was chosen for the comparative test below. With a 30 X 30 grid, the time taken was found to be 10 percent more than with a 24 X 24 grid.

To check the pressure and flow rate accuracy, friction factor ($f = 2d\Delta P/\rho Lu^2$) data was obtained for different Reynolds numbers ($Re = Ud/v$). The results are compared with the classical relation $f = 64/Re$ in Figure 3.3. The results indicate excellent agreement. Maximum deviation is less than one percent, as expected.

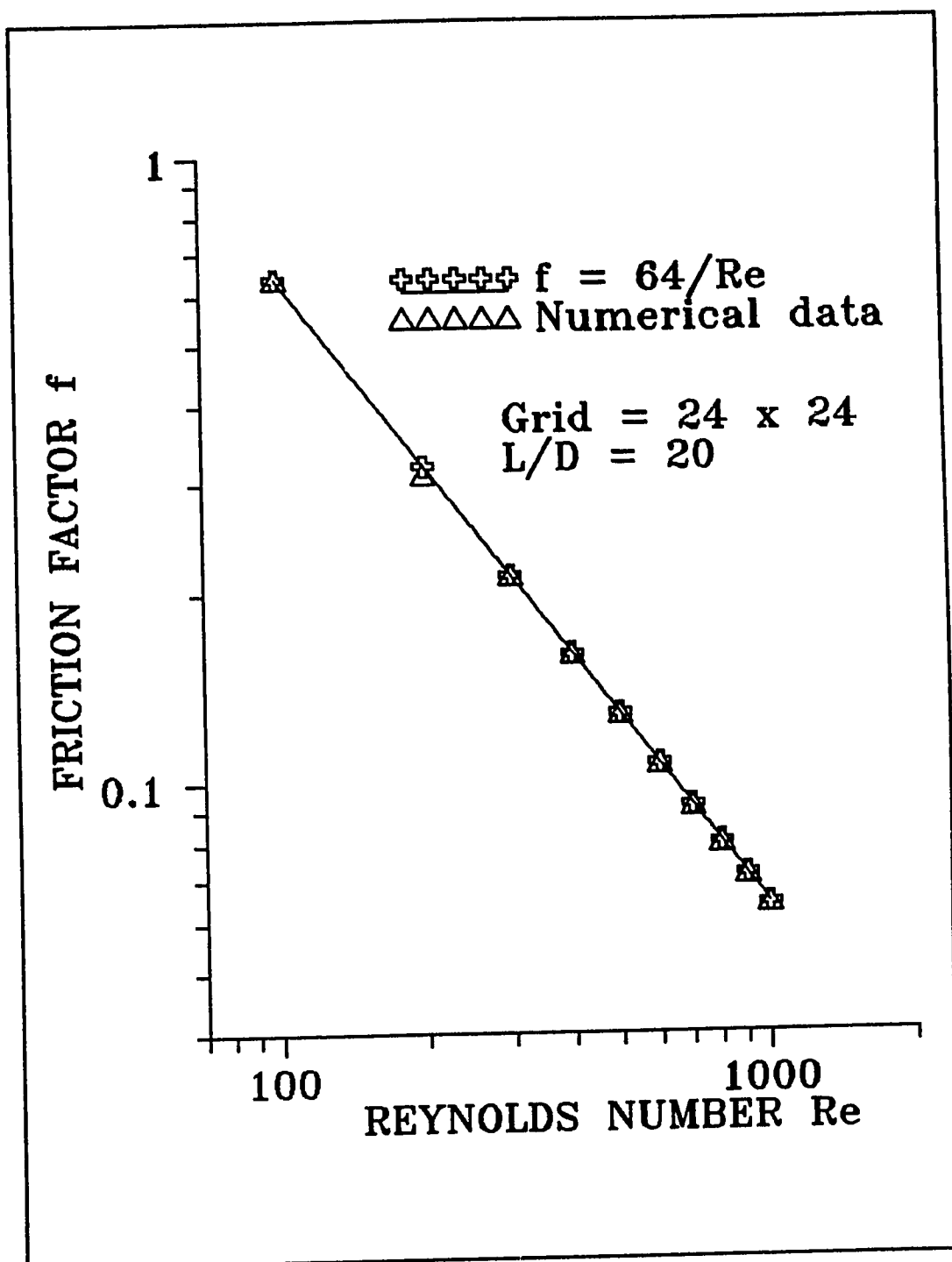


FIGURE 3.3 COMPARISON OF FRICTION FACTOR DATA FOR A CIRCULAR TUBE

The following convergence criteria were used for the bayonet tube :

Table 3

Function	Nodal average change over two successive iterations (%)
u	10^{-4}
v	10^{-2}
w	10^{-2}
p	6×10^{-3}
source	5×10^{-3}

A grid of $41 \times 41 \times 20$, with the respective grid lines in the x-, r- and θ -directions, was used. This grid has approximately double grid lines in the x- and r-directions as compared to the grid for a straight pipe. This was chosen, since now we are dealing with two pipes instead of single pipe dealt before. Also the complexity of the flow pattern demands a finer grid to include the effects of vortex and recirculation. An optimum relaxation factor of 0.72 was used. Test with a grid of $61 \times 61 \times 40$ indicated a percentage Euler number change of less than 2%, while the time taken to run the program was increased by 10%. The percentage mass error between inlet and outlet is less than 0.6 percent.

The two dimensional results were checked for uniqueness by using different initial velocity and pressure fields. The solution remained unchanged. The three dimensional results were not checked for uniqueness.

Chapter 4

Frictional Characteristics With Central Admission

4.1 Introduction

In this chapter, the effect of the principal bayonet tube parameters on the overall pressure drop in the tube is discussed in the absence of heat transfer. The pressure drop is expressed nondimensionally as the Euler number. The definition of Euler number described in equation (2.35), section 2.3, is used. The nondimensional parameters studied were : Reynolds number (Re), length to diameter ratio (L/D), area ratio (F_i/F_a) and the clearance ratio (H/D).

These parameters represent the fluid flow rate and the system geometry. Parameter definitions are given in section 2.3. During the study of each parametric effect, the other parameters are held constant at a set of reference values. These were $Re \approx 1000$, $L/D \approx 20$, $H/D \approx 1$ and $F_i/F_o \approx 0.47$, chosen to represent a practical situation [15]. Flow behaviour is restricted to a cylindrical end geometry with the thickness of the inner tube being neglected. In addition, flow in the tube is taken to be steady and laminar with the fluid properties held constant. This chapter deals only with admission of the fluid into the inner tube; a fully developed (parabolic) velocity profile is assumed. Chapter 5 deals with fluid admission into the annulus between the inner and the outer tube, again with a parabolic entry profile.

The results have been plotted as graphs and velocity field diagrams. Where available, the experimental data is also displayed. This enables direct comparisons to be made. The experimental data plotted is the nearest available data representing the given conditions. More on this will be discussed later.

The velocity field diagrams have been plotted using a Plot 3D package. The vectors in the diagrams represent the resultant velocity with the arrowheads pointing in the direction of the fluid flow. The length of the vector provides the magnitude of the velocity non-dimensionalized by a characteristic velocity. Since the main flow is in the axial direction, the characteristic velocity

was obtained by balancing the pressure drop term in the axial momentum equation, equation (2.15), with the radial viscous term. The characteristic velocity thus obtained was equal to $4Kv/D$, K being L/D , L the length and D the outer tube diameter.

4.2 Effect of Reynolds number

The effect of the Reynolds number on the Euler number is shown in Figure 4.1. As expected, the Euler number decreases monotonically with an increase in the Reynolds number, here plotted on a logarithmic scale. An increase in the (laminar) Reynolds number from 200 to 1000 results in a 73.5% decrease in the Euler number. This trend is not unexpected given the shape of the curve in Figure 3.3, where the friction factor data for a fully developed laminar flow in a circular duct is plotted.

The numerical prediction is seen to lie consistently below the experimental data, the deviations being larger at Reynolds numbers near the two extremes of the curve. The experimental points (1) and (4) are above the numerical curve by 23.5% and 12.3%, respectively. This is because the experimental points do not represent exactly the same conditions used for numerical prediction. Experimental point (1) is plotted for $F_i/F_a = 0.229$. As will be seen later, the pressure drop for an area ratio of 0.229 is 20% more than that at 0.474 (see section 4.4). Also point (4) is for a clearance ratio of 0.748.

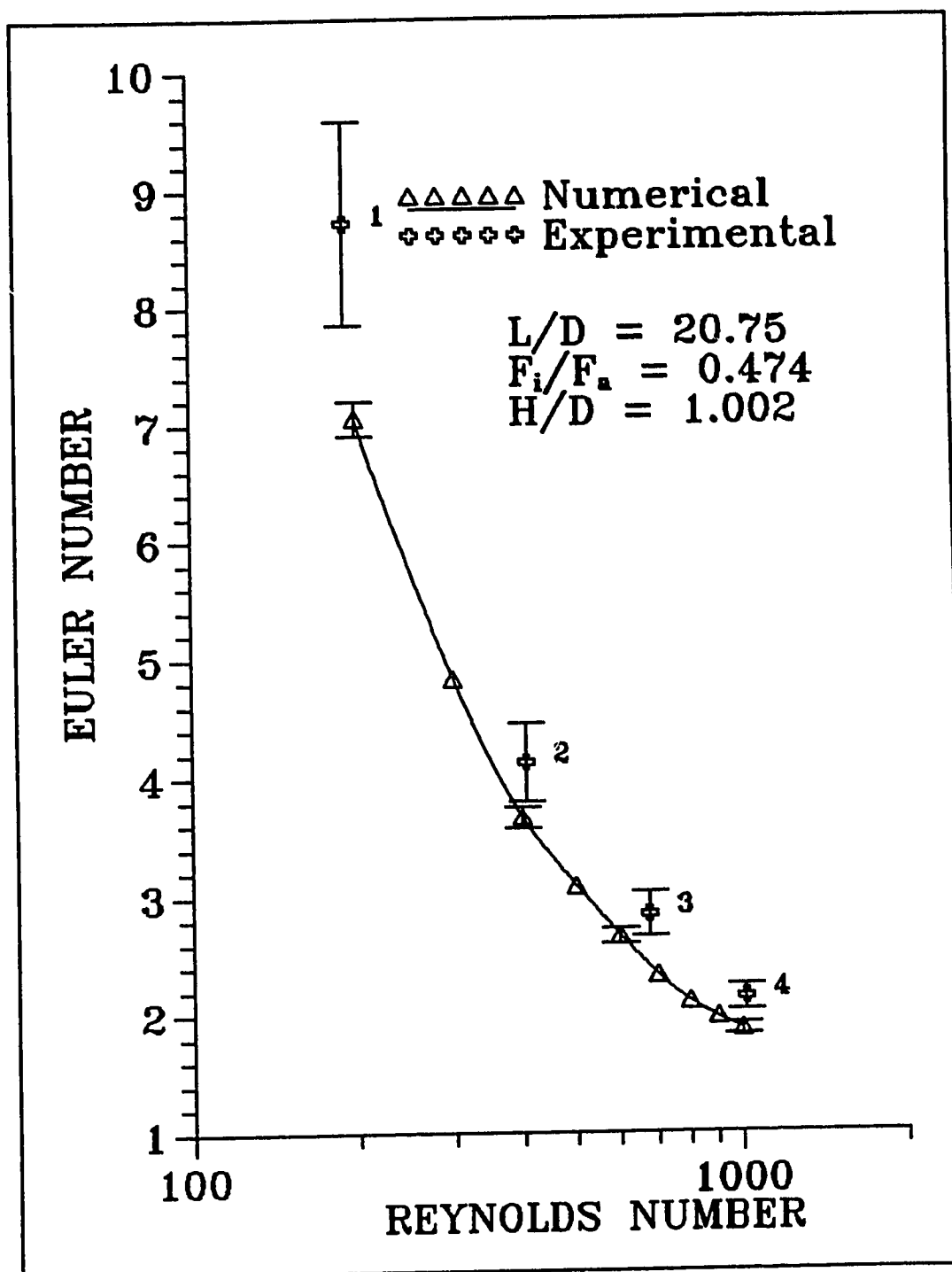


FIGURE 4.1 EFFECT OF REYNOLDS NUMBER ON EULER NUMBER

The Euler number for H/D between 0.5 to 1.0 is greater than for $H/D = 1.0$ (see section 4.5); for $H/D = 0.748$, in particular, it is 12.5% more. Agreement at these points is thus within the experimental error shown. The discrepancy at points (1) and (2) is difficult to explain.

The flow pattern for Reynolds numbers of 200 and 1000 were studied, the respective velocity fields being plotted in Figure 4.2, the left hand side of which provides the "standard" flow field for future comparison. A ring vortex is observed in the end clearance zone. This vortex was found to be stable in an axisymmetric form. As the fluid moves away from the sealed end, the vortex gets narrower. At $Re = 200$, it has split into a few small secondary vortices before reattaching at the outside of the inner tube. At $Re = 1000$, the velocity is higher and the circulation within the vortex is also faster than at lower Reynolds numbers. At higher mass flow rates, the formation of a stronger vortex with more vigorous circulation may lead to slope variation with increased Reynolds numbers. A stronger vortex implies a greater dissipation rate which in turn implies a greater pressure drop.

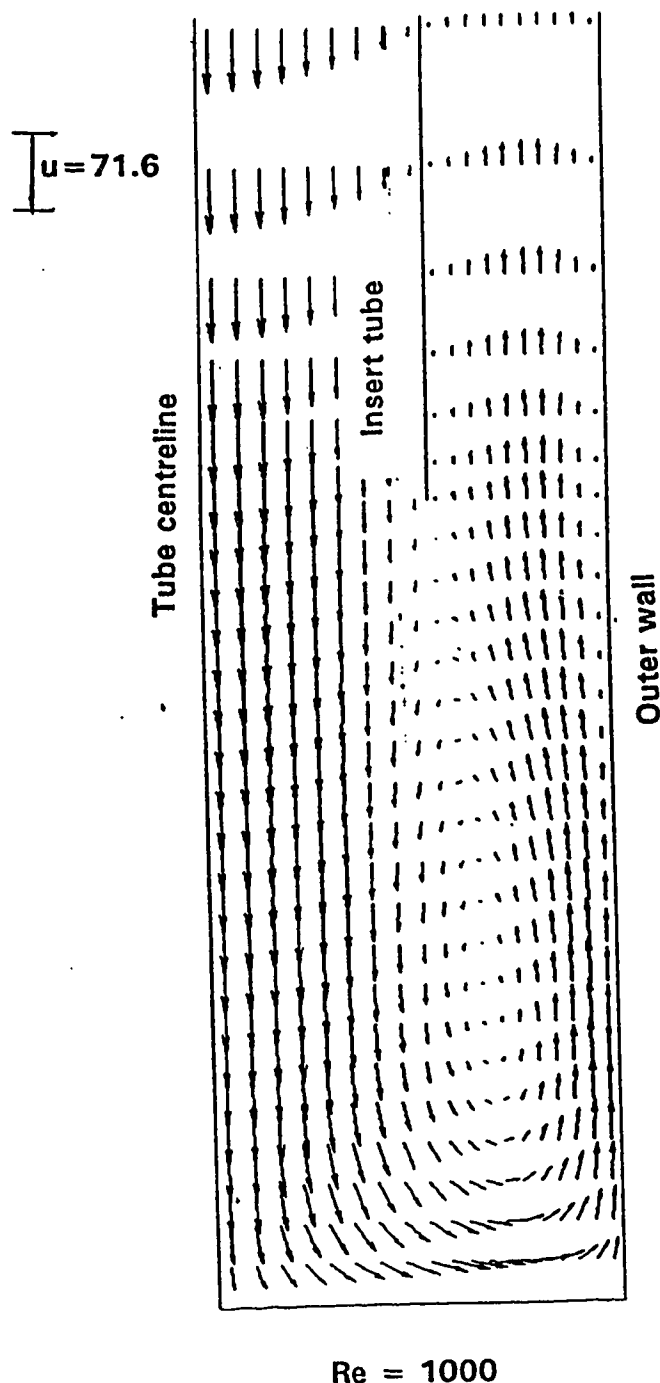
4.3 Effect of Length-diameter ratio

The effect of length-diameter ratio L/D on the Euler number is shown in Figure (4.3). As expected, the Euler number increases with an increase in the

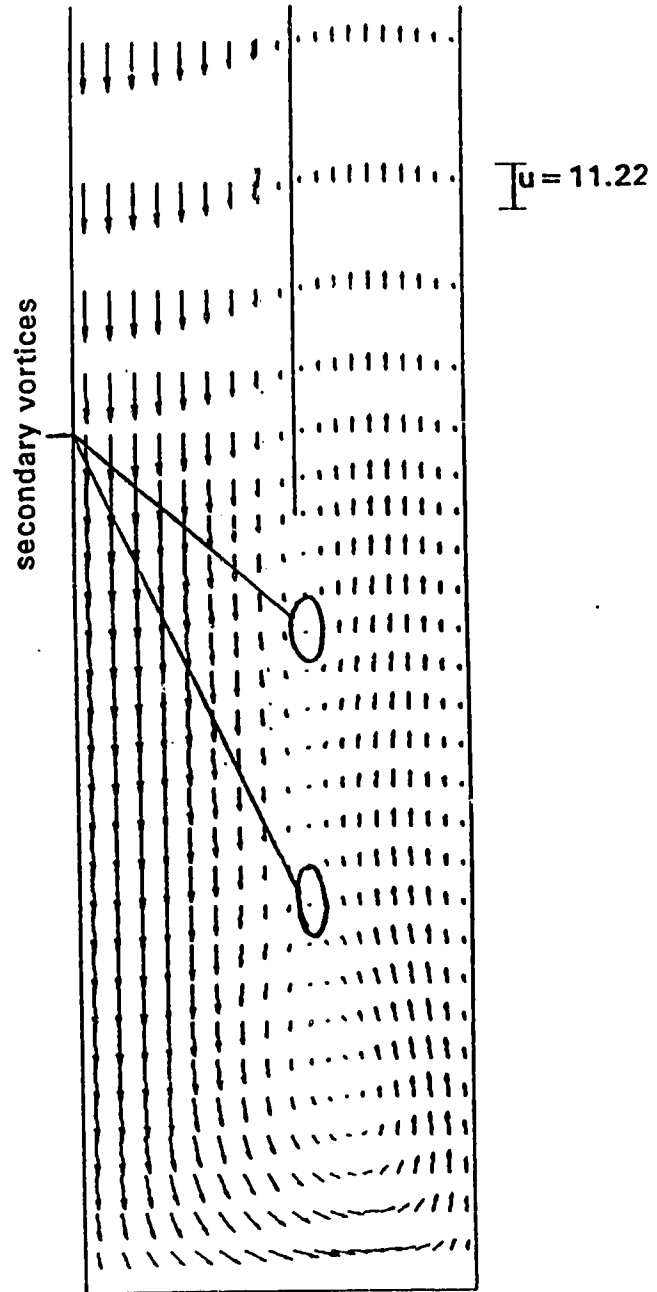
$L/D = 20$
 $F_i/F_a = 0.47$
 $H/D = 1$

$L/D = 20.75$
 $F_i/F_a = 0.474$
 $H/D = 1.002$

51



$Re = 1000$



$Re = 200$

FIGURE 4.2 VELOCITY PROFILE FOR $Re = 1000$ AND 200

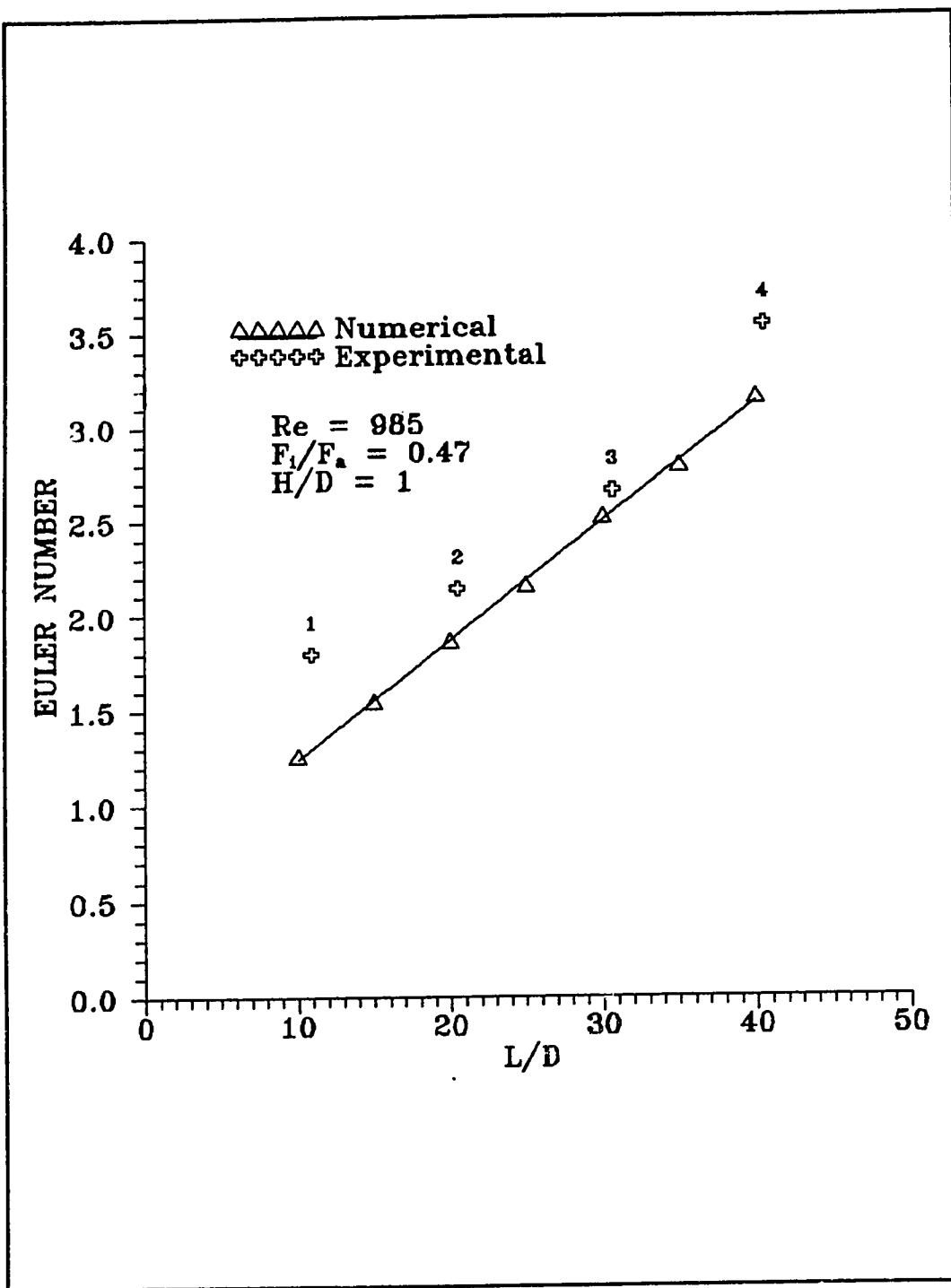


FIGURE 4.3 EFFECT OF LENGTH-DIAMETER RATIO ON EULER NUMBER

length-diameter ratio. This linear trend is expected to continue for L/D values greater than 40 because the skin friction loss increases in proportion to the tube surface area.

At L/D = 30, corresponding to experimental point (3), the numerical results are within 10% experimental data. For other values, the deviation is due to variations in the experimental parameters. Point (1) for example, is for a Reynolds number of 689. As seen in the previous section, a decrease in the mass flow rate results in an increase in the pressure drop. Hence, point (1) should lie 27% above the numerical data. Point (2) is for H/D = 0.748 implying that it should lie 12.6% above the numerical curve. Also point (4) should be a higher value, since it is for a clearance ratio of 0.982, which creates a 2% greater Euler number than for a clearance ratio of 1.0 (see section 4.5). Agreement for points (2) and (4) is therefore within experimental error of 10%. However, the "corrected" experimental point (1) still lies slightly above the numerical curve. The neglect of the inner tube thickness in the numerical study suggests that for L/D = 10, the pressure drop may be less than in the experiment. It will be seen later that a ring vortex extends between the mouth of the inner tube and the sealed end of the outer tube. A change in the inner tube thickness will thus effect the vortex flow pattern. At low L/D values, the inertial and the viscous forces, being small, may be unable to overcome the changes in the flow pattern introduced by the inner tube thickness. Thus the

numerical pressure drop values, which are obtained assuming no inner tube thickness, are below the experimental results obtained with certain inner tube thickness.

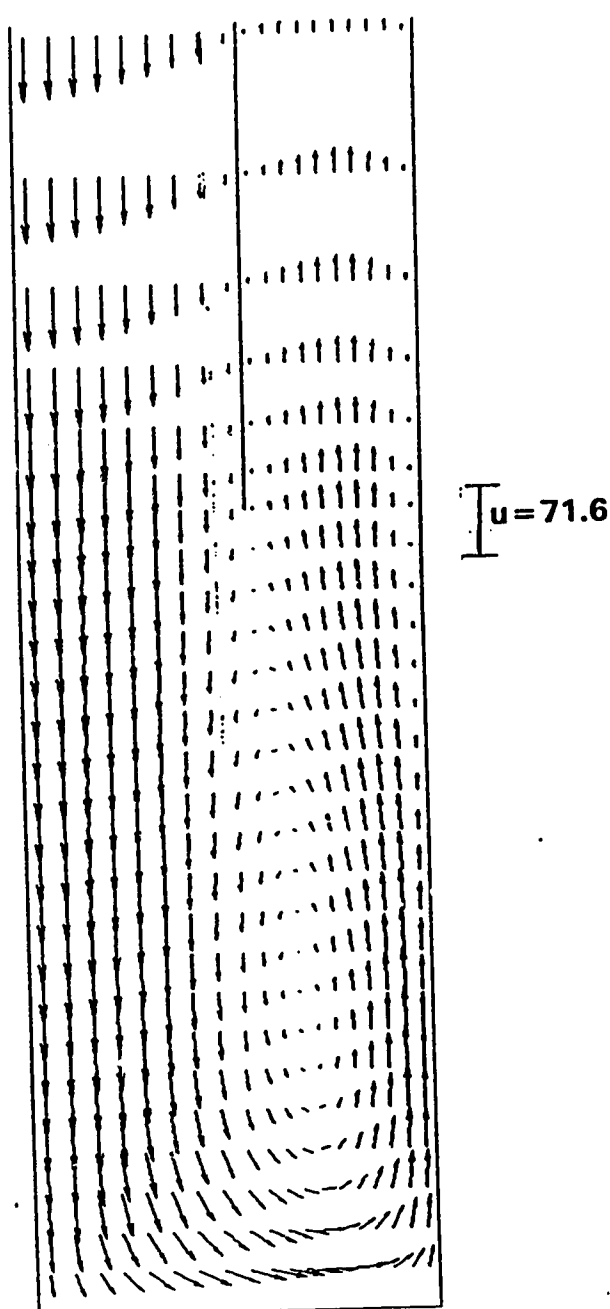
The velocity flow fields for L/D ratios of 10 and 40 are plotted in Figures 4.4 and 4.5, respectively. For both, $L/D = 10$ and $L/D = 40$, the vortex extends from the bottom of the clearance space to the inner end of the inside tube. The curve being a straight line, suggests that its slope remains unaffected as long as the vortex pattern is the same in the clearance zone. Conversely, a change in pattern would imply a changing slope.

4.4 Effect of Area ratio

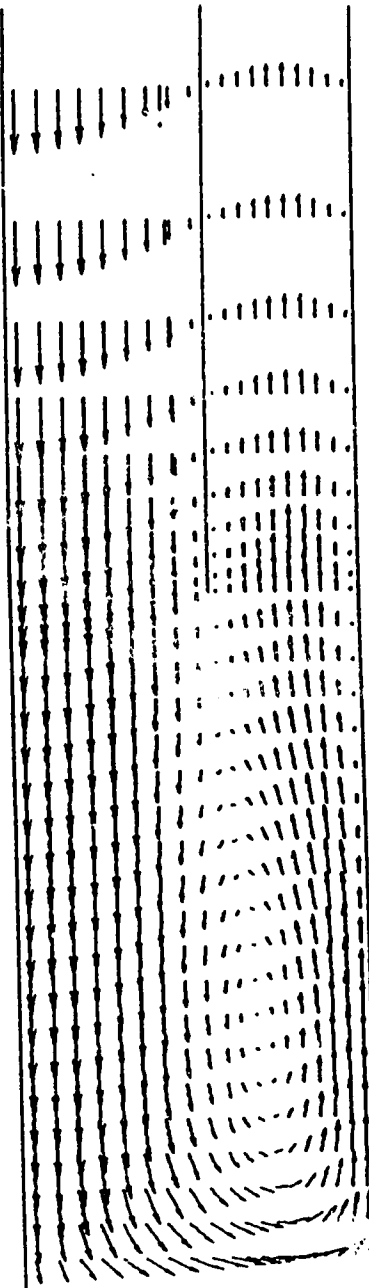
The effect of the area ratio, F_i/F_a , on the Euler number, is illustrated in Figure 4.6. The change of the Euler number with the area ratio is not monotonic. A characteristic minimum is noted. This occurs at $F_i/F_a \approx 0.47$. Appearance of this minimum is not unexpected. In fact, it might be expected that this minimum would occur at $F_i/F_a = 1.0$, when the inertial contribution to the pressure drop is theoretically zero i.e. when sudden contraction or expansion does not occur. However, this prescription of the inertial behaviour does not account for the space created by the end clearance or the effluent

$Re = 1000$
 $F_i/F_a = 0.47$
 $H/D = 1$

$Re = 965$
 $F_i/F_a = 0.47$
 $H/D = 1$ 55



$L/D = 20$



$L/D = 10$

FIGURE 4.4 VELOCITY PROFILE FOR $L/D = 20$ AND 10

$Re = 1000$
 $F_i/F_a = 0.47$
 $H/D = 1$

$Re = 965$
 $F_i/F_a = 0.47$
 $H/D = 1$

56

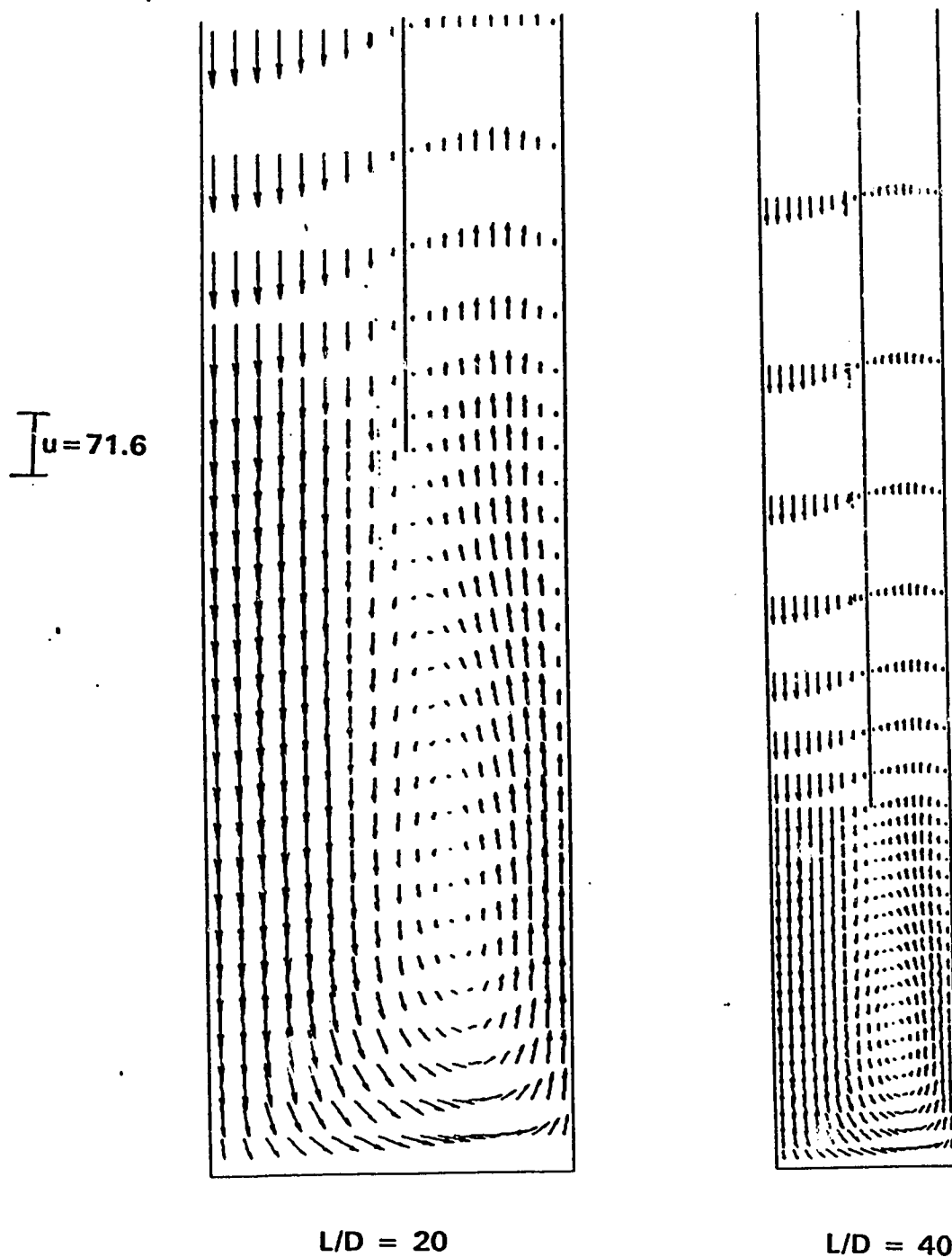


FIGURE 4.5 VELOCITY PROFILE FOR $L/D = 20$ AND 40

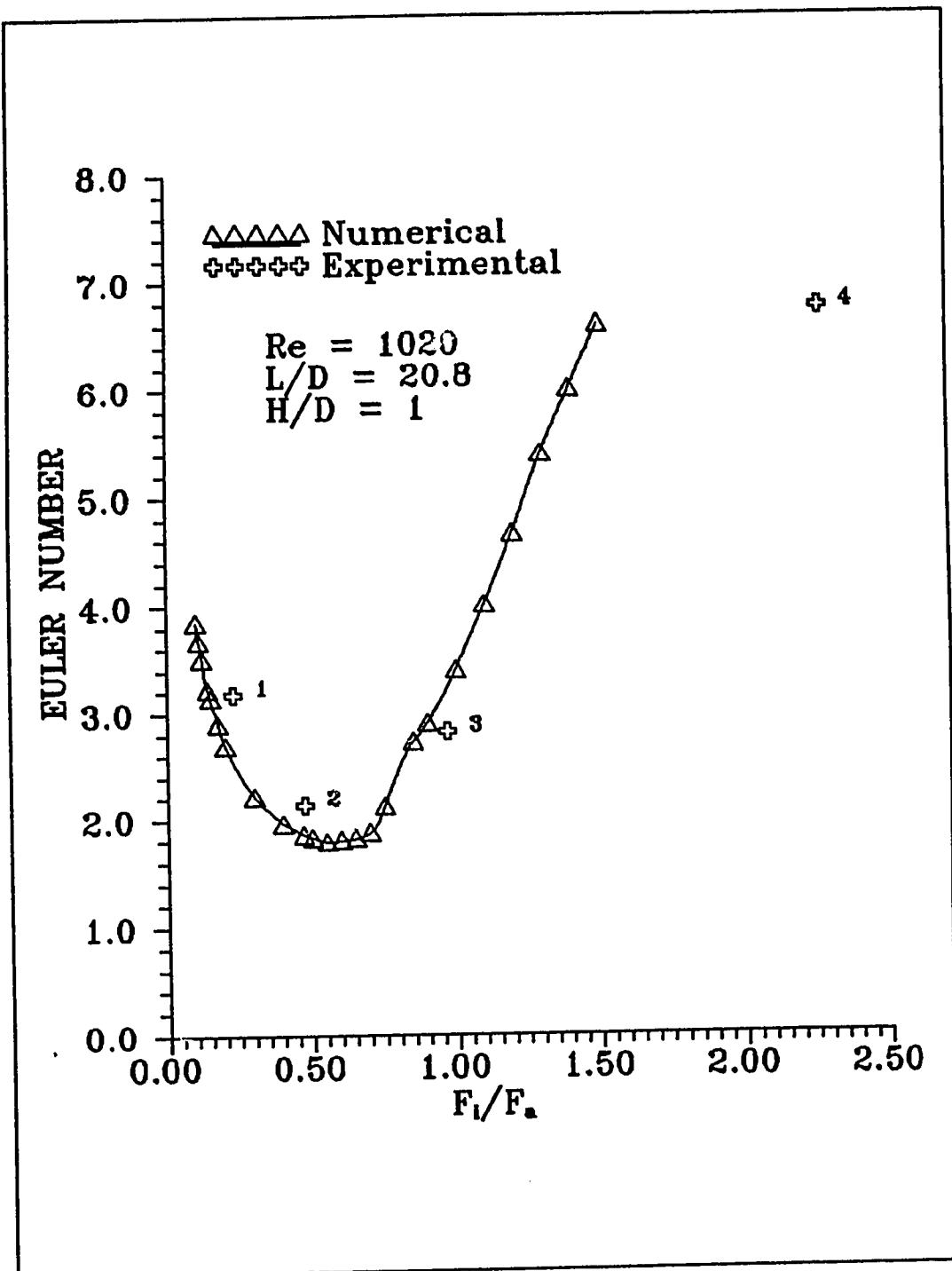


FIGURE 4.6 EFFECT OF AREA RATIO
ON EULER NUMBER

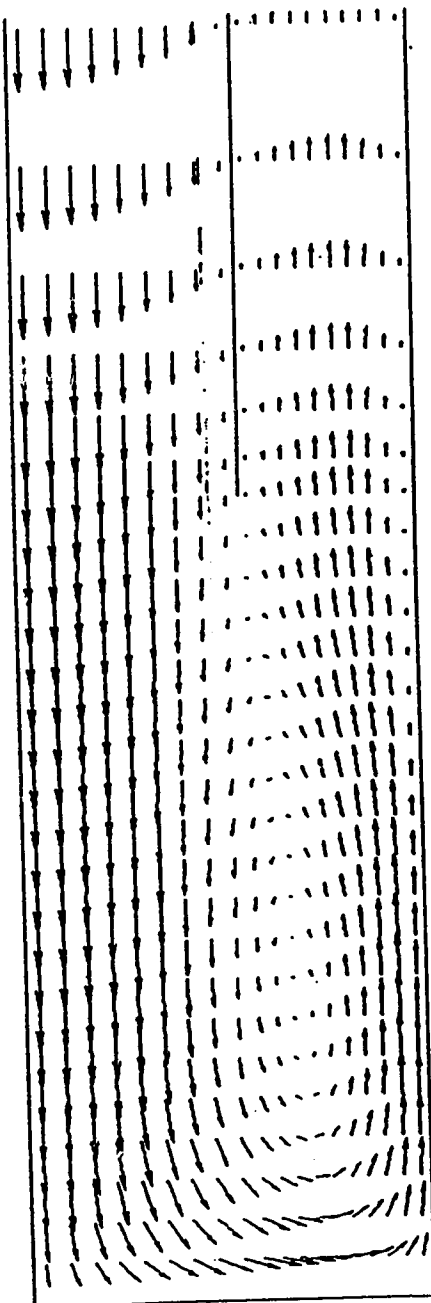
flow behaviour in the end zone. It is evident from the figure that the pressure drop is controlled by the smaller of F_i and F_a .

Experimental points (1) and (2) are above the numerical data, but point (1) is for a Reynolds number of 689, and point (2) is for a clearance ratio of 0.789 ; these parametric deviations result in higher pressure drops of 24% and 10%, respectively. Thus the corrected Euler numbers for points (1) and (2) are within the experimental error of 10%. The deviations are large at higher area ratios. As will be discussed later, the flow at higher area ratios is three dimensional. The numerical solution for three dimensional flow not being tested for uniqueness, allows that more than one velocity field may occur for the same conditions at higher area ratios.

The velocity field for $F_i/F_a = 0.2$ is plotted in Figure 4.7 and for $F_i/F_a = 1.5$ in Figures 4.8 and 4.9. For $F_i/F_a = 0.2$, the ring vortex again exists in the clearance space. In addition, a weak secondary vortex exists on the outer tube. These vortices account for greater pressure drop at this area ratio. At even lower area ratios, the flow within the secondary vortex becomes more vigorous. This offers more resistance, resulting in higher pressure drops. For area ratios increased above 0.2, the secondary vortex diminishes and at $F_i/F_a \approx 0.47$, it vanishes completely resulting in a minimum, with a single ring vortex in the clearance space. For area ratios greater than the minimum, fluid starts

$Re = 1000$
 $L/D = 20$
 $H/D = 1$

$u=71.6$

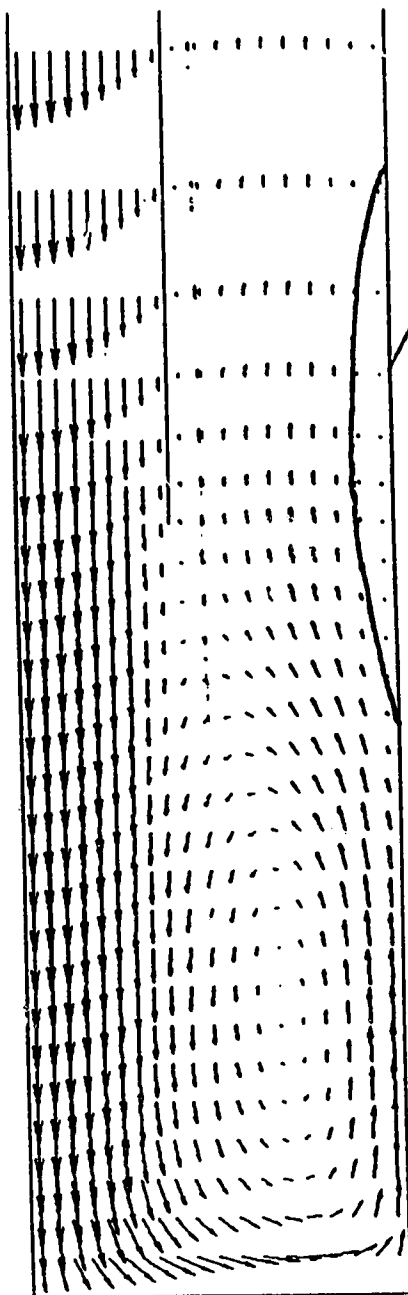


$F_i/F_a = 0.47$

$Re = 1020$
 $L/D = 20.8$
 $H/D = 1$

59

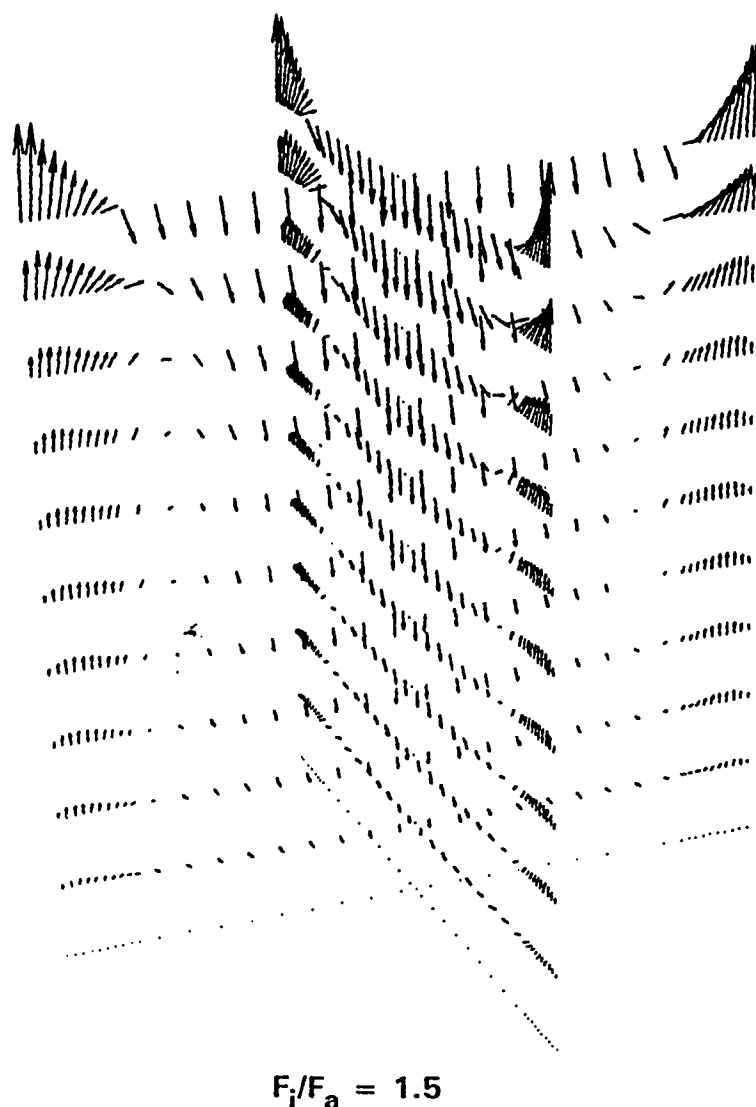
secondary vortex



$F_i/F_a = 0.2$

FIGURE 4.7 VELOCITY PROFILE FOR $F_i/F_a = 0.47$ AND 0.2

$Re = 1020$
 $L/D = 20.8$
 $H/D = 1$



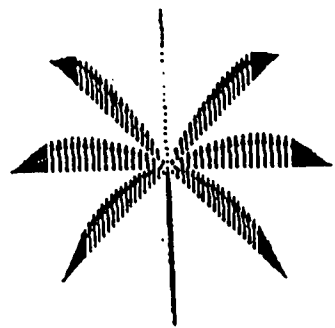
$F_i/F_a = 1.5$

**FIGURE 4.8 VELOCITY PROFILE IN THREE DIMENSIONS
FOR $F_i/F_a = 1.5$**

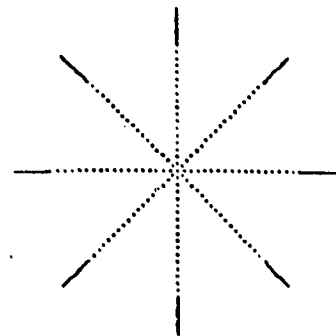
$Re = 1020$

$L/D = 20$

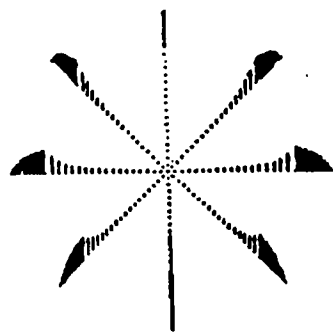
$H/D = 1$



$x' = 0.05 H$

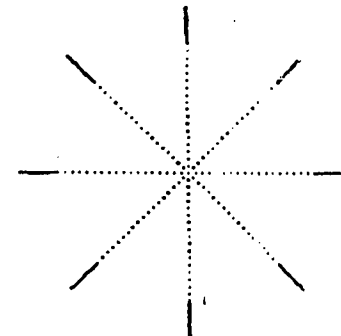


$x' = 0.5 H$



$x' = H$

$F_i/F_a = 1.5$



$x' = 9.9 H$

$x' = 1 - x$

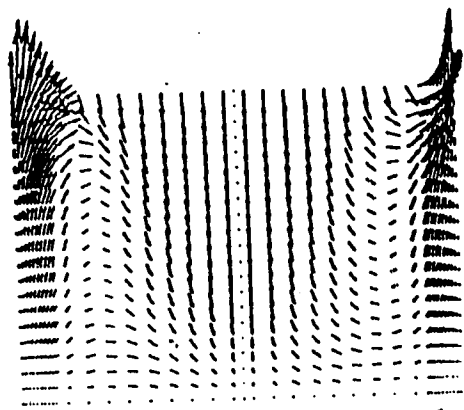
**FIGURE 4.9 VELOCITY PROFILE IN R- θ PLANE
FOR $F_i/F_a = 1.5$**

moving in the circumferential direction; this begins near the sealed end of the outer tube. With increased area ratios , it becomes more predominant near the sealed end and starts appearing in other regions of the tube. This results in a more complex circulation.

For an area ratio of 1.5 (see Figures 4.8 and 4.9), the three dimensional effects are considerable at the bottom. At mid height ($X' = 0.5 H$) in the clearance zone (see Figure 4.9), these effects vanish and the flow is axisymmetric. However, they evolve again at the end of the inner tube ($X' = H$), being more dominant in the annular space and near the inside wall of the inner tube. This suggests that the decreased exit area is responsible for their origin. They gradually die out as the fluid advances upwards. At even higher area ratios, it is expected that the three dimensional effects may extend towards the mouth of the annulus.

A photograph from the visual study conducted by Lock and Wu [15], is shown in Figure 4.10. A comparative velocity field from this study for the same conditions, confirms the three dimensional effects, but only qualitatively; at least, they are clearly not axisymmetric.

$Re = 100$
 $L/D = 20$
 $H/D = 0.5$



$F_i/F_a = 2.26$

**FIGURE 4.10 VELOCITY PROFILE IN X-R PLANE
FOR $F_i/F_a = 2.26$**

4.5 Effect of Clearance Ratio

The effect of clearance ratio on the Euler number is shown in Figure 4.11. A comparison with experimental data indicates deviations at experimental points (2) and (4). At point (2), the deviation is 7%, which is within the range of the experimental error of 10%. For point (4), the deviation is 16%, which is slightly more than the experimental error. As will be seen later, at $H/D = 2$, a ring vortex extends from the mouth of the inner tube to the sealed end of the outer tube. The vortex being attached to the inner tube mouth at one end, a change in vortex pattern with wall thickness is possible. This study neglecting the inner tube length, a slightly lower Euler number at $H/D = 2$ is possible.

For very small clearances, that is $H/D < 0.1$, the effect of reducing H/D is to produce a high pressure gradient. This is due to two factors : the reduced clearance space and a flow separation phenomenon, as explained later. For $H/D > 1$, the pressure drop is nearly constant, as expected. For $0.1 < H/D < 1$, two extrema are observed, representing a minimum and a maximum which occur at $H/D \approx 0.2$ and 0.4 , respectively.

Velocity fields for $H/D = 0.2, 0.4, 0.8$ and 2.0 are plotted in Figures 4.12 to 4.15, respectively. At $H/D = 0.2$, a ring of separation is observed on the outside of inner tube. Also a small secondary vortex is observed in the

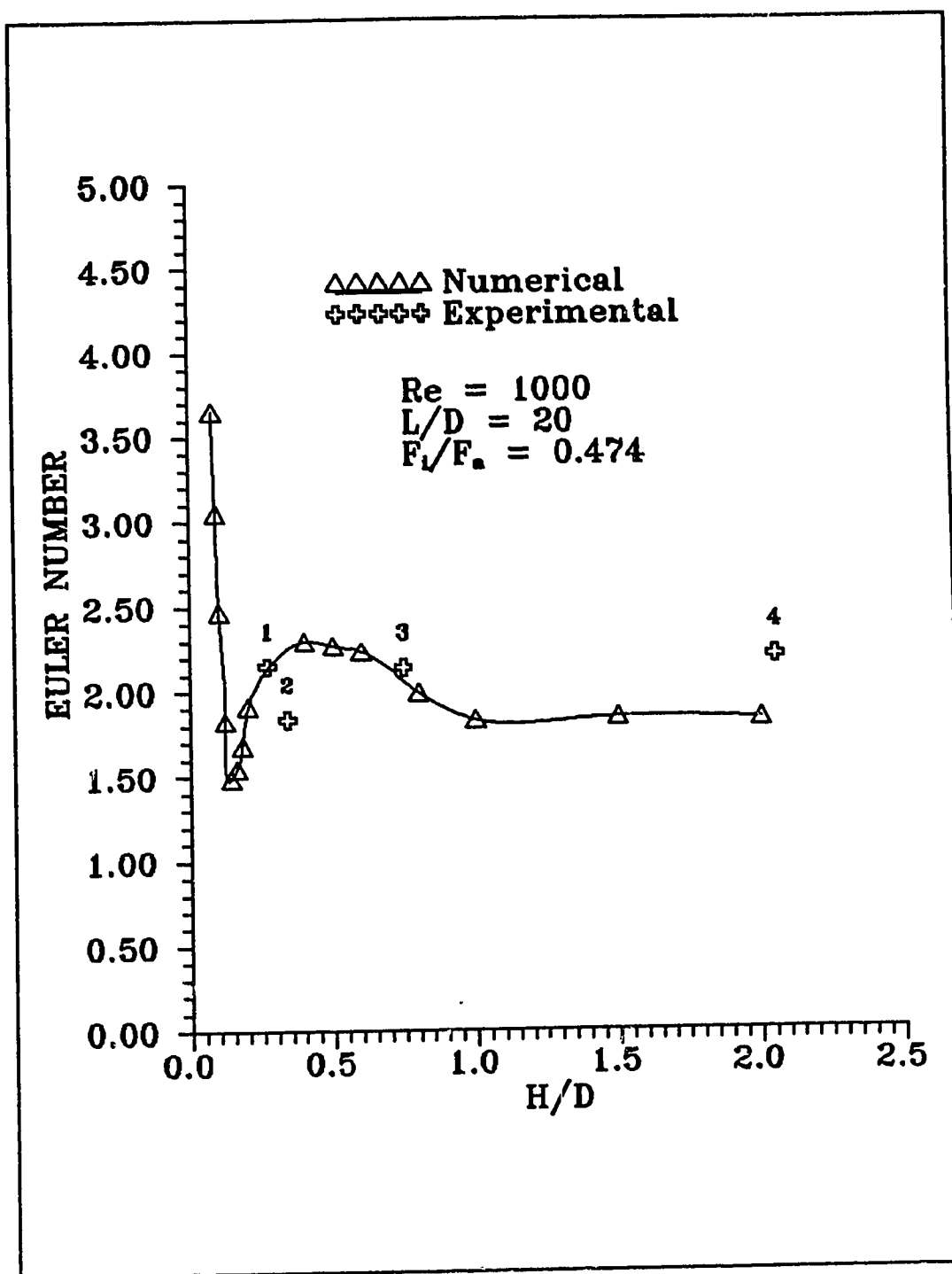
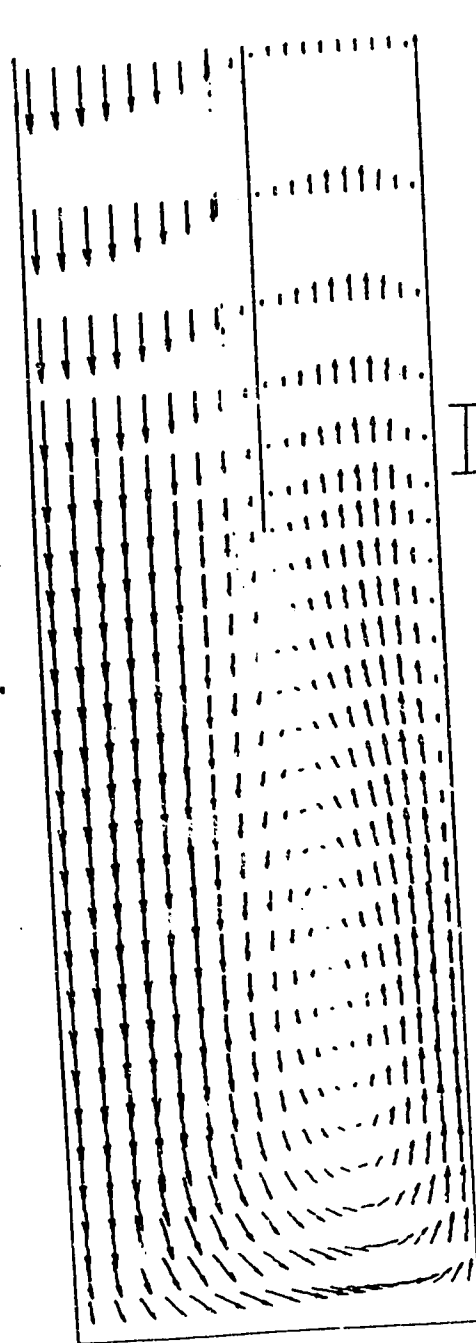


FIGURE 4.11 EFFECT OF CLEARANCE RATIO
ON EULER NUMBER

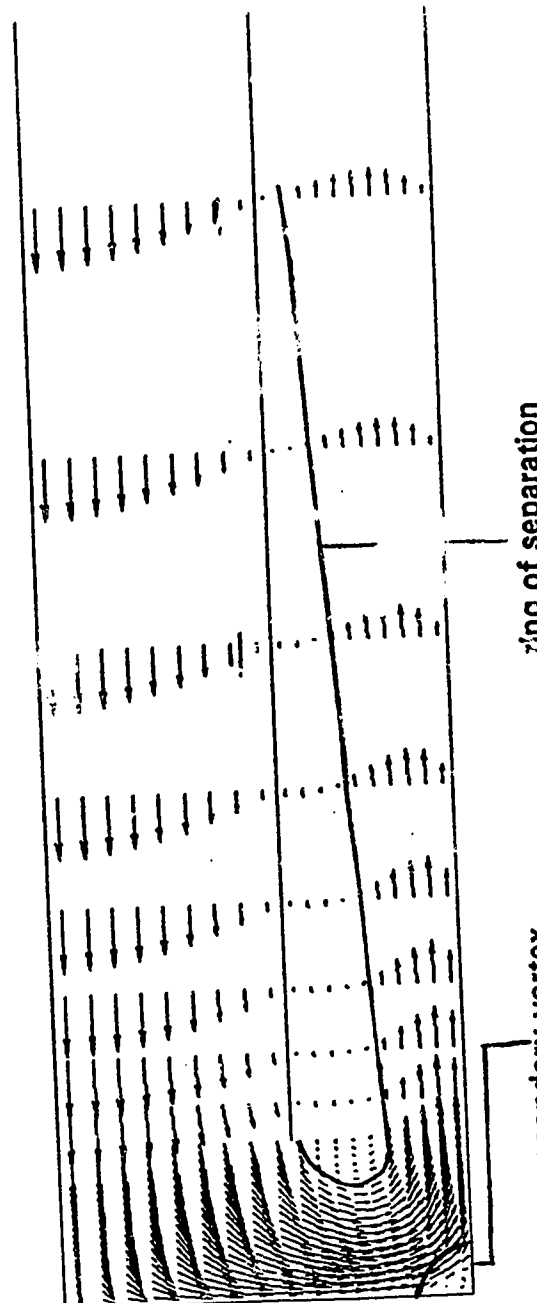
$Re = 1000$
 $L/D = 20$
 $F_i/F_a = 0.47$

$Re = 1000$
 $L/D = 20$
 $F_i/F_a = 0.474$

66



$H/D = 1$



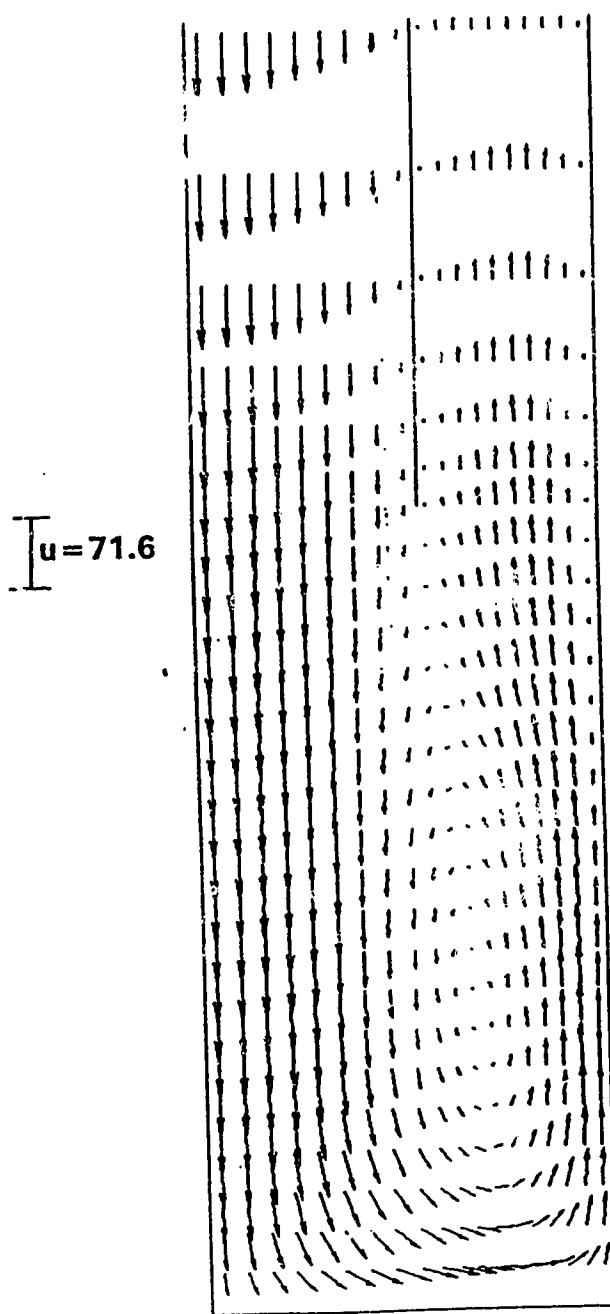
$H/D = 0.2$

FIGURE 4.12 VELOCITY PROFILE FOR $H/D = 1.0$ AND 0.2

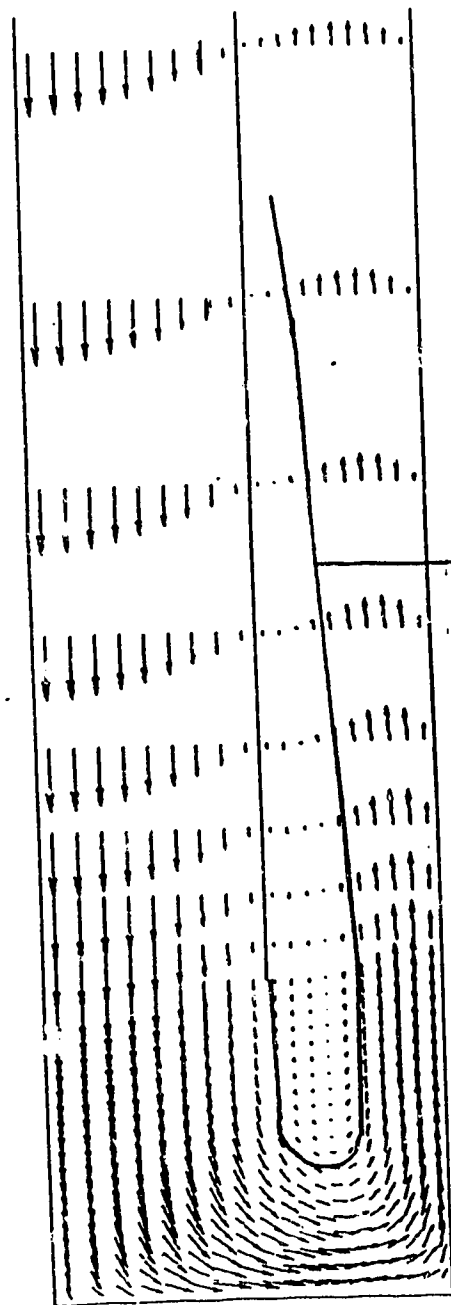
$Re = 1000$
 $L/D = 20$
 $F_i/F_a = 0.47$

$Re = 1000$
 $L/D = 20$
 $F_i/F_a = 0.474$

67



$H/D = 1$



$H/D = 0.4$

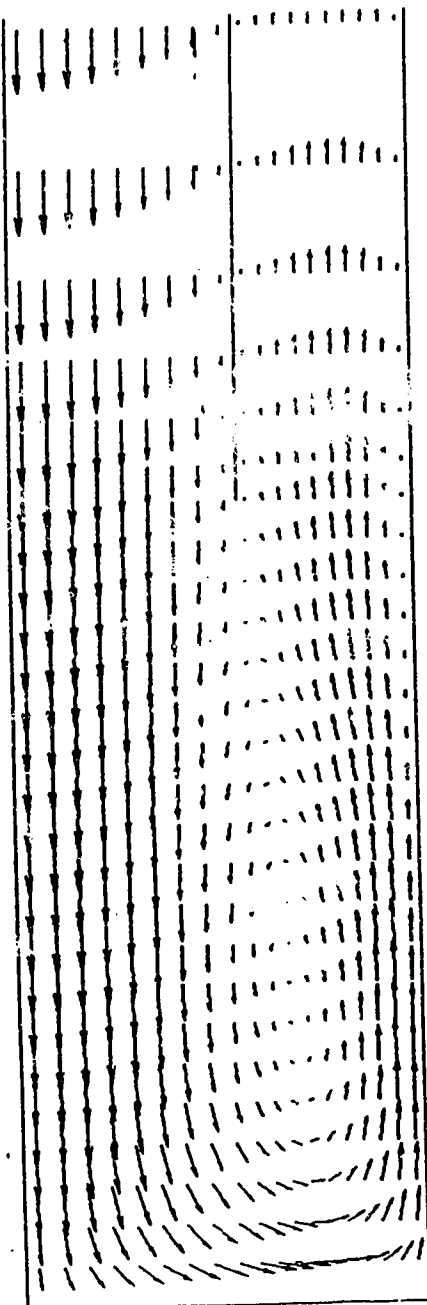
FIGURE 4.13 VELOCITY PROFILE FOR $H/D = 1.0$ AND 0.4

$Re = 1000$
 $L/D = 20$
 $F_i/F_a = 0.47$

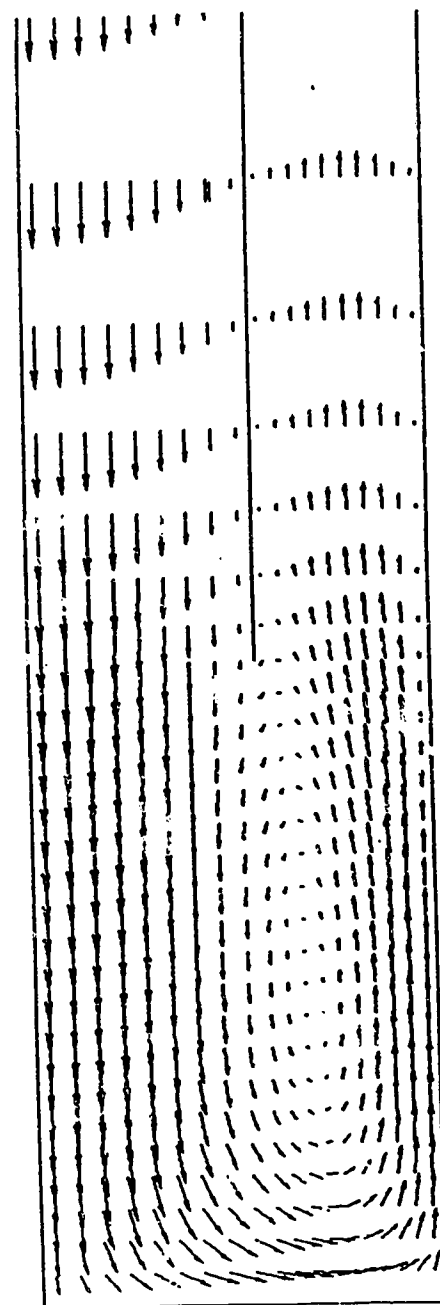
$Re = 1000$
 $L/D = 20$
 $F_i/F_a = 0.474$

68

$u = 71.6$



$H/D = 1.0$



$H/D = 0.8$

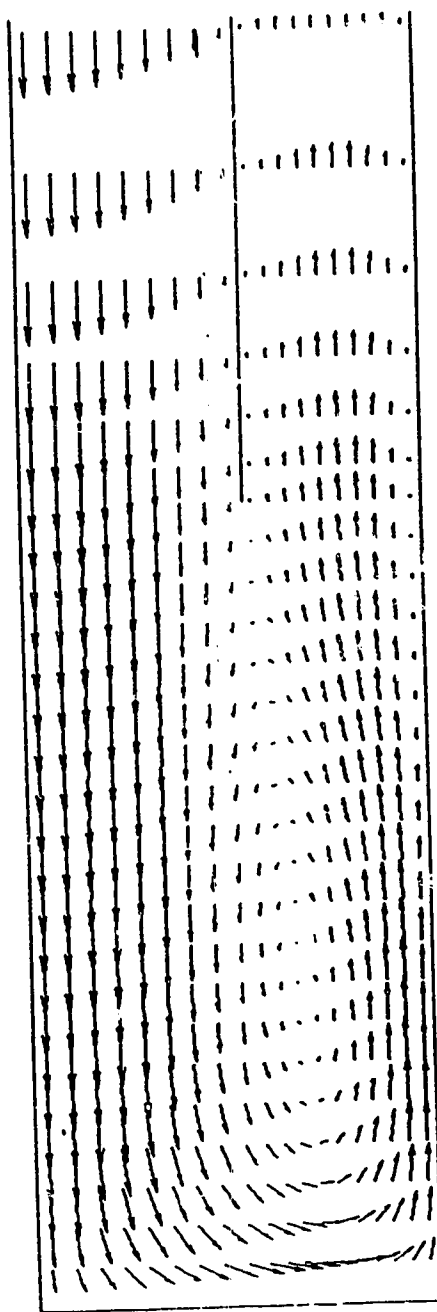
FIGURE 4.14 VELOCITY PROFILE FOR $H/D = 1.0$ AND 0.8

$Re = 1000$
 $L/D = 20$
 $F_i/F_a = 0.47$

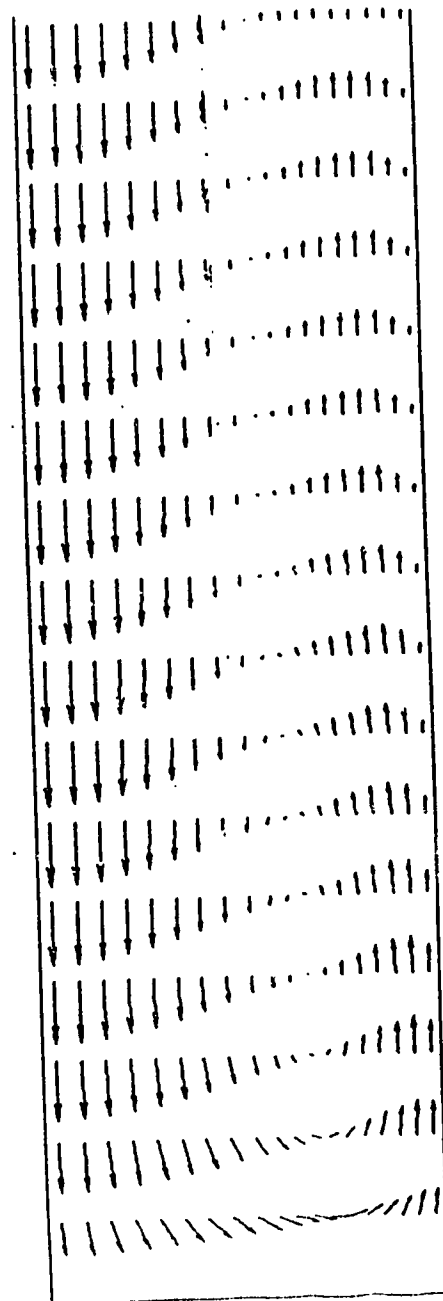
$Re = 1000$
 $L/D = 20$
 $F_i/F_a = 0.474$

69

$u=71.6$



$H/D = 1$

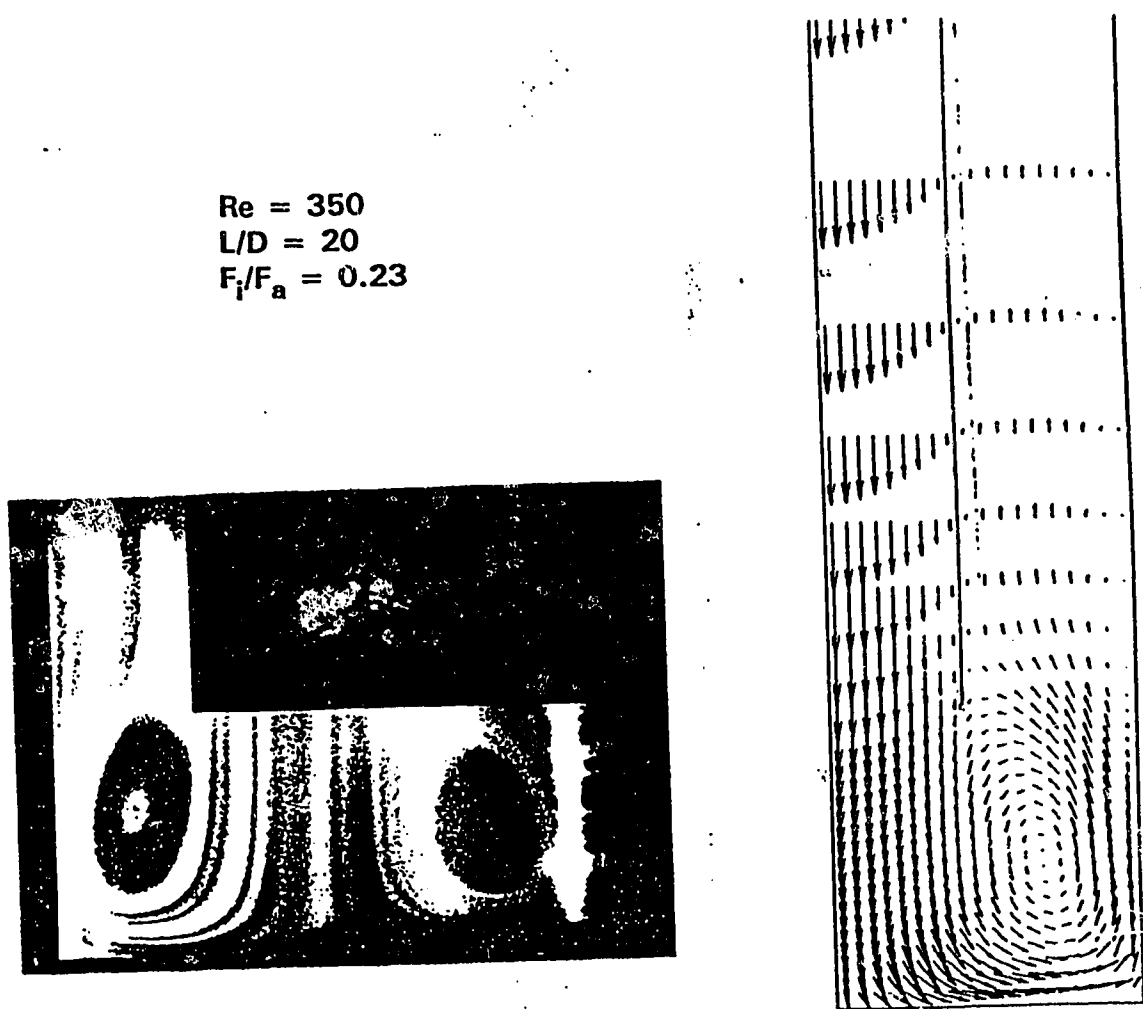


$H/D = 2$

FIGURE 4.15 VELOCITY PROFILE FOR $H/D = 1.0$
AND 2.0

bottom right hand corner. The fluid motion within this vortex is clockwise. For clearance ratios less than the minimum, corresponding to $H/D \approx 0.2$ in the figure, the secondary corner vortex becomes even bigger with a further decrease in the clearance ratio. This, along with the ring of separation accounts for a higher pressure drop at lower H/D . At $H/D = 0.2$, the secondary corner vortex has nearly collapsed thus accounting for the minimum. For clearance ratios between 0.2 and 0.4, the ring of separation grows further accounting for greater pressure drops. At $H/D = 0.4$, corresponding to the maximum in Figure 4.13, the ring of separation is noted again. The small corner vortex no longer exists. At $H/D = 0.8$, near the inflection point in Figure 4.11, the ring of separation is seen evolving into a torodial vortex. This suggests that for H/D values between 0.4 and 1.0, the ring growth into a full fledged vortex accounts for decreasing pressure drops with increased H/D . For $H/D = 1.0$ (the reference condition), a full fledged vortex is observed at the mouth of the inner tube. For $H/D = 2.0$, the same pattern exists, except that the vortex is more elongated, resulting in an Euler number value nearly the same as for $H/D = 1$.

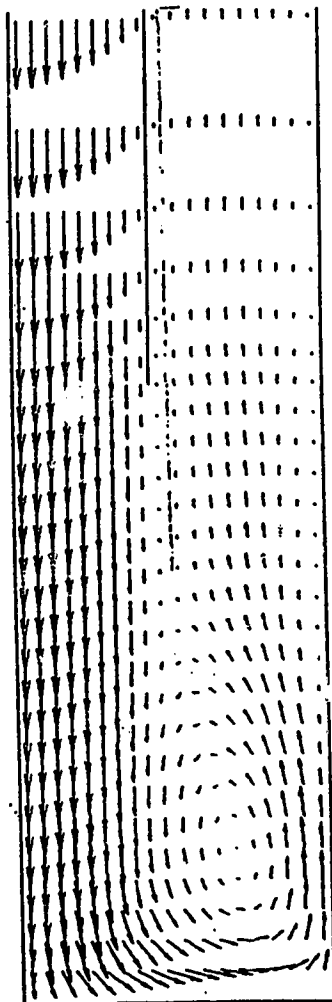
Velocity profiles from this study are compared with the photographs of Lock and Wu [15] (see Figures 4.16 and 4.17). The flow patterns are very similar.



$H/D = 0.5$

FIGURE 4.16 VELOCITY PROFILE FOR $H/D = 0.5$

$Re = 350$
 $L/D = 20$
 $F_i/F_a = 0.23$



$H/D = 1$

FIGURE 4.17 VELOCITY PROFILE FOR $H/D = 1.0$

Chapter 5

Frictional Characteristics

With Annular Admission

5.1 Introduction

In annular admission the fluid enters at the top of the annulus between the inner and the outer tube. Since, the flow direction is now reversed, a change in the flow pattern, especially in the vicinity of the clearance zone, is expected. This will bring changes in the frictional characteristics. In this chapter the parametric influence on the pressure drop for a 'Reverse Flow' is studied. Data is plotted separately with Reynolds number, length-diameter ratio, flow

area ratio and the clearance ratio as the independent variables ; the Euler number remains the dependent variable (see Figures 5.1, 5.2, 5.3 and 5.5). The definitions for the dependent and the independent variables are the same as in the previous chapter. The inlet velocity profile is fully developed (parabolic). Data for central fluid admission is also plotted for comparative purpose.

5.2 Effect of Reynolds number

The Euler number again decreases with an increase in the Reynolds number, as shown in Figure 5.1. The Euler number values are evidently greater than those observed for central admission. The curve is also less steep. However, this change in pressure drop is not unexpected. For example, F_i/F_a of 0.474 implies an entrance area 2.1 times the exit area. As seen in the previous section, the fluid entrance area plays an important role in determining the pressure loss. Therefore, for annular admission, F_i/F_a of 0.474 corresponds to an area ratio of about 2.1 in central admission. The curve for central admission reflects a three dimensional flow with a higher pressure drop for this condition.

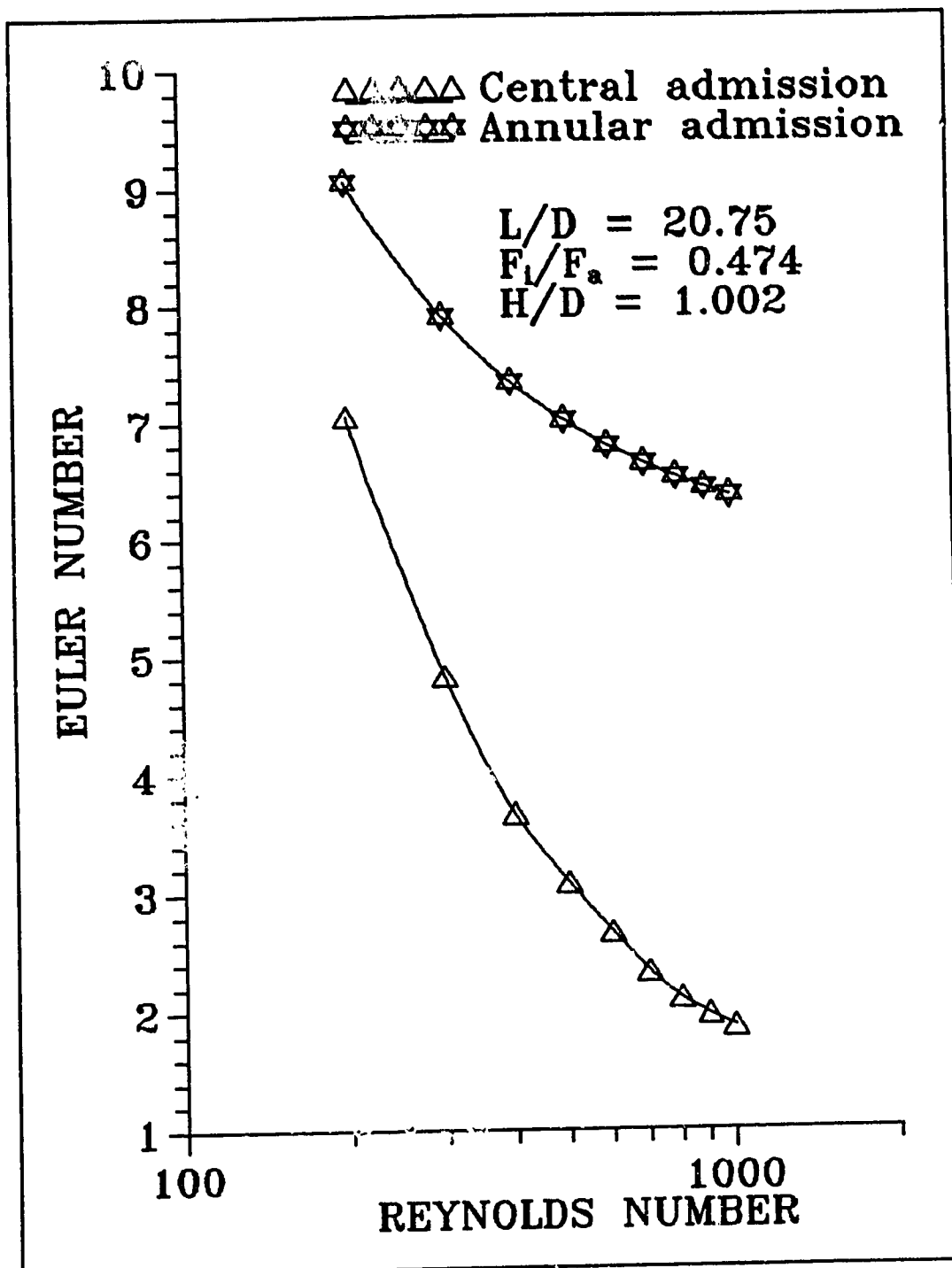


FIGURE 5.1 EFFECT OF REYNOLDS NUMBER
ON EULER NUMBER

5.3 Effect of length-diameter ratio

The effect of length-diameter ratio, L/D, on Euler number is shown in Figure 5.2. As expected, the Euler number increases with L/D. The Euler number for annular admission is greater than for the central admission for reasons explained in the previous section. However a higher slope for annular admission was not expected. In fact, the same slope as for central admission might be expected. But this explanation does not take into consideration the changes in the end clearance zone flow pattern introduced by reversed flow direction. More on the end clearance flow pattern will be discussed in the following sections, when velocity profiles are plotted. Evidently, the higher slope for annular admission suggests that the already three dimensional flow pattern becomes more disorderly at higher L/D.

5.4 Effect of area ratio

The results for the effect of the area ratio on the Euler number are plotted in Figure 5.3. The general trend is same as for central admission. However, now the minimum occurs at $F_i/F_a \approx 0.8$, in contrast to the central admission, where it occurs at $F_i/F_a \approx 0.47$; $0.8 \neq 1/0.47$.

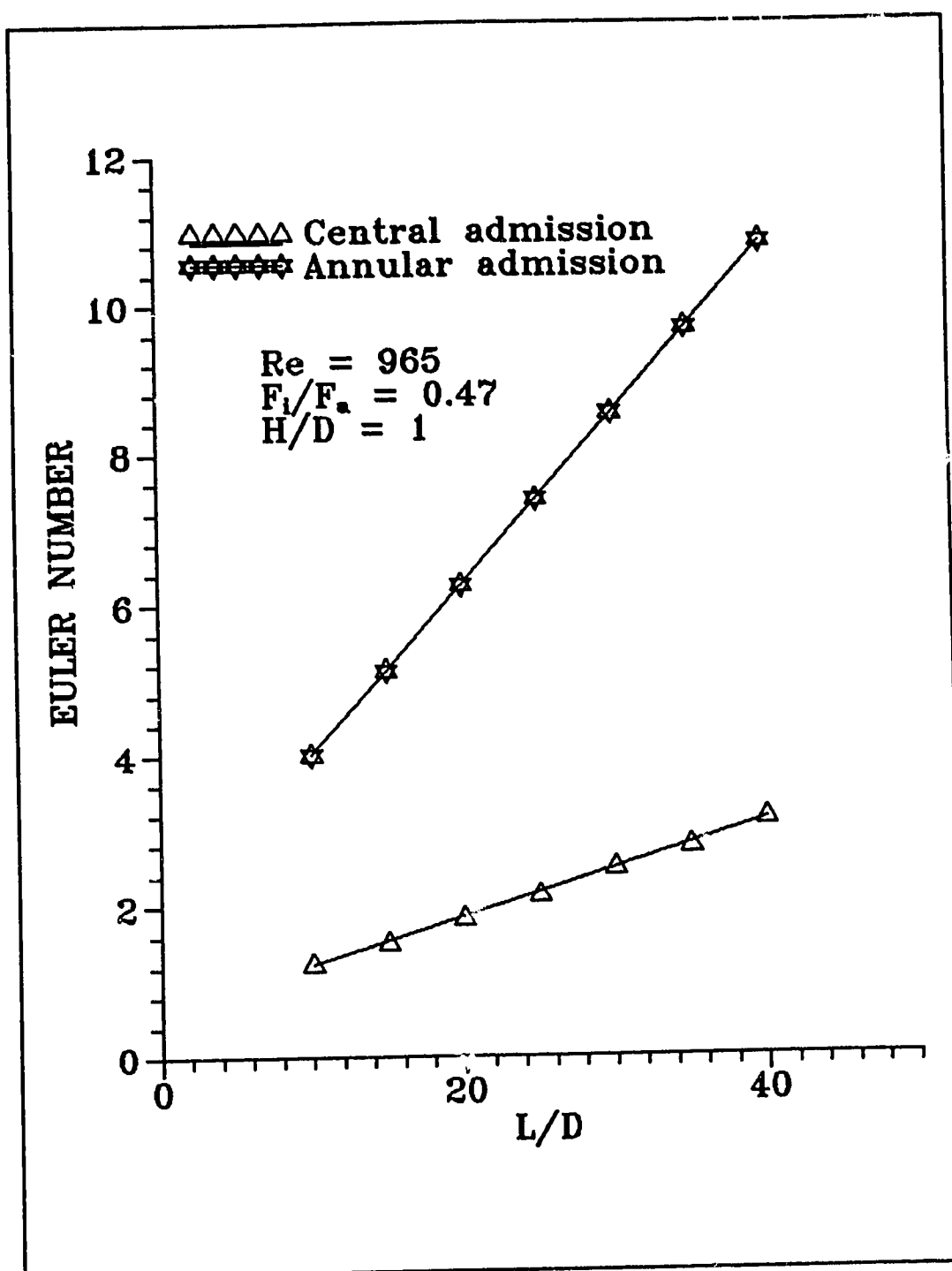


FIGURE 5.2 EFFECT OF LENGTH-DIAMETER RATIO
ON EULER NUMBER

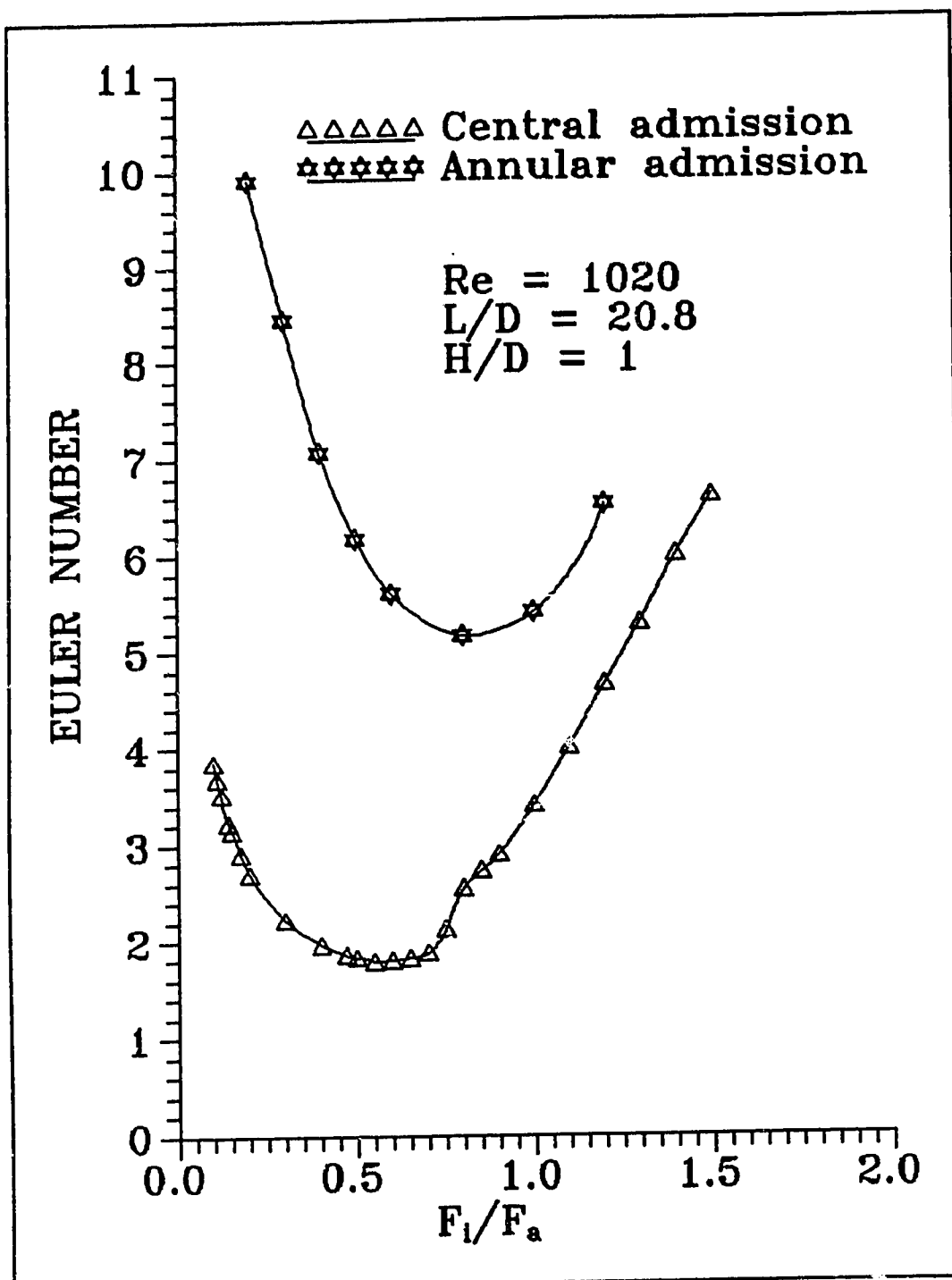


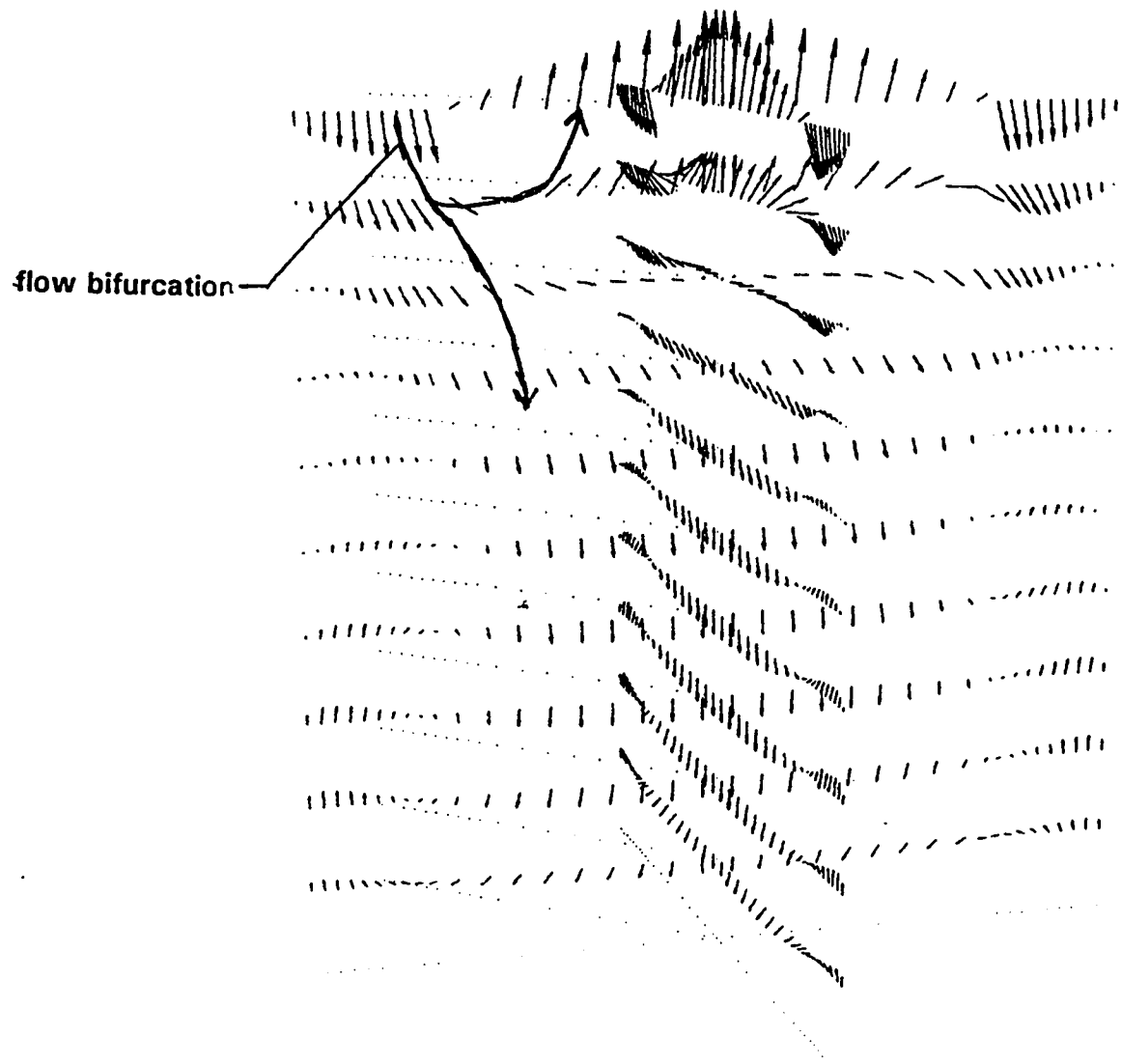
FIGURE 5.3 EFFECT OF AREA RATIO
ON EULER NUMBER

The trend of the curve is not unexpected. Starting from the highest F_i/F_a value on the curve, a decrease in the area ratio, implying an increase in the entrance area, results in a decreased pressure drop. This is expected, considering the slope of the curve for the central admission which shows that an increase in the entrance area would result in an increasing Euler number in the same region. After reaching a minimum, a slope upwards is also expected. However, it was expected that the minimum would occur at the same point as for central admission. To investigate this difference, the flow field for $F_i/F_i = 0.8$ is plotted in Figure 5.4. The figure reveals a complex three dimensional pattern in the clearance space. Its implication is not very clear to the author. It appears that the fluid bifurcates after entering the clearance space. While one stream of the fluid leaves through the inner tube, the other forms into a vortex which resolves into a complex three dimensional pattern accounting for higher frictional losses.

5.5 Effect of clearance ratio

The effect of clearance ratio is shown in Figure 5.5. For H/D values less than those plotted, converged solutions could not be obtained; these are of little practical value. The flow may be turbulent at these clearance ratios. In contrast to the central admission, the flow field is already three dimensional and a decrease in the clearance area further complicates the process.

$Re = 1020$
 $L/D = 20.8$
 $H/D = 1$



$$F_i/F_a = 0.8$$

FIGURE 5.4 VELOCITY PROFILE FOR $F_i/F_a = 0.8$

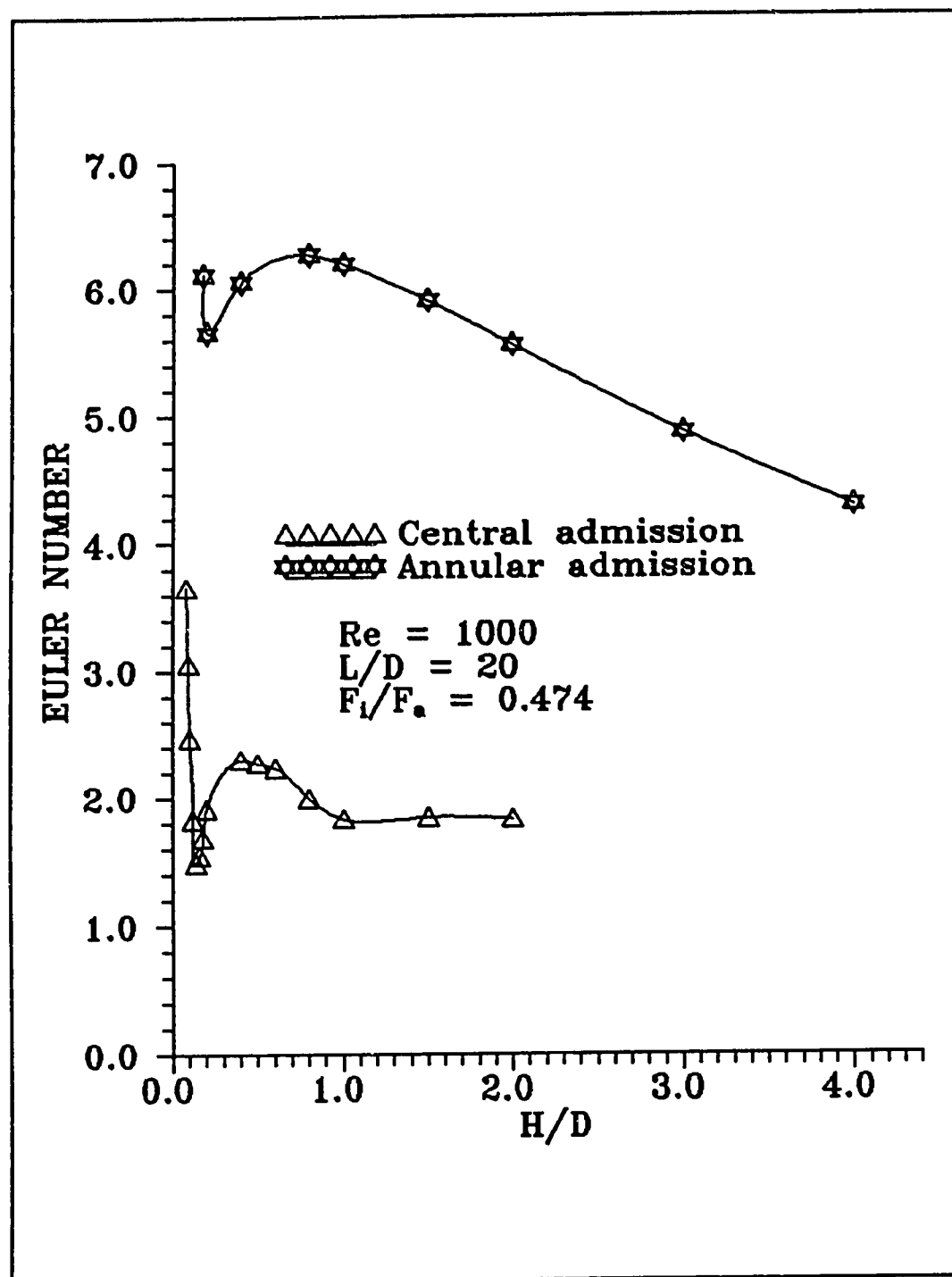


FIGURE 5.5 EFFECT OF CLEARANCE RATIO
ON EULER NUMBER

The velocity fields for H/D ratios of 0.2, 0.8 and 3.0 are plotted in Figures 5.6 to 5.8, respectively. A complicated three dimensional pattern accounting for higher dissipation is evident for H/D values of 0.2 and 0.8. As observed in the previous section, the fluid bifurcates after entering the clearance space. The vortical action is greater for H/D = 0.8, and this may account for greater frictional losses at H/D = 0.8. At H/D = 3.0, Figure 5.8 indicates that three dimensional effects are less pronounced. Hence the drop in the curve with further increase in H/D is not unexpected.

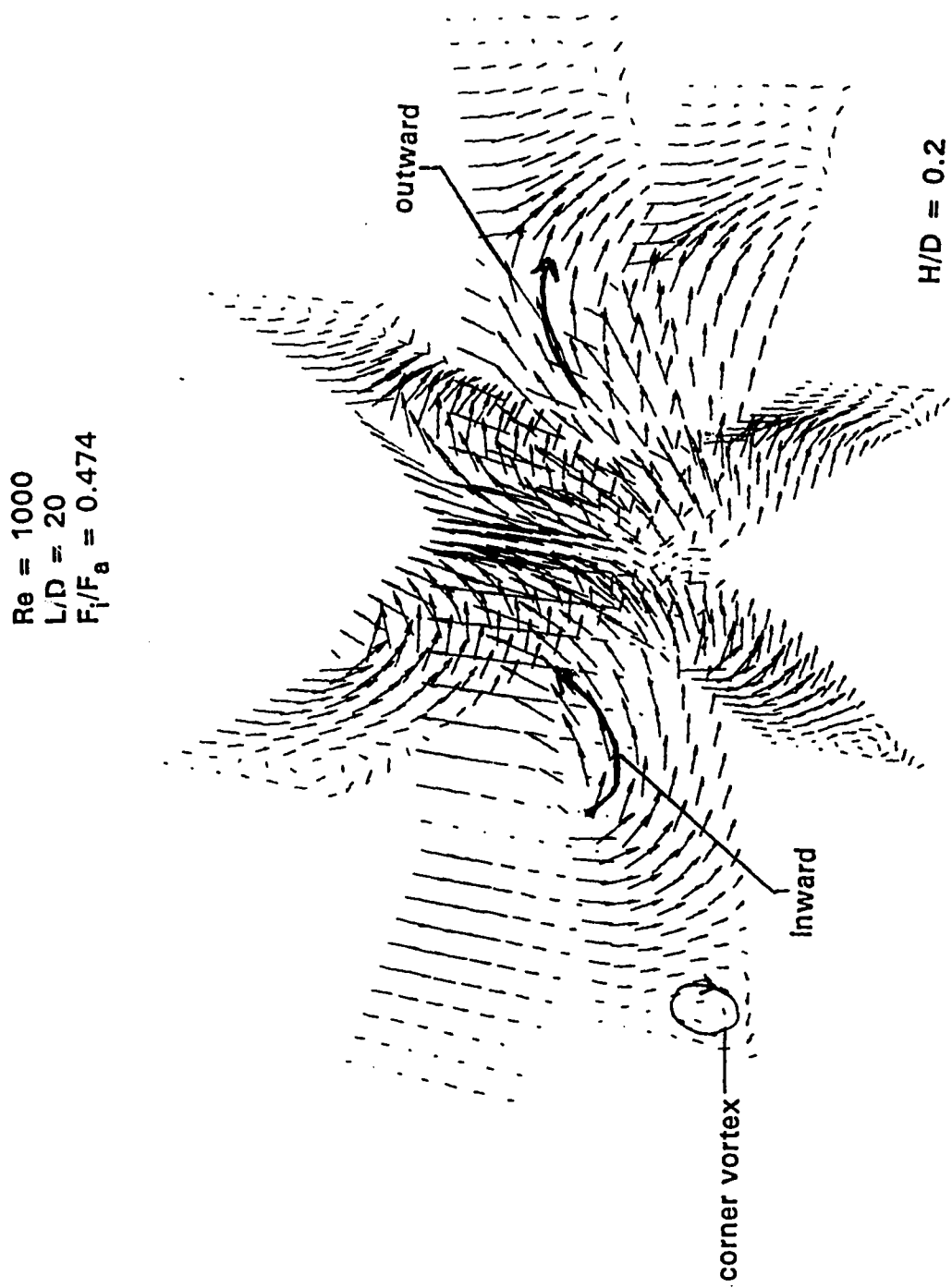


FIGURE 5.6 VELOCITY PROFILE FOR $H/D = 0.2$

$Re = 1000$
 $L/D = 20$
 $F_i/F_a = 0.474$

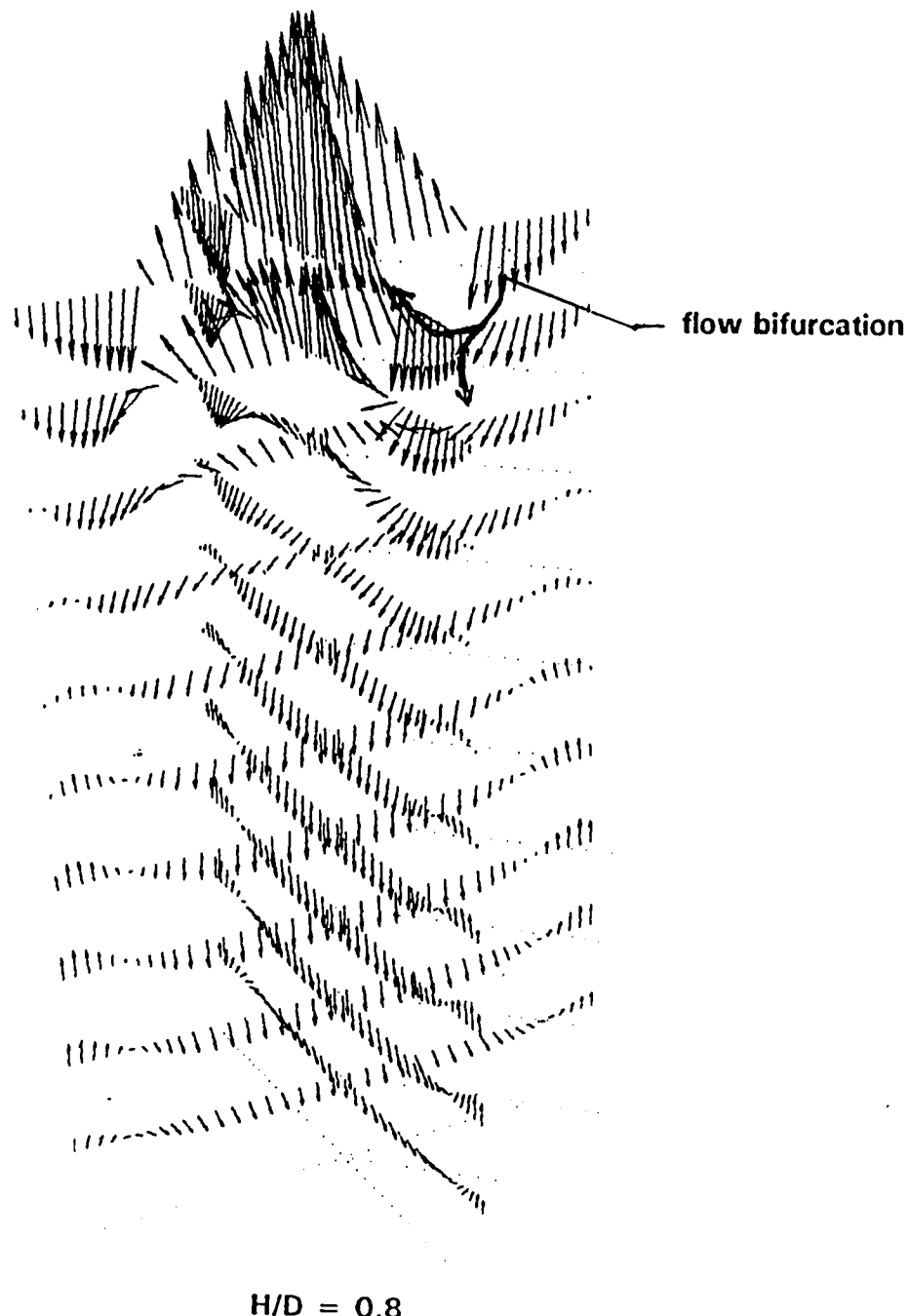
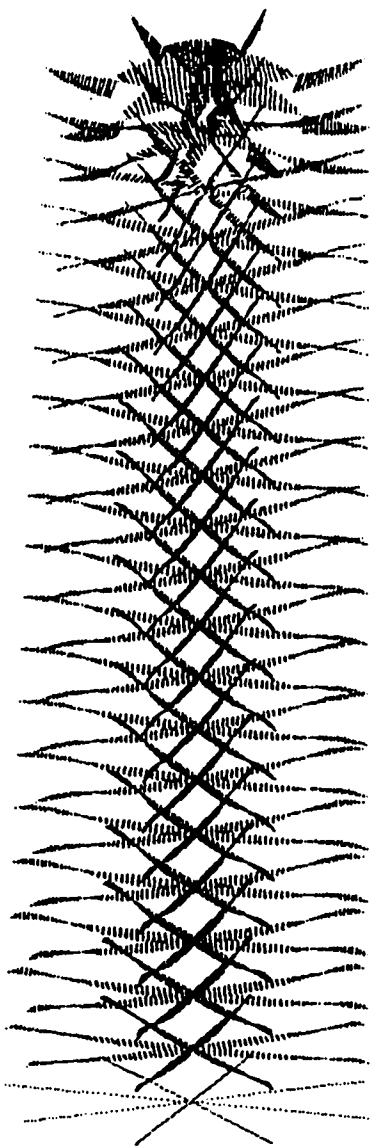


FIGURE 5.7 VELOCITY PROFILE FOR $H/D = 0.8$

$Re = 1000$
 $L/D = 20$
 $F_i/F_a = 0.474$

85



$H/D = 3$

FIGURE 5.8 VELOCITY PROFILE FOR $H/D = 3$

Chapter 6

Conclusions and Recommendations

The results of a numerical study of the frictional characteristics of a bayonet tube under steady laminar conditions have been presented. Data have been obtained with a cylindrical end geometry and a constant property fluid. The results are plotted with Reynolds number, Re, length-diameter ratio, L/D, area ratio, F_i/F_a , and clearance ratio H/D as the independent variables and Euler number, Eu, as the dependent variable. Two fluid entrance conditions are considered : fluid entry at the centre of the inner tube and at the annulus between the inner and the outer tube.

For central admission, the effects of Reynolds number and length-diameter ratio were as expected. The Euler number decreased with Re and

increased with L/D. A characteristic minimum was noted in the effect of area ratio at values lower than expected. An examination of the flow pattern revealed a ring vortex in the clearance zone accounting for a low pressure drop. For area ratios less than the minimum the existence of a secondary vortex along with the primary vortex accounted for higher pressure drops. For F_i/F_a values greater than the minimum, three dimensional effects resulted in higher frictional losses. Varying H/D created a secondary corner vortex accounting for higher pressure drops at low values. A diminishing secondary vortex along with a ring of separation corresponded to the minimum in the curve; a ring of separation alone corresponds to the maximum. An asymptotic value of E_u , yielded a stable ring vortex.

For annular admission, comparatively higher values for Euler number were attributed to higher entrance areas. The effect of Reynolds number and L/D ratio were qualitatively similar to those observed for central admission. A different flow pattern in the end clearance zone accounted for a minimum value of F_i/F_a greater than expected. A more organised flow accounted for lower pressure losses at higher H/D.

As a result of this study, the following recommendations for future work are made :

1. At high velocities the flow may not be laminar. The turbulent behaviour of the fluid is worth exploring.
2. During start-up, shutdown and upset conditions, the flow in the tube becomes transient. In the process industries this affects the flow downstream. A study of flow behaviour under unsteady conditions is recommended.
3. This study is for a cylindrical end geometry of the tube. Since the flow pattern in the end zone plays an important role in determining the overall pressure drop, a study of other end geometries is desirable.
4. Deviation of the numerical solutions from experimental results at higher area ratios suggests that more than one flow pattern may exist. A study of other solutions is desirable.
5. Variable fluid properties may affect the flow pattern, resulting in different frictional characteristics. A study of flow with variable fluid properties is required.
6. Since the bayonet tube is a heat exchanger, a study of the heat transfer characteristics of the tube is required. This, coupled with the pressure drop results of this study, can be used to construct an optimal tube design.

References

- [1] BAUM, A.J. (1978). Optimum Design of a bayonet tube heat exchanger. Proc. 6 th Int. Heat Transf. Conf., Toronto, 4, 285-9
- [2] HURD, N.L. (1946). Mean temperature difference in field or bayonet tube. Ind. Eng. Chem., 38 (12), 1266-71
- [3] FRAAS, A.P. (1973). A potassium-steam binary vapour cycle for better fuel economy and reduced thermal pollution. J. Eng. Power, 95, 53-63
- [4] ZHANG, Y.M. and ZHANG, H.Q. (1988). Experimental investigation of flow characteristics about tip heat transfer in bayonet tube (in Chinese) Huagong Jixie, 15(2), 96-102
- [5] HINCHEY, P. (1984). Key aspects of the design and specification of individual items of plant. In Heat Exchanger Design Handbook, vol. 3, pp. 3.16.2-1 - 3.16.2-15 (ed. by B.A. Bolding and M. Prescott), Hemisphere Publishing Co., Washington, D.C.

- [6] LUU, M. and GRANT, K.W. (1985). Thermal and fluid design of a bayonet tube heat exchanger for high-temperature waste heat recovery. In Ind. Heat Exchangers, pp 159-73 (ed. A.J. HAYES, W.W. WANG, S.C.RICHLEN and E.S.TABB).
- [7] FUKUSAKO, S., SEKI, N., and YAMADA, M. (1987). Heat removal characteristics of a combined system of concentric-tube thermosyphon and heat pump. JSME Int. J., 30 (264), 936-44.
- [8] JAHNS, H.O., MILLER, T.W., POWER, L.D., RICKEY, W.P., TAYLOR, T.P., and WHEELER, J.A. (1973). Permafrost protection for pipelines on permafrost, 2 nd Int. Conf. on Permafrost, pp. 673-84. National Academy Press, Washington.
- [9] LOCK, G.S.H. (1986). Control of spring run-off in northern rivers: the ice veil concept. Polar Rec. 23 (145), 451-7
- [10] COOPER, I.S. (1967). Cryogenic surgery. In Engineering in the practice of medicine, Ch. 12 pp. 122-41 (ed. B.L. Segal and D.G. Kilpatrick), Williams and Wilkins, Baltimore
- [11] HAYNES, F.D. and ZARLING, J.P. (1982). A comparative study of thermosyphon used for freezing soil. ASME Paper # 82-WA/HT-40.

- [12] LOCK, G.S.H. and KIRCHNER, J.D. (1988). Performance of an air filled, open thermosyphon tube with particular reference to wind augmentation. *Int. J. Heat Mass Transfer*, 31 (11), 2357-64
- [13] LOCK, G.S.H. and KIRCHNER, J.D. (1990). Wind augmented heat transfer in an open thermosyphon tube with large length-diameter ratios. *J. Heat Transfer*, 112 (1), 71-7
- [14] YANG, S.L. and HSIEH, C.K. (1988). Fluid flow and heat transfer in a single pass, return-flow, bayonet heat exchanger. *Proc. ASME. AIChE. Nat. Heat Transfer Conf.*, Houston, 3., 355-64
- [15] LOCK, G.S.H. and WU, M. (1991). Laminar frictional behaviour of a bayonet tube. *Proc. 3 rd Sym. on Cold Regions Heat Transfer*, Fairbanks, pp 425-40
- [16] LOCK, G.S.H. and WU, M. (1992). Laminar heat transfer in an air filled bayonet tube. *Proc. 11 th Int. Conf. on Offshore Mechanics, and Artic Engineering*, Calgary.
- [17] PATANKAR, S.V., and SPALDING, D.B. (1972). A calculation procedure for heat, mass and momentum transfer in three dimensional parabolic flow. *Int. J. of Heat and Mass Transfer*, Vol. 15, pp 1787-1806

- [18] PATANKAR, S.V. (1980). Numerical heat transfer and fluid flow. Hemisphere Publishing Co., Washington, D.C.
- [19] VAN DOORMAAL, J.P. and RAITHBY, G.D. (1984). Enhancement of the SIMPLE Method for predicting incompressible fluid flows. Numerical Heat Transfer, Vol. 7, pp 147-63
- [20] BARAKAT, H.Z. and CLARK, J.A. (1966). Analytical and experimental study of transient laminar natural convection flows in partially filled containers. Proc. of 3 rd Int. Heat Transf. Conf., Vol. 2, pp 152-62
- [21] RUNCHAL, A.K. (1972). Convergence and accuracy of three finite difference schemes for a two-dimensional conduction and convection problems. Int. J. of Num. Meth. in Engineering, Vol. 4, pp 541-50

Appendix A

Listing of Computer Program

```

C
C-----This program determines the velocity and pressure
C      distribution in a bayonet tube.
C
C-----SYMBOL DEFINITION
C
C      X(I) = i th axial distance
C      R(J) = j th radial distance
C      TH(K) = k th circumferential distance
C      U(I,J,K) = (i,j,k) th node axial velocity
C      V(I,J,K) = (i,j,k) th node radial velocity
C      W(I,J,K) = (i,j,k) th node circumferential velocity
C      P(I,J,K) = (i,j,k) th node pressure
C
C      IMPLICIT REAL (A-H,O-Z)
PARAMETER(ID = 50,JD = 50,LD = 30)
COMMON/VEL/U(ID,JD,LD),V(ID,JD,LD),W(ID,JD,LD),
' P(ID,JD,LD)
COMMON/XINDEX/X(ID),XU(ID),XDIF(ID),XCV(ID)
COMMON/RINDEX/R(JD),RV(JD),RDIF(JD),RCV(JD)
COMMON/TINDEX/TH(JD),TV(JD),TDIF(JD),TCV(JD)
DIMENSION ULB(JD),DXA(JD),TA(JD),RI(JD),RA(JD)
DIMENSION AP(ID,JD,LD),AE(ID,JD,LD),AW(ID,JD,LD),
' AN(ID,JD,LD),AS(ID,JD,LD),AT(ID,JD,LD),AB(ID,JD,LD)
DIMENSION S(ID,JD,LD),DU(ID,JD,LD),DV(ID,JD,LD),
' DWA(ID,JD,LD),Z(ID,JD,LD),PW(ID,JD,LD)
DIMENSION S8(ID,JD),T(ID,JD,LD),S7(ID,JD),Y(ID,JD,LD)
DIMENSION PC(ID,JD,LD),USTR(ID,JD,LD),VSTR(ID,JD,LD),
' WSTR(ID,JD,LD),TE2(ID,JD,LD)
DIMENSION WLB(JD),ALB(JD),PULB(JD),ULB1(JD)
DIMENSION SP(JD),DRA(JD),PR(JD),BT(JD),BTA(JD)
DIMENSION Q(ID,JD,LD,5),PU(ID,JD,LD),PV(ID,JD,LD)
DIMENSION PUA1(JD),PUT1(JD),TE1(JD),PU1(JD)
DIMENSION QF1(ID,JD),QF2(ID,JD),QFA1(ID,JD),QFA2(ID,JD)
DIMENSION QO(JD),SUMR(JD),THETA(JD),SUMX1(JD),SUMRA1(JD)
DIMENSION QQ(ID,JD,LD),PRE(ID,JD,LD)
DIMENSION TT(ID,JD),YY(ID,JD)
DIMENSION SUMX(JD),SUMRA(JD),SUMU(JD),SUMT(JD),PUP1(JD)
DIMENSION PUK(ID,JD,LD),PVK(ID,JD,LD),PWK(ID,JD,LD)
DIMENSION USS(ID,JD),VSS(ID,JD),PSS(ID,JD),EP(JD)
REAL*8 ERRU,ERRV,ERRW,SERR,ERRP
C
C-----Read in and write out the input data

```

C

```

PRINT*, "INLET = ?"
READ*, INLET
PRINT*, "M = ?", "IM = ?", "N = ?", "IN = ?", "KM = ?"
READ*, M, IM, N, IN, KM
PRINT*, "RF = ?"
READ*, RF
PRINT*, "H = ?"
READ*, H
PRINT*, "Fi/Fa = ?", "H/D = ?"
READ*, AR, CL
UT = 0.000001
VT = 0.000001
WT = 0.000001
PT = 0.00001
THC = 44.0/7.0
TOL = 0.0001
PRINT*, "REN = ?"
READ*, REN
PRINT*, "RELAU = ?"
READ*, RELAU
RELAU = RELAU
RELAW = RELAU
NITER = 1000
NP = 2
NPP = 2

OPEN(20,FILE = 'U.DAT',FORM = 'UNFORMATTED')
OPEN(21,FILE = 'V.DAT',FORM = 'UNFORMATTED')
OPEN(22,FILE = 'P.DAT',FORM = 'UNFORMATTED')
READ(20)((USS(I,J),I = 1,M),J = 1,N)
READ(21)((VSS(I,J),I = 1,M),J = 1,N)
READ(22)((PSS(I,J),I = 1,M),J = 1,N)
CLOSE(20)
CLOSE(21)
CLOSE(22)

DO I = 1,M
  DO J = 1,N
    DO K = 1,KM
      U(I,J,K) = USS(I,J)
      V(I,J,K) = VSS(I,J)
      W(I,J,K) = 0.0
      USTR(I,J,K) = 0.0
    END DO
  END DO
END DO

```

```

VSTR(I,J,K) = 0.0
WSTR(I,J,K) = 0.0
P(I,J,K) = PSS(I,J)
PC(I,J,K) = 0.0
END DO
END DO
END DO
IF(INLET.EQ.1)THEN
  DO K=1,KM
    U(2,1,K)=U(2,2,K)
  END DO
ENDIF
C
C          WRITE(6,*)" DATA USED IN THIS RUN ARE:"
C          WRITE(6,*)"M =",M,"N =",N,"KM =",KM,"REYNOLDS NUM =",RENOL
C          WRITE(6,*)"H =",H
C
C-----Calculate annular and inside radius
C
RRY=(1.0+(1.0/AR))**0.5
RII=1.0/RRY
RAA=1.0-RII
C
C          WRITE(6,*)"RII =",RII,"RAA =",RAA
XA=CL/H
XI=1.0-XA
RENOL=REN*(1.0+RRY)
C
C-----Calculate block velocity profile
C
SP(1)=0.0
SR=1/FLOAT(IN-2)
SP(2)=SP(1)+SR/2
DO J=3,IN-1
  SP(J)=SP(J-1)+SR
END DO
SP(IN)=SP(IN-1)+SR/2.0
DO J=1,IN
  ULB(J)=2.0*RENOL*(1.0-SP(J)**2.0)/(4.0*H)
END DO
C
C          WRITE(6,*)"ULB(J),J=1,IN"
C          WRITE(6,5)(ULB(J),J=1,IN)
IF(INLET.EQ.1)THEN
  INM=IN+((N-IN-1)/2.0)
  SUM1=0.0

```

```

DO J=INM,N-1
  IF(J.GT.INM)SUM1 = SUM1 + 1/(FLOAT(N-1-INM))
  EP(J) = SUM1
END DO
DO J=INM,N-1
  ALB(J) = 2.0*RENOL*(1.0-(EP(J))**2.0)/(4.0*H)
END DO
IS = 0
DO J=INM,IN,-1
  ISS = INM+IS
  ALB(J) = ALB(ISS)
  IS = IS + 1
END DO
ENDIF
C
  RENOL1 = RENOL/(4.0*H)
  RENOL = 4.0*H
C
C-----Generate mesh
C
C      Calculate radial grid locations
C
  RV(2) = 0.0
  DR1 = RII/FLOAT(IN-2)
  DO J = 3,IN
    RV(J) = RV(J-1) + DR1
  END DO
  R(1) = 0.0
  DO J = 2,IN-1
    R(J) = 0.5 * (RV(J) + RV(J + 1))
  END DO
  R(IN) = RV(IN)
  DO J = 2,IN
    RDIF(J) = R(J)-R(J-1)
  END DO
  DO J = 2,IN-1
    RCV(J) = RV(J + 1)-RV(J)
  END DO
C
  DR2 = RAA/FLOAT(N-IN-1)
  DO J = IN + 1,N-1
    RV(J) = RV(J-1) + DR2
  END DO
  DO J = IN + 1,N-1

```

```

R(J)=0.5*(RV(J-1)+RV(J))
END DO
R(N)=RV(N-1)
DO J=IN,N
  RDIF(J)=R(J)-R(J-1)
END DO
DO J=IN,N-1
  RCV(J)=RV(J+1)-RV(J)
END DO
C
C   Calculate circumferential grid locations
C
TV(2)=0.0
DT1=1.0/FLOAT(KM-2)
DO K=3,KM
  TV(K)=TV(K-1)+DT1
  WRITE(6,*)"K =",K,"TV(K) =",TV(K)
END DO
TH(1)=0.0
DO K=2,KM-1
  TH(K)=0.5*(TV(K)+TV(K+1))
END DO
TH(KM)=TV(KM)
DO K=2,KM
  TDIF(K)=TH(K)-TH(K-1)
END DO
DO K=2,KM-1
  TCV(K)=TV(K+1)-TV(K)
END DO
C
C   Calculate axial grid locations
C
XU(2)=0.0
DIST=(RF)**(1.0/FLOAT(IM-3))
COUNT=0.0
DIST2=0.0
DO I=1,IM-2
  ISUM=ISUM+1
  DIST1=DIST**COUNT
  WRITE(6,*)"I =",I,"DIST1 =",DIST1
  DIST2=DIST1+DIST2
  COUNT=COUNT+1.0
END DO
DX1=XI/DIST2

```

```

DO J = 3,IM
  XU(J) = XU(J-1) + DX1
  DX1 = DX1 * DIST
END DO
X(1)=0.0
DO J = 2,IM-1
  X(J) = 0.5 * (XU(J) + XU(J+1))
END DO
X(IM) = XU(IM)
DO J = 2,M
  XDIF(J) = X(J)-X(J-1)
END DO
DO J = 2,IM-1
  XCV(J) = XU(J+1)-XU(J)
END DO

```

C

```

DX2 = XA/FLOAT(M-IM-1)
DO J = IM + 1,M-1
  XU(J) = XU(J-1) + DX2
END DO
DO J = IM + 1,M-1
  X(J) = 0.5 * (XU(J-1) + XU(J))
END DO
X(M) = XU(M-1)
DO J = IM,M
  XDIF(J) = X(J)-X(J-1)
END DO
DO J = IM,M-1
  XCV(J) = XU(J+1)-XU(J)
END DO

```

C

C-----Calculate the mass at the inlet

C

```

ULB1(2) = ULB(1)
ULB1(IN) = ULB(IN)
SUMA = 0.0
ISWICH = 0
DO J = 3,IN-1
  PULB(J) = (ULB(J-1) + ULB(J)) * RV(J)/2.0
  IF(ISWICH.EQ.0)THEN
    PULB(J) = 4.0 * PULB(J)
    ISWICH = 1
  ELSE
    PULB(J) = 2.0 * PULB(J)
  END IF
END DO

```

```

      ISWICH=0
      ENDIF
      SUMA = SUMA + PULB(J)
    END DO
    UIN=DR1*(SUMA)*2.0/(3.0*R(IN)**2.0)
    SINN=DR1*(SUMA)/3.0
    SINN2=SINN*2.0*3.14

    DO I=1,M-1
      DO J=1,N-1
        DO K=1,KM-1
          IF(I.EQ.IM)GO TO 115
          IF(J.EQ.IN)GO TO 115
          P(I,J,K)=PSS(I,J)
115      END DO
        END DO
      END DO

      IF(INLET.EQ.0)THEN
        DO J=IN+1,N-1
          DO K=2,KM-1
            P(2,J,K)=0.0
          END DO
        END DO
      ENDIF
      IF(INLET.EQ.1)THEN
        DO J=2,IN-1
          DO K=2,KM-1
            P(2,J,K)=0.0
          END DO
        END DO
      ENDIF

C
C-----Iteration begins here
C
      HH4=4.0*H*H
      ITER=0
555  CONTINUE
      ITER=ITER+1
      WRITE(6,*)"ITERATION NUMBER =",ITER
C
C-----Specify B.C. for U-equation
C
C      Boundary indices are (2,M-1,1,N,1,KM)

```

```

C      Entrance B.C. (u = ULB(J))
C
C      DO K = 2,KM-1
      DO J = 2,IN-1
          AP(2,J,K) = 1.0
          IF(INLET.EQ.0)THEN
              AE(2,J,K) = 0.0
              S(2,J,K) = ULB(J)
          ELSE
              AE(2,J,K) = 1.0
              S(2,J,J) = 0.0
          ENDIF
      END DO
C      Closed end B.C.(u = 0.0)
C
C      DO J = 2,N-1
          AP(M-1,J,K) = 1.0
          AW(M-1,J,K) = 0.0
          S(M-1,J,K) = 0.0
      END DO
C      Centre B.C.(du/dr = 1.0)
C
C      DO I = 3,M-2
          AP(I,1,K) = 1.0
          AN(I,1,K) = 1.0
          S(I,1,K) = 0.0
      END DO
C      Inner tube (inside) b.c.(u = 0.0)
C
C      DO I = 3,IM
          AP(I,IN,K) = 1.0
          AS(I,IN,K) = 0.0
          S(I,IN,K) = 0.0
      END DO
C      Outer tube (inside) B.C.(u = 0.0)
C
C      DO I = 3,M-2
          AP(I,N,K) = 1.0
          AS(I,N,K) = 0.0

```

```

      S(I,N,K)=0.0
      END DO
C
C   Exit B.C.
C
      DO J=IN+1,N-1
        AP(2,J,K)=1.0
        IF(INLET.EQ.0)THEN
          AE(2,J,K)=1.0
          S(2,J,K)=0.0
        ELSE
          AE(2,J,K)=0.0
          S(2,J,K)=ALB(J)
        ENDIF
      END DO
C
C   Inner Tube (outside) B.C.(u=0.0)
C
      DO I=3,IM
        AP(I,IN,K)=1.0
        AN(I,IN,K)=0.0
        S(I,IN,K)=0.0
      END DO
    END DO
C
C   Circumferential B.C.
C
      DO I=3,M-2
        DO J=2,N-1
          AP(I,J,1)=1.0
          AT(I,J,1)=1.0
          S(I,J,1)=0.0
          AP(I,J,KM)=1.0
          AB(I,J,KM)=0.0
          S(I,J,KM)=U(I,J,1)
        END DO
      END DO
C
C----- Calculate coefficients of velocity, U
C
      CALL COEFFU(M,N,KM,RENOL,H,RELAU,DU,AP,AE,AW,AN,AS,AT,AB,S,
      ' IM,IN,THC)
C
C-----Calculate U,using solver TDMA

```

```

C
C     CALL TDMA(AP,AE,AW,AN,AS,AT,AB,S,2,M-1,1,N,1,KM,.FALSE.,NP,UT,
' USTR,RD,M,N,IM,IN,KM,1)
C
C     Specify B.C.for V-equation
C
C     Boundary indices are (1,M,2,N-1,1,KM)
C
C     Entrance B.C.(v = 0.0)
C
DO K=2,KM-1
  DO J=3,IN-1
    AP(1,J,K)=1.0
    IF(INLET.EQ.0)THEN
      AE(1,J,K)=0.0
      S(1,J,K)=0.0
    ELSE
      AE(1,J,K)=1.0
      S(1,J,K)=0.0
    ENDIF
  END DO
C
C     Closed end b.c.(v = 0.0)
C
DO J=3,N-2
  AP(M,J,K)=1.0
  AW(M,J,K)=0.0
  S(M,J,K)=0.0
END DO
C
C     Centre B.C.(dv/dr = 0.0)
C
DO I=2,M-1
  AP(I,2,K)=1.0
  AN(I,2,K)=0.0
  S(I,2,K)=0.0
END DO
C
C     Inner tube (inside) B.C.(v = 0.0)
C
DO I=2,IM
  AP(I,IN,K)=1.0
  AS(I,IN,K)=0.0
  S(I,IN,K)=0.0

```

```

    END DO
C
C   Outer tube (inside) B.C.(v=0.0)
C
DO I=2,M-1
  AP(I,N-1,K) = 1.0
  AS(I,N-1,K) = 0.0
  S(I,N-1,K) = 0.0
END DO
C
C   Exit B.C.(dv/dx = 0)
C
DO J=IN+1,N-2
  AP(1,J,K) = 1.0
  IF(INLET.EQ.0)THEN
    AE(1,J,K) = 1.0
    S(1,J,K) = 0.0
  ELSE
    AE(1,J,K) = 0.0
    S(1,J,K) = 0.0
  ENDIF
END DO
C
C   Inner tube (outside) B.C.(v=0.0)
C
DO I=2,IM
  AP(I,IN,K) = 1.0
  AN(I,IN,K) = 0.0
  S(I,IN,K) = 0.0
END DO
END DO
DO I=2,M-1
  DO J=3,N-2
    AP(I,J,1) = 1.0
    AT(I,J,1) = 1.0
    S(I,J,1) = 0.0
    AP(I,J,KM) = 1.0
    AB(I,J,KM) = 0.0
    S(I,J,KM) = V(I,J,1)
  END DO
END DO
C
C-----Calculate coefficients of velocity,V
C

```

```

    CALL COEFFV(M,N,KM,RENOL,H,RELAV,DV,AP,AE,AW,AN,AS,AT,AB,S,
    , IM,IN,THC)
C
C-----Calculate V,using solver TDMA
C
    CALL TDMA(AP,AE,AW,AN,AS,AT,AB,S,1,M,2,N-1,1,KM,.FALSE.,NP,VT,
    , VSTR,RD,M,N,IM,IN,KM,2)
C
C     Specify B.C.for w-equation
C
C     Boundary indices are (1,M,1,N,2,KM)
C
C     Entrance B.C.(w = 0.0)
C
    DO K = 3,KM-1
        DO J = 2,IN-1
            AP(1,J,K) = 1.0
            IF(INLET.EQ.0)THEN
                AE(1,J,K) = 0.0
                S(1,J,K) = 0.0
            ELSE
                AE(1,J,K) = 1.0
                S(1,J,K) = 0.0
            ENDIF
        END DO
C
C     Closed end b.c.(w = 0.0)
C
    DO J = 2,N-1
        AP(M,J,K) = 1.0
        AW(M,J,K) = 0.0
        S(M,J,K) = 0.0
    END DO
C
C     Centre B.C.(dw/dr = 0.0)
C
    DO I = 2,M-1
        AP(I,1,K) = 1.0
        AN(I,1,K) = 1.0
        S(I,1,K) = 0.0
    END DO
C
C     Inner tube (inside) B.C.(w = 0.0)
C

```

```

DO I=2,IM
  AP(I,IN,K) = 1.0
  AS(I,IN,K) = 0.0
  S(I,IN,K) = 0.0
END DO
C
C Outer tube (inside) B.C.(w=0.0)
C
DO I=2,M-1
  AP(I,N,K) = 1.0
  AS(I,N,K) = 0.0
  S(I,N,K) = 0.0
END DO
C
C Exit B.C.(dw/dx = 0)
C
DO J=IN+1,N-1
  AP(1,J,K) = 1.0
  IF(INLET.EQ.0)THEN
    AE(1,J,K) = 1.0
    S(1,J,K) = 0.0
  ELSE
    AE(1,J,K) = 0.0
    S(1,J,K) = 0.0
  ENDIF
END DO
C
C Inner tube (outside) B.C.(w=0.0)
C
DO I=2,IM
  AP(I,IN,K) = 1.0
  AN(I,IN,K) = 0.0
  S(I,IN,K) = 0.0
END DO
END DO
C
C Circumferential B.C.
C
DO I=2,M-1
  DO J=2,N-1
    AP(I,J,2) = 1.0
    AT(I,J,2) = 1.0
    S(I,J,2) = 0.0
    AP(I,J,KM) = 1.0
  END DO
END DO

```

```

      AB(I,J,KM)=0.0
      S(I,J,KM)=W(I,J,2)
334    END DO
      END DO
C
C-----Calculate coefficients of velocity,W
C
      CALL COEFFW(M,N,KM,RENOL,H,RELAWS,DWA,AP,AE,AW,AN,AS,AT,AB,S,
      ' IM,IN,THC)
C
C-----Calculate W,using solver TDMA
C
      CALL TDMA(AP,AE,AW,AN,AS,AT,AB,S,1,M,1,N,2,KM,.FALSE.,NP,WT,
      ' WSTR,RD,M,N,IM,IN,KM,3)
C
C-----Solve pressure correction equation with new velocity
C     field
C
      DO I=2,M-1
        DO J=2,N-1
          DO K=2,KM-1
            IF(I.EQ.IM)GO TO 114
            IF(J.EQ.IN)GO TO 114
            PC(I,J,K)=0.0
114      END DO
        END DO
      END DO

      SOURCE=0.0
      NPT=0.0
      JCAT=0
      KA=2
      KB=IM
      KC=2
      KD=IN-1
540    IF(JCAT.EQ.1)THEN
        KA=IM+1
        KB=M-1
        KC=2
        KD=N-1
      ENDIF
      IF(JCAT.EQ.2)THEN
        KA=2
        KB=IM
      ENDIF
    
```

```

KC = IN + 1
KD = N-1
ENDIF

DO I=KA,KB
  DO J=KC,KD
    DO K=2,KM-1
      IF(J.EQ.IN)GO TO 142
      IF(I.EQ.IM)GO TO 142
      DELT=TCV(K)
      IF(I.LT.IM)DELX=XCV(I)
      IF(I.GT.IM)DELX=XCV(I-1)
      IF(J.LT.IN)DELR=RCV(J)
      IF(J.GT.IN)DELR=RCV(J-1)
      RE=R(J)
      RW=R(J)
      RN=RV(J+1)
      RS=RV(J)
      RT=R(J)
      RB=R(J)
      IF(J.GT.IN)THEN
        RN=RV(J)
        RS=RV(J-1)
      ENDIF
C
C-----Calculate pressure coefficients
C
      IF(I.LT.IM)THEN
        AE(I,J,K)=DU(I+1,J,K)*RE*RE*DELR*DELT
        IF(I.NE.2)AW(I,J,K)=DU(I,J,K)*RW*RW*DELR*DELT
        IF(I.EQ.2)AW(I,J,K)=0.0
        IF(J.LT.IN)THEN
          IF(J.NE.IN-1)AN(I,J,K)=HH4*D(V(I,J+1,K)*
          ,RN*RN*DELX*DELT
          ,IF(J.NE.2)AS(I,J,K)=HH4*D(V(I,J,K)*RS*RS*
          ,DELX*DELT
          ,IF(J.EQ.IN-1)AN(I,J,K)=0.0
          ,IF(J.EQ.2)AS(I,J,K)=0.0
        ENDIF
        IF(J.GT.IN)THEN
          IF(J.EQ.IN+1)AS(I,J,K)=0.0
          IF(J.EQ.N-1)AN(I,J,K)=0.0
          IF(J.NE.IN+1)AS(I,J,K)=HH4*D(V(I,J-1,K)*
          ,RS*RS*DELX*DELT
        ,
      
```

```

        IF(J.NE.N-1)AN(I,J,K)=HH4*DVi(J,K)*
        RN*RN*DELX*DELT
    ENDIF
ENDIF
IF(I.GT.IM)THEN
    AW(I,J,K)=DU(I-1,J,K)*RW*RW*DELR*DELT
    IF(I.NE.M-1)AE(I,J,K)=DU(I,J,K)*RE*RE*DELR*DELT
    IF(I.EQ.M-1)AE(I,J,K)=0.0
    IF(J.LT.IN)THEN
        IF(J.EQ.2)AS(I,J,K)=0.0
        IF(J.NE.2)AS(I,J,K)=HH4*DVi(J+1,K)*RN*RN*DELX*DELT
        *RS*RS*DELX*DELT
        AN(I,J,K)=HH4*DVi(J+1,K)*RN*RN*DELX*DELT
    ENDIF
    IF(J.GT.IN)THEN
        IF(J.EQ.N-1)AN(I,J,K)=0.0
        IF(J.NE.N-1)AN(I,J,K)=HH4*DVi(J,K)*RN*RN*
        DELT*DELX
        AS(I,J,K)=HH4*DVi(J-1,K)*RS*RS*DELX*DELT
    ENDIF
ENDIF
IF(K.NE.KM-1)AT(I,J,K)=HH4*RT*DELX*DELR*
DWA(I,J,K+1)/(THC*THC)
IF(K.NE.2)AB(I,J,K)=HH4*RB*DELX*DELR*
DWA(I,J,K)/(THC*THC)
IF(K.EQ.2)AB(I,J,K)=0.0
IF(K.EQ.KM-1)AT(I,J,K)=0.0

C
C      Boundary condition
C
IF(INLET.EQ.0)THEN
    IF(J.GT.IN)THEN
        IF(I.EQ.2)AE(I,J,K)=0.0
    ENDIF
ELSE
    IF(J.LT.IN)THEN
        IF(I.EQ.2)AE(I,J,K)=0.0
    ENDIF
ENDIF
AP(I,J,K)=AE(I,J,K)+AW(I,J,K)+AN(I,J,K)+AS(I,J,K)+

AT(I,J,K)+AB(I,J,K)

C
C      Source term calculation
C

```

```

IF(I.LT.IM)S(I,J,K) = (USTR(I,J,K)-USTR(I+1,J,K))*  

RE*RE*DELR*DELT  

IF(I.GT.IM)S(I,J,K) = (USTR(I-1,J,K)-USTR(I,J,K))*  

RE*RE*DELR*DELT  

IF(J.LT.IN)S(I,J,K) = S(I,J,K) + (VSTR(I,J,K)*  

RS*RS-VSTR(I,J+1,K)*RN*RN)*DELX*DELT  

IF(J.GT.IN)S(I,J,K) = S(I,J,K) + (VSTR(I,J-1,K)*  

RS*RS-VSTR(I,J,K)*RN*RN)*DELX*DELT  

S(I,J,K) = S(I,J,K) + (WSTR(I,J,K)-WSTR(I,J,K+1))*  

RT*DELX*DELR  

SOURCE = SOURCE + S(I,J,K)  

NPT = NPT + 1.0
142    END DO
        END DO
    END DO

JCAT = JCAT + 1
IF(JCAT.LT.3)GO TO 540
C
C-----Specify pressure at exit boundary
C
    DO K = 2,KM-1
C      DO J = 2,IN-1
        IF(INLET.EQ.0)THEN
            DO J=IN+1,N-1
                AP(2,J,K)=1.0
                AE(2,J,K)=0.0
                AW(2,J,K)=0.0
                AN(2,J,K)=0.0
                AS(2,J,K)=0.0
                AT(2,J,K)=0.0
                AB(2,J,K)=0.0
                S(2,J,K)=0.0
            END DO
        ELSE
            DO J = 2,IN-1
                AP(2,J,K)=1.0
                AE(2,J,K)=0.0
                AW(2,J,K)=0.0
                AN(2,J,K)=0.0
                AS(2,J,K)=0.0
                AT(2,J,K)=0.0
                AB(2,J,K)=0.0
                S(2,J,K)=0.0
            END DO
        END IF
    END DO

```

```

END DO
ENDIF
END DO

SOURCE=SOURCE/NPT
WRITE(6,*)"PSOURCE =",SOURCE
WRITE(6,*)"NPT =",NPT

WRITE(6,*)"PC(I,J,2),J = 2,IN-1"
WRITE(6,*)(PC(2,J,2),J = 2,IN-1)
WRITE(6,*)"P(2,J,3),J = 2,IN-1"
WRITE(6,*)(P(2,J,3),J = 2,IN-1)

CALL TDMA(AP,AE,AW,AN,AS,AT,AB,S,1,M,1,N,1,KM,.TRUE.,NPP,PT,
          PC,RD,M,N,IM,IN,KM,3)

WRITE(6,*)"PC(I,J,3),J = IN + 1,N-1"
WRITE(6,*)(PC(2,J,3),J = IN + 1,N-1)
WRITE(6,*)"P(2,J,3),J = IN + 1,N-1"
WRITE(6,*)(P(2,J,3),J = IN + 1,N-1)

C
C-----Calculate the new pressure field
C
DO 135 K = 2,KM-1
  DO 135 I = 2,M-1
    DO 135 J = 2,N-1
      IF(J.EQ.IN)GO TO 135
      IF(I.EQ.IM)GO TO 135
      P(I,J,K)=P(I,J,K)+RELAP*PC(I,J,K)
135 CONTINUE

C
C-----Calculate the new U velocity field
C
ICAT=0
164 IF(ICAT.EQ.0)THEN
  KA=3
  KB=IM
  KC=2
  KD=IN-1
ENDIF
IF(ICAT.EQ.1)THEN
  KA=IM+1
  KB=M-2
  KC=2

```

```

KD = N-1
ENDIF
IF(ICAT.EQ.2)THEN
  KA = 3
  KB = IM
  KC = IN + 1
  KD = N-1
ENDIF
DO I=KA,KB
  DO J=KC,KD
    DO K = 2,KM-1
      IF(J.EQ.IN)GO TO 101
      IF(I.LT.IM)USTR(I,J,K) = USTR(I,J,K) + DU(I,J,K)*
        (PC(I-1,J,K)-PC(I,J,K))
      IF(I.EQ.IM)USTR(I,J,K) = USTR(I,J,K) + DU(I,J,K)*
        (PC(IM-1,J,K)-PC(IM+1,J,K))
      IF(I.GT.IM)USTR(I,J,K) = USTR(I,J,K) + DU(I,J,K)*
        (PC(I,J,K)-PC(I+1,J,K))
    101   END DO
    END DO
  ICAT = ICAT + 1
  IF(ICAT.LT.3)GO TO 164
C
C-----Calculate the new V velocity field
C
ICAT = 0
168 IF(ICAT.EQ.0)THEN
  KA = 2
  KB = IM
  KC = 3
  KD = IN-1
ENDIF
IF(ICAT.EQ.1)THEN
  KA = IM + 1
  KB = M-1
  KC = 3
  KD = N-2
ENDIF
IF(ICAT.EQ.2)THEN
  KA = 2
  KB = IM
  KC = IN + 1
  KD = N-2

```

```

ENDIF
DO I=KA,KB
  DO J=KC,KD
    DO K = 2,KM-1
      IF(I.EQ.IM)GO TO 102
      IF(J.LT.IN)VSTR(I,J,K)=VSTR(I,J,K)+HH4*DVA(I,J,K)*
      ' (PC(I,J-1,K)-PC(I,J,K))
      ' IF(J.EQ.IN)VSTR(I,J,K)=VSTR(I,J,K)+HH4*
      ' DV(I,J,K)*(PC(I,IN-1,K)-PC(I,IN+1,K))
      ' IF(J.GT.IN)VSTR(I,J,K)=VSTR(I,J,K)+HH4*
      ' DV(I,J,K)*(PC(I,J,K)-PC(I,J+1,K))
102   END DO
    END DO
  ICAT=ICAT+1
  IF(ICAT.LT.3)GO TO 168
C
C-----Calculate the new W velocity field
C
  ICAT=0
178 IF(ICAT.EQ.0)THEN
  KA=2
  KB=IM
  KC=2
  KD=IN-1
ENDIF
IF(ICAT.EQ.1)THEN
  KA=IM+1
  KB=M-1
  KC=2
  KD=N-1
ENDIF
IF(ICAT.EQ.2)THEN
  KA=2
  KB=IM
  KC=IN+1
  KD=N-1
ENDIF
DO I=KA,KB
  DO J=KC,KD
    DO K = 3,KM-1
      IF(I.EQ.IM)GO TO 103
      IF(J.EQ.IN)GO TO 103
      WSTR(I,J,K)=WSTR(I,J,K)+HH4*DWA(I,J,K)*

```

```

      '      (PC(I,J,K-1)-PC(I,J,K))/(THC*THC)
103    END DO
      END DO
      END DO
      ICAT=ICAT+1
      IF(ICAT.LT.3)GO TO 178
C
C-----Calculate velocity and pressure errors
C
      CALL CRIT(U,USTR,2,M-1,1,N,1,KM,ERRU,IM,IN,KM,1)
      CALL CRIT(V,VSTR,1,M,2,N-1,1,KM,ERRV,IM,IN,KM,2)
      CALL CRIT(W,WSTR,1,M,1,N,2,KM,ERRW,IM,IN,KM,3)

      SUM=0.0
      POINT=0.0
      DO I=2,M-1
        DO J=2,N-1
          DO K=2,KM-1
            IF(I.EQ.IM)GO TO 24
            IF(J.EQ.IN)GO TO 24
            C=PC(I,J,K)
            B=P(I,J,K)
            IF(B.EQ.0.0)GO TO 24
            DIFF=C/B
            DIFF=DIFF*DIFF
            SUM=SUM+DIFF
24        POINT=POINT+1.0
          END DO
        END DO
      END DO
      SUM=SQRT(SUM)
      IF(ITER.EQ.1)SUMI=SUM
      IF(ITER.GT.1)THEN
        SDI=SUM/SUMI
        WRITE(6,*)"SUMI =",SUMI
        WRITE(6,*)"PDIFFERENCE =",SDI
      ENDIF
      ERRP=SUM/POINT
C
      WRITE(6,*)"ERRP =",ERRP
      WRITE(6,*)"ERRU =",ERRU,"ERRV =",ERRV
      WRITE(6,*)"ERRW =",ERRW
C
      DO I=2,M-1

```

```

DO J=1,N
  DO K=1,KM
    IF(I.GT.IM)THEN
      IF(J.EQ.IN)GO TO 121
    ENDIF
    U(I,J,K)=USTR(I,J,K)
121   END DO
    END DO
  END DO
  DO I=1,M
    DO J=2,N-1
      DO K=1,KM
        IF(I.EQ.IM)GO TO 120
        V(I,J,K)=VSTR(I,J,K)
120   END DO
    END DO
  END DO
  DO I=1,M
    DO J=1,N
      DO K=2,KM
        IF(I.EQ.IM)GO TO 129
        IF(I.GT.IM)THEN
          IF(J.EQ.IN)GO TO 129
        ENDIF
        W(I,J,K)=WSTR(I,J,K)
129   END DO
    END DO
  END DO
  DO I=2,M-1
    DO J=1,N
      U(I,J,1)=U(I,J,2)
      U(I,J,KM)=U(I,J,KM-1)
    END DO
  END DO
  DO I=2,M-1
    DO K=1,KM
      U(I,1,K)=U(I,2,K)
    END DO
  END DO
1 FORMAT(18E14.5)
2 FORMAT(12E11.3)
3 FORMAT(10E11.3)
4 FORMAT(9E11.3)

```

```

5 FORMAT(F20.16)
6 FORMAT(20E22.8,2F15.4)
7 FORMAT(20E24.8,3F15.4)

C
C-----Plot the resultant velocity
C
DO K = 1,KM
  DO J = 1,N-1
    PU(1,J,K) = U(2,J,K)
    XU(1) = 0.0
  END DO

  DO I = 2,M-1
    DO J = 2,N-1
      IF(J.LT.IN)PU(I,J,K) = (U(I,J-1,K) + U(I,J,K))/2.0
      IF(J.GT.IN)PU(I,J,K) = (U(I,J,K) + U(I,J+1,K))/2.0
      IF(J.EQ.2)PU(I,J,K) = U(I,J-1,K)
      IF(J.EQ.N-1)PU(I,J,K) = U(I,J+1,K)
      IF(I.LT.IM+1)THEN
        IF(J.EQ.IN)PU(I,J,K) = U(I,J,K)
      ELSE
        IF(J.EQ.IN)PU(I,J,K) = (U(I,J-1,K) + U(I,J+1,K))/2.0
      ENDIF
    END DO
  END DO
END DO
DO J = 2,N-1
  DO K = 1,KM
    PUK(1,J,K) = U(2,J,K)
  END DO
  DO I = 2,M-1
    DO K = 2,KM
      PUK(I,J,K) = (PU(I,J,K-1) + PU(I,J,K))/2.0
      IF(K.EQ.2)PUK(I,J,K) = PU(I,J,K-1)
      IF(K.EQ.KM)PUK(I,J,K) = PU(I,J,K)
    END DO
  END DO
END DO
DO K = 2,KM
  DO I = 1,M-1
    PV(I,1,K) = 0.0
    RV(1) = 0.0
  END DO
  DO J = 2,N-1

```

```

DO I=2,M-1
  IF(I.LT.IM)PV(I,J,K)=(V(I-1,J,K)+V(I,J,K))/2.0
  IF(I.GT.IM)PV(I,J,K)=(V(I,J,K)+V(I+1,J,K))/2.0
  IF(I.EQ.2)PV(I,J,K)=V(I-1,J,K)
  IF(I.EQ.IM)PV(I,J,K)=(V(I-1,J,K)+V(I+1,J,K))/2.0
  IF(I.EQ.M-1)PV(I,J,K)=V(I+1,J,K)
  PV(IM,IN,K)=0.0
END DO
ENDDO
END DO
DO I=1,M-1
  DO K=1,KM
    PVK(I,1,K)=0.0
  END DO
  DO J=2,N-1
    DO K=2,KM
      PVK(I,J,K)=(PV(I,J,K-1)+PV(I,J,K))/2.0
      IF(K.EQ.2)PVK(I,J,K)=PV(I,J,K-1)
      IF(K.EQ.KM)PVK(I,J,K)=PV(I,J,K)
    END DO
  END DO
END DO
DO J=2,N-1
  DO I=1,M-1
    PW(I,J,1)=0.0
    TV(1)=0.0
  END DO
  DO K=2,KM
    DO I=2,M-1
      IF(I.LT.IM)PW(I,J,K)=(W(I-1,J,K)+W(I,J,K))/2.0
      IF(I.GT.IM)PW(I,J,K)=(W(I,J,K)+W(I+1,J,K))/2.0
      IF(I.EQ.2)PW(I,J,K)=W(I-1,J,K)
      IF(I.EQ.IM)PW(I,J,K)=(W(I-1,J,K)+W(I+1,J,K))/2.0
      IF(I.EQ.M-1)PW(I,J,K)=W(I+1,J,K)
      PW(IM,IN,K)=0.0
    END DO
  END DO
END DO
DO I=2,M-1
  DO J=1,N-1
    PWK(I,J,1)=0.0
  END DO
  DO K=2,KM
    DO J=2,N-1

```

```

IF(J.LT.IN)PWK(I,J,K)=(PW(I,J-1,K)+PW(I,J,K))/2.0
IF(J.GT.IN)PWK(I,J,K)=(PW(I,J,K)+PW(I,J+1,K))/2.0
IF(J.EQ.2)PWK(I,J,K)=PW(I,J-1,K)
IF(J.EQ.N-1)PWK(I,J,K)=PW(I,J+1,K)
IF(I.LT.IM+1)THEN
    IF(J.EQ.IN)PWK(I,J,K)=PW(I,J,K)
ELSE
    IF(J.EQ.IN)PWK(I,J,K)=(PW(I,J-1,K)+PW(I,J+1,K))/2.0
ENDIF
END DO
END DO
END DO
C
C-----Calculate average pressure at the entrance
C
DO K=1,KM
    DO J=1,N
        P(1,J,K)=P(2,J,K)
    END DO
END DO
DO K=1,KM
    P(2,IN,K)=P(2,IN-1,K)
    P(3,IN,K)=P(3,IN-1,K)
    P(2,N-1,K)=P(2,N-2,K)
    P(3,N-1,K)=P(3,N-2,K)
END DO
DO J=1,N
    P(2,J,KM)=P(2,J,KM-1)
    P(3,J,KM)=P(3,J,KM-1)
    P(2,J,1)=P(2,J,2)
    P(3,J,1)=P(3,J,2)
END DO
DO K=1,KM
    PRE(1,2,K)=P(2,1,K)
    PRE(2,2,K)=P(3,1,K)
    PRE(1,IN,K)=P(2,IN,K)
    PRE(2,IN,K)=P(3,IN,K)
    PRE(1,N-1,K)=P(2,N-1,K)
    PRE(2,N-1,K)=P(3,N-1,K)
    DO J=3,IN-1
        PRE(1,J,K)=(P(2,J,K)+P(2,J-1,K))/2.0
        PRE(2,J,K)=(P(3,J,K)+P(3,J-1,K))/2.0
    END DO
    DO J=IN+1,N-2

```

```

PRE(1,J,K) = (P(2,J,K) + P(2,J+1,K))/2.0
PRE(2,J,K) = (P(3,J,K) + P(3,J+1,K))/2.0
IF(J.EQ.N-2)THEN
  PRE(1,J,K) = P(2,J,K)
  PRE(2,J,K) = P(3,J,K)
ENDIF
END DO
END DO
DO J=2,IN
  T(1,J,2)=PRE(1,J,1)
  T(2,J,2)=PRE(2,J,1)
  T(1,J,KM)=PRE(1,J,KM)
  T(2,J,KM)=PRE(2,J,KM)
  DO K=3,KM-1
    T(1,J,K)=(PRE(1,J,K)+PRE(1,J,K-1))/2.0
    T(2,J,K)=(PRE(2,J,K)+PRE(2,J,K-1))/2.0
  END DO
END DO
DO J=IN+1,N-1
  T(1,J,2)=PRE(1,J,1)
  T(1,J,KM)=PRE(1,J,KM)
  T(2,J,2)=PRE(2,J,1)
  T(2,J,KM)=PRE(2,J,KM)
  DO K=3,KM-1
    T(1,J,K)=(PRE(1,J,K)+PRE(1,J,K-1))/2.0
    T(2,J,K)=(PRE(2,J,K)+PRE(2,J,K-1))/2.0
  END DO
END DO
DO K=2,KM
  SUMX(K)=0.0
  SUMX1(K)=0.0
  ISWICH=0
  DO J=2,IN
    IF(ISWICH.EQ.0)THEN
      QQ(1,J,K)=2.0*T(1,J,K)*RV(J)
      QQ(2,J,K)=2.0*T(2,J,K)*RV(J)
      IF(J.EQ.2.OR.J.EQ.IN)THEN
        QQ(1,J,K)=QQ(1,J,K)/2.0
        QQ(2,J,K)=QQ(2,J,K)/2.0
      ENDIF
      ISWICH=1
    ELSE
      QQ(1,J,K)=4.0*T(1,J,K)*RV(J)
      QQ(2,J,K)=4.0*T(2,J,K)*RV(J)
    ENDIF
  END DO
END DO

```

```

ISWICH=0
ENDIF
SUMX(K)=SUMX(K)+QQ(1,J,K)
SUMX1(K)=SUMX1(K)+QQ(2,J,K)
END DO
SUMX(K)=SUMX(K)*DR1/(3.0)
SUMX1(K)=SUMX1(K)*DR1/3.0
END DO
SUM=0.0
SUME=0.0
ISWICH=0
DO K=2,KM
IF(ISWICH.EQ.0)THEN
  SUM1=2.0*SUMX(K)
  SUM2=2.0*SUMX1(K)
  IF(K.EQ.2.OR.K.EQ.KM)THEN
    SUM1=SUM1/2.0
    SUM2=SUM2/2.0
  ENDIF
  ISWICH=1
ELSE
  SUM1=4.0*SUMX(K)
  SUM2=4.0*SUMX1(K)
  ISWICH=0
ENDIF
SUM=SUM+SUM1
SUME=SUME+SUM2
END DO
SUM=SUM*DT1/(3.0)
SUM=SUM*2.0/(R(IN)**2.0)
PAVV=SUM
SUME=SUME*DT1/3.0
SUME=SUME*2.0/(R(IN)**2.0)
PAVV1=SUME
DO K=2,KM
  SUMX(K)=0.0
  SUMX1(K)=0.0
  ISWICH=0
  DO J=IN,N-1
    IF(ISWICH.EQ.0)THEN
      QQ(1,J,K)=2.0*T(1,J,K)*RV(J)
      QQ(2,J,K)=2.0*T(2,J,K)*RV(J)
      IF(J.EQ.IN)THEN
        QQ(1,J,K)=2.0*T(1,J+1,K)*RV(J)
      ENDIF
    ENDIF
  END DO
END DO

```

```

    QQ(2,J,K) = 2.0*T(2,J+1,K)*RV(J)
ENDIF
IF(J.EQ.IN.OR.J.EQ.N-1)THEN
    QQ(1,J,K) = QQ(1,J,K)/2.0
    QQ(2,J,K) = QQ(2,J,K)/2.0
ENDIF
ISWICH = 1
ELSE
    QQ(1,J,K) = 4.0*T(1,J,K)*RV(J)
    QQ(2,J,K) = 4.0*T(2,J,K)*RV(J)
    ISWICH = 0
ENDIF
SUMX(K) = SUMX(K) + QQ(1,J,K)
SUMX1(K) = SUMX1(K) + QQ(2,J,K)
END DO
SUMX(K) = SUMX(K)*DR2/(3.0)
SUMX1(K) = SUMX1(K)*DR2/3.0
END DO
SUM = 0.0
SUME = 0.0
ISWICH = 0
DO K = 2,KM
    IF(ISWICH.EQ.0)THEN
        SUM1 = 2.0*SUMX(K)
        SUM2 = 2.0*SUMX1(K)
        IF(K.EQ.2.OR.K.EQ.KM)THEN
            SUM1 = SUM1/2.0
            SUM2 = SUM2/2.0
        ENDIF
        ISWICH = 1
    ELSE
        SUM1 = 4.0*SUMX(K)
        SUM2 = 4.0*SUMX1(K)
        ISWICH = 0
    ENDIF
    SUM = SUM + SUM1
    SUME = SUME + SUM2
END DO
SUM = SUM*DT1/(3.0)
SUM = SUM*2.0/(1.0-(R(IN)**2.0))
PAVVA = SUM
SUME = SUME*DT1/3.0
SUME = SUME*2.0/(1.0-(R(IN)**2.0))
PAVVA1 = SUME

```

```

WRITE(6,*)
WRITE(6,*)"PAVVA =",PAVVA,"P(2,IN+2,2) =",P(2,IN+2,2)
WRITE(6,*)
PAV=0.0
POINT=0.0
DO K=2,KM-1
  DO J=2,IN-1
    PAV=SUM+P(2,J,K)
    POINT=POINT+1.0
  END DO
END DO
PAV=PAV/POINT
WRITE(6,*)"AVERAGE PRESSURE =",PAVV

C
C-----Calculate exit velocity
C
DO K=1,KM
  ISWICH=0
  SUMR(K)=0.0
  DO J=IN+1,N-2
    PR(J)=(U(2,J+1,K)+U(2,J,K))*RV(J)/2.0
    IF(ISWICH.EQ.0)THEN
      PR(J)=4.0*PR(J)
      ISWICH=1
    ELSE
      PR(J)=2.0*PR(J)
      ISWICH=0
    ENDIF
    SUMR(K)=SUMR(K)+PR(J)
  END DO
  SUMR(K)=(SUMR(K))*DR2/3.0
END DO
ISWICH=0
SUM=0.0
DO K=3,KM-1
  PR(K)=(SUMR(K)+SUMR(K-1))/2.0
  IF(ISWICH.EQ.0)THEN
    PR(K)=4.0*PR(K)
    ISWICH=1
  ELSE
    PR(K)=2.0*PR(K)
    ISWICH=0
  ENDIF
  SUM=SUM+PR(K)

```

```

    END DO
    SUM = (SUMR(2) + SUMR(KM) + SUM) * DT1/3.0
    UAN = SUM * 2.0 / (1.0 - RII ** 2.0)
    IF(INLET.EQ.1)THEN
C
C-----Calculate exit velocity
C
    DO K = 1,KM
        ISWICH = 0
        SUMR(K) = 0.0
        DO J = 3,IN-1
            PR(J) = (U(2,J-1,K) + U(2,J,K)) * RV(J)/2.0
            IF(ISWICH.EQ.0)THEN
                PR(J) = 4.0 * PR(J)
                ISWICH = 1
            ELSE
                PR(J) = 2.0 * PR(J)
                ISWICH = 0
            ENDIF
            SUMR(K) = SUMR(K) + PR(J)
        END DO
        SUMR(K) = (SUMR(K)) * DR1/3.0
    END DO
    ISWICH = 0
    SUM = 0.0
    DO K = 3,KM-1
        PR(K) = (SUMR(K) + SUMR(K-1))/2.0
        IF(ISWICH.EQ.0)THEN
            PR(K) = 4.0 * PR(K)
            ISWICH = 1
        ELSE
            PR(K) = 2.0 * PR(K)
            ISWICH = 0
        ENDIF
        SUM = SUM + PR(K)
    END DO
    SUM = (SUMR(2) + SUMR(KM) + SUM) * DT1/3.0
    UIN = SUM * 2.0 / (RII ** 2.0)
    ENDIF
    IF(INLET.EQ.1)SOUT = -3.14 * 2.0 * SUM
    IF(INLET.EQ.0)SINN = RENOL1 * 3.14 * (R(IN) ** 2.0)
    IF(INLET.EQ.1)SINN = RENOL1 * 3.14 * (1.0 - R(IN)) ** 2.0
    WRITE(6,*)"SINN1 =", SINN
    WRITE(6,*)"SINN2 =", SINN2

```

```

SOUT1 = -3.14*2.0*SUMR(3)
WRITE(6,*)
WRITE(6,*)"SOUT1 =",SOUT1
WRITE(6,*)
IF(INLET.EQ.0)SOUT = -3.14*2.0*SUM
WRITE(6,*)"SOUT =",SOUT
SERR = ((SINN-SOUT)/SINN)*100.0
WRITE(6,*)"MASS IN =",SINN,"MASS OUT =",SOUT
WRITE(6,*)"PERCENTAGE MASS ERROR =",SERR
SOURCE = ABS(SOURCE)
IF(ITER.EQ.NITER)THEN
  WRITE(6,*)"NOT CONVERGED AFTER 1000 ITERATIONS"
  GO TO 777
END IF
C
C-----Calculate the Euler number
C
PDIFF = PAVV-P(2,IN+2,2)
PDIFF = PDIFF + ((P(2,2,2)-P(3,2,2)) + (P(3,IN+2,2)-P(2,IN+2,2)))/2.0
EU = (PDIFF)*2.0 + 2.0*(RENOL1**2.0)*
  '(1.0-(0.75*(AR**2.0)))
EU = EU/((UAN**2.0)*(RRY**4.0))
IF(INLET.EQ.1)THEN
  PDIFF = P(2,IN+2,2) + ((P(2,IN+2,2)-P(3,IN+2,2)) + (P(3,2,2)-
    P(2,2,2))/2.0
  EU = (PDIFF)*2.0 + 2.0*(UIN**2.0)*(1.0-(0.75*(AR**2.0)))
  EU = EU/((RENOL1**2.0)*(RRY**4.0))
ENDIF
WRITE(6,*)"EU =",EU
WRITE(6,*)"PERCENTAGE MASS ERROR =",SERR
C
C-----Specify the convergence criteria
C
IF(ERRU.GT.0.00001)GO TO 555
IF(ERRP.GT.0.0005)GO TO 555
IF(ERRV.GT.0.001)GO TO 555
IF(ERRW.GT.0.001)GO TO 555
IF(INLET.EQ.0)THEN
  IF(SERR.GT.0.6.OR.SERR.LT.0.0)GO TO 555
ELSE
  IF(SERR.GT.0.6.OR.SERR.LT.0.0)GO TO 555
ENDIF
777  CONTINUE

```

```

      WRITE(6,*)"NO OF ITERATIONS =",ITER
      WRITE(6,*)"MASS SOURCE AFTER FINAL ITERATION =",SOURCE
      WRITE(6,*)"CORRECTED PRESSURE FIELD"
      WRITE(6,7)((P(I,J,2),J=2,N-1),I=2,M-2)
      WRITE(6,*)"CORRECTED U-FIELD"
      WRITE(6,7)((U(I,J,2),I=2,M-1),J=N,1,-1)
      WRITE(6,*)"CORRECTED V-FIELD"
      WRITE(6,7)((V(I,J,2),I=1,M),J=N-1,2,-1)

C
C-----Input data for Plot3d package
C
      XU(1)=0.0
      XU(M)=0.0
      RV(1)=0.0
      RV(N)=0.0
      TV(1)=0.0
      TV(KM)=0.0
      IDM=M-1
      JDM=N-1
      KDM=KM-1
      DO I=1,M-1
        DO J=1,N-1
          DO K=1,KM-1
            THETA(K)=6.28*TV(K)
            T(I,J,K)=XU(I)
            Y(I,J,K)=RV(J)*COS(THETA(K))
            Z(I,J,K)=RV(J)*SIN(THETA(K))
            U(I,J,K)=0.0
            V(I,1,K)=0.0
            W(I,J,1)=0.0
            Q(I,J,K,1)=1.0
            Q(I,J,K,2)=PUK(I,J,K)
            Q(I,J,K,3)=PVK(I,J,K)
            Q(I,J,K,4)=PWK(I,J,K)
            Q(I,J,K,5)=0.0
          END DO
        END DO
      END DO

C
      OPEN(12,FILE='GRIDX.DAT',FORM='UNFORMATTED')
      OPEN(14,FILE='VELQ.DAT',FORM='UNFORMATTED')
      WRITE(12)IDM,JDM,KDM
      WRITE(12)((((T(I,J,K),I=1,IDM),J=1,JDM),K=1,KDM),
      '     (((Y(I,J,K),I=1,IDM),J=1,JDM),K=1,KDM),

```

```

' (((Z(I,J,K),I = 1,IMD),J = 1,JDM),K = 1,KDM)
WRITE(14)IDM,JDM,KDM
WRITE(14)A,B,C,D
WRITE(14)((((Q(I,J,K,NX),I = 1,IMD),J = 1,JDM),K = 1,KDM),
' NX = 1,5)
CLOSE(12)
CLOSE(14)
STOP
END

C
C-----This subroutine applies solver TDMA to calculate
C      unknown nodal values
C
C      SUBROUTINE TDMA(AP,AE,AW,AN,AS,AT,AB,S,IL,IR,JB,JT,
' KS,KT,FLAG,NPS,TO,X,E,M,N,IM,IN,KM,ILET)
C
C      IMPLICIT REAL (A-H,O-Z)
C      PARAMETER(ID = 50,JD = 50,LD = 30)
C      DIMENSION AP(ID,JD,LD),AE(ID,JD,LD),AW(ID,JD,LD),AN(ID,JD,LD),
' AS(ID,JD,LD),AT(ID,JD,LD),AB(ID,JD,LD)
C      DIMENSION X(ID,JD,LD),S(ID,JD,LD)
C      DIMENSION P(JD),Q(JD)
C      DIMENSION A(JD),B(JD),C(JD),D(JD)
C      LOGICAL FLAG
C
C-----Make double sweep N-pass times or until RELERR
C      becomes small.
C
C      ISWICH=0
C      DO 333 ITER = 1,NPS
319  DO 444 ILOOP = 1,2
C
C-----Set the sweep direction
C
C-----Sweep from left to right boundary beginning from
C      J=bottom or J=top
C
C      IF(ISWICH.EQ.0)THEN
        K1 = KS + 1
        K2 = KT - 1
        KINC = 1
      ELSE
        K1 = KT - 1
        K2 = KS + 1
      ENDIF
    ENDIF
  ENDIF
END

```

```

KINC=-1
ENDIF
DO K=K1,K2,KINC
IF(ISWICH.EQ.0)ICAT=0
IF(ISWICH.EQ.1)ICAT=2
502 IF(ICAT.EQ.0)THEN
  KE=JB
  KF=IN
  KL=IL
  KR=IR
ENDIF
IF(ICAT.EQ.2)THEN
  KE=IN
  KF=JT
  KL=IL
  KR=IR
ENDIF
IF(ICAT.EQ.1)THEN
  KL=IM
  KR=IR
  KE=IN-1
  KF=IN+1
ENDIF
IF(ISWICH.EQ.0)THEN
  J1=KE+1
  JINC=1
  J2=KF-1
ELSE
  J1=KF-1
  JINC=-1
  J2=KE+1
ENDIF

170 DO J=J1,J2,JINC
C
C-----Set up the TD-Matrix
C
C      IF(ICAT.EQ.2)GO TO 155
      DO I=KL+1,KR-1

        IF(I.GT.IM)THEN
          IF(ILET.EQ.1.OR.ILET.EQ.3)THEN
            IF(J.EQ.IN)GO TO 12
          ENDIF
        ENDIF
      ENDIF
    ENDIF
  ENDIF
ENDIF

```

```

ENDIF

IF(ILET.EQ.2.OR.ILET.EQ.3)THEN
  IF(I.EQ.IM)GO TO 12
ENDIF
A(I)=AP(I,J,K)
B(I)=AE(I,J,K)
C(I)=AW(I,J,K)
D(I)=S(I,J,K)+AN(I,J,K)*X(I,J+1,K)+AS(I,J,K)*X(I,J-1,K)
IF(ILET.EQ.1.OR.ILET.EQ.3)THEN
  IF(I.GT.IM)THEN
    IF(J.EQ.IN-1)D(I)=S(I,J,K)+AN(I,J,K)*X(I,IN+1,K)+AS(I,J,K)*X(I,J-1,K)
    IF(J.EQ.IN+1)D(I)=S(I,J,K)+AN(I,J,K)*X(I,J+1,K)+AS(I,J,K)*X(I,IN-1,K)
  ENDIF
ENDIF
D(I)=D(I)+AT(I,J,K)*X(I,J,K+1)+AB(I,J,K)*X(I,J,K-1)

12  END DO
IF(FLAG.EQV..TRUE.)THEN
  KL=KL+1
  KR=KR-1
  GO TO 15
END IF
C(KL)=0
B(KR)=0

C
C  Left B.C.
C
A(KL)=AP(KL,J,K)
B(KL)=AE(KL,J,K)
D(KL)=S(KL,J,K)

C
C  Right B.C.
C
A(KR)=AP(KR,J,K)
C(KR)=AW(KR,J,K)
D(KR)=S(KR,J,K)

C
C  Calculate P(I)&Q(I)
C
15  P(KL)=B(KL)/A(KL)
    Q(KL)=D(KL)/A(KL)
    DO I=KL+1,KR

```

```

DENOM=A(I)-C(I)*P(I-1)
IF(ILET.EQ.2.OR.ILET.EQ.3)THEN
  IF(I.EQ.IM)GO TO 92
  IF(I.EQ.IM + 1)DENOM=A(I)-C(I)*P(IM-1)
ENDIF
P(I)=B(I)/DENOM
Q(I)=(D(I) + C(I)*Q(I-1))/DENOM
IF(ILET.EQ.2.OR.ILET.EQ.3)THEN
  IF(I.EQ.IM + 1)Q(I)=(D(I) + C(I)*Q(IM-1))/DENOM
ENDIF

92    END DO
C
C-----Obtain solution by back substitution
C
X(KR,J,K)=Q(KR)

DO I=KR-1,KL,-1
  X(I,J,K)=P(I)*X(I+1,J,K)+Q(I)
  IF(ILET.EQ.2.OR.ILET.EQ.3)THEN
    IF(I.EQ.IM)GO TO 14
    IF(I.EQ.IM-1)X(I,J,K)=P(I)*X(IM+1,J,K)+Q(I)
  ENDIF
14    END DO

IF(FLAG.EQV..TRUE.)THEN
  KL=KL-1
  KR=KR+1
ENDIF
END DO
IF(ILET.EQ.2)THEN
  IF(ISWICH.EQ.0)ICAT=ICAT+1
  IF(ISWICH.EQ.1)ICAT=ICAT-1
ELSE
  IF(ISWICH.EQ.0)ICAT=ICAT+2
  IF(ISWICH.EQ.1)ICAT=ICAT-2
ENDIF
IF(ISWICH.EQ.0)THEN
  IF(ICAT.LT.3)GO TO 502
ELSE
  IF(ICAT.EQ.1.OR.ICAT.EQ.0)GO TO 502
ENDIF
END DO
C

```

C-----Sweep from bottom to top(begin from left or right)

C

C-----Set up TD-Matrix

C

```
IF(ISWICH.EQ.0)ICAT=0
IF(ISWICH.EQ.1)ICAT=2
```

```
501 IF(ICAT.EQ.0)THEN
```

```
KA = IL
KB = IM + 1
KC = JB
KD = IN
```

ENDIF

```
IF(ICAT.EQ.1)THEN
```

```
KA = IM
KB = IR
KC = JB
KD = JT
```

ENDIF

```
IF(ICAT.EQ.2)THEN
```

```
KA = IM-1
KB = IL + 2
KC = IN
KD = JT
```

ENDIF

```
IF(ISWICH.EQ.0)THEN
```

```
I1 = KA + 1
IINC = 1
I2 = KB-1
```

```
IF(ICAT.EQ.2)IINC = -1
```

ELSE

```
IF(ICAT.EQ.2)THEN
```

```
I1 = KB-1
IINC = 1
I2 = KA + 1
```

ENDIF

```
IF(ICAT.EQ.1)THEN
```

```
I1 = KA + 1
IINC = 1
I2 = KB-1
```

ENDIF

```
IF(ICAT.EQ.0)THEN
```

```
I1 = KB-2
IINC = -1
I2 = KA + 1
```

```

ENDIF
ENDIF

DO I=I1,I2,IINC
  IF(ILET.EQ.2.OR.ILET.EQ.3)THEN
    IF(I.EQ.IM)GO TO 100
  ENDIF
  DO K=K1,K2,KINC
    DO J=KC+1,KD-1
      IF(ILET.EQ.1.OR.ILET.EQ.3)THEN
        IF(I.GT.IM)THEN
          IF(J.EQ.IN)GO TO 9
        ENDIF
      ENDIF
      A(J)=AP(I,J,K)
      B(J)=AN(I,J,K)
      C(J)=AS(I,J,K)
      D(J)=S(I,J,K)+AE(I,J,K)*X(I+1,J,K)+AW(I,J,K)*X(I-1,J,K)

      IF(ILET.EQ.2.OR.ILET.EQ.3)THEN
        IF(I.EQ.IM-1)D(J)=S(I,J,K)+AE(I,J,K)*
          X(IM+1,J,K)+AW(I,J,K)*X(I-1,J,K)
        IF(I.EQ.IM+1)D(J)=S(I,J,K)+AE(I,J,K)*
          X(I+1,J,K)+AW(I,J,K)*X(IM-1,J,K)
      ENDIF
      D(J)=D(J)+AT(I,J,K)*X(I,J,K+1)+AB(I,J,K)*X(I,J,K-1)
9   END DO
C
IF(FLAG.EQV..TRUE.)THEN
  KC=KC+1
  KD=KD-1
  GO TO 45
ENDIF
C(KC)=0
B(KD)=0
C
C      Bottom B.C.
C
A(KC)=AP(I,KC,K)
B(KC)=AN(I,KC,K)
D(KC)=S(I,KC,K)
C
C      Top B.C.
A(KD)=AP(I,KD,K)
C(KD)=AS(I,KD,K)

```

```

D(KD) = S(I,KD,K)
C
C      Calculate P(J)&Q(J)
C
45   P(KC) = B(KC)/A(KC)
      Q(KC) = D(KC)/A(KC)

      DO J=KC+1,KD
          DENOM = A(J)-C(J)*P(J-1)
          IF(ILET.EQ.1.OR.ILET.EQ.3)THEN
              IF(I.GT.IM)THEN
                  IF(J.EQ.IN)GO TO 91
                  IF(J.EQ.IN+1)DENOM = A(J)-C(J)*P(IN-1)
              ENDIF
          ENDIF
          P(J) = B(J)/DENOM
          Q(J) = (D(J)+C(J)*Q(J-1))/DENOM
          IF(ILET.EQ.1.OR.ILET.EQ.3)THEN
              IF(I.GT.IM)THEN
                  IF(J.EQ.IN+1)Q(J) = (D(J)+C(J)*Q(IN-1))/DENOM
              ENDIF
          ENDIF
      91   END DO
C
C-----Solution by back substitution
C
      X(I,KD,K) = Q(KD)
      DO J=KD-1,KC,-1
          X(I,J,K) = P(J)*X(I,J+1,K) + Q(J)
          IF(ILET.EQ.1.OR.ILET.EQ.3)THEN
              IF(I.GT.IM)THEN
                  IF(J.EQ.IN)GO TO 115
                  IF(J.EQ.IN-1)X(I,J,K) = P(J)*X(I,IN+1,K) + Q(J)
              ENDIF
          ENDIF
      115  END DO
      IF(FLAG.EQV..TRUE.)THEN
          KC = KC-1
          KD = KD + 1
      ENDIF
      END DO
100  END DO
      IF(ISWICH.EQ.0)ICAT = ICAT + 1
      IF(ISWICH.EQ.1)ICAT = ICAT-1
  
```

```
IF(ISWICH.EQ.0)THEN
  IF(ICAT.LT.3)GO TO 501
ELSE
  IF(ICAT.EQ.1.OR.ICAT.EQ.0)GO TO 501
ENDIF

IF(ISWICH.EQ.0)ICAT=0
IF(ISWICH.EQ.1)ICAT=2

C
C-----Sweep in the circumferential direction
C
5020 IF(ICAT.EQ.0)THEN
  KE=JB
  KF=IN
  KL=IL
  KR=IR
ENDIF
IF(ICAT.EQ.2)THEN
  KE=IN
  KF=JT
  KL=IL
  KR=IR
ENDIF
IF(ICAT.EQ.1)THEN
  KL=IM
  KR=IR
  KE=IN-1
  KF=IN+1
ENDIF
IF(ISWICH.EQ.0)THEN
  J1=KE+1
  JINC=1
  J2=KF-1
ELSE
  J1=KF-1
  JINC=-1
  J2=KE+1
ENDIF
1700 DO J=J1,J2,JINC
IF(ILET.EQ.1.OR.ILET.EQ.3)THEN
  IF(I.GT.IM)THEN
    IF(J.EQ.IN)GO TO 1702
  ENDIF
ENDIF
```

```

DO I=KL+1,KR-1
IF(ILET.EQ.2.OR.ILET.EQ.3)THEN
  IF(I.EQ.IM)GO TO 1701
ENDIF
C
C-----Set up TD-Matrix
C
DO K=KS+1,KT-1
  A(K)=AP(I,J,K)
  B(K)=AT(I,J,K)
  C(K)=AB(I,J,K)
  D(K)=S(I,J,K)+AN(I,J,K)*X(I,J+1,K)+AS(I,J,K)*X(I,J-1,K)

  IF(ILET.EQ.1.OR.ILET.EQ.3)THEN
    IF(I.GT.IM)THEN
      IF(J.EQ.IN-1)D(K)=S(I,J,K)+AN(I,J,K)*X(I,IN+1,K)+AS(I,J,K)*X(I,J-1,K)
      IF(J.EQ.IN+1)D(K)=S(I,J,K)+AN(I,J,K)*X(I,J+1,K)+AS(I,J,K)*X(I,IN-1,K)
    ENDIF
  ENDIF
  IF(ILET.EQ.1)THEN
    D(K)=D(K)+AE(I,J,K)*X(I+1,J,K)+AW(I,J,K)*X(I-1,J,K)
  ENDIF
  IF(ILET.EQ.2.OR.ILET.EQ.3)THEN
    IF(I.LT.IM-1.OR.I.GT.IM+1)D(K)=D(K)+AE(I,J,K)*X(I+1,J,K)+AW(I,J,K)*X(I-1,J,K)
    IF(I.EQ.IM-1)D(K)=D(K)+AE(I,J,K)*X(IM+1,J,K)+AW(I,J,K)*X(I-1,J,K)
    IF(I.EQ.IM+1)D(K)=D(K)+AE(I,J,K)*X(I+1,J,K)+AW(I,J,K)*X(IM-1,J,K)
  ENDIF
END DO
IF(FLAG.EQV..TRUE.)THEN
  KS=KS+1
  KT=KT-1
  GO TO 1555
END IF
C(KS)=0
B(KT)=0
C
C Left B.C.
C

```

```

A(KS)=AP(I,J,KS)
B(KS)=AT(I,J,KS)
D(KS)=S(I,J,KS)

C
C Right B.C.
C
A(KT)=AP(I,J,KT)
C(KT)=AB(I,J,KT)
D(KT)=S(I,J,KT)

C
C-----Calculate P(I)&Q(I)
C
1555   P(KS)=B(KS)/A(KS)
        Q(KS)=D(KS)/A(KS)
        DO K=KS+1,KT
          DENOM=A(K)-C(K)*P(K-1)
          P(K)=B(K)/DENOM
          Q(K)=(D(K)+C(K)*Q(K-1))/DENOM

922    END DO

C
C-----Obtain solution by back substitution
C
X(I,J,KT)=Q(KT)

DO K=KT-1,KS,-1
  X(I,J,K)=P(K)*X(I,J,K+1)+Q(K)
144    END DO

IF(FLAG.EQV..TRUE.)THEN
  KS=KS-1
  KT=KT+1
ENDIF

1701  END DO
1702  END DO

IF(ILET.EQ.2)THEN
  IF(ISWICH.EQ.0)ICAT=ICAT+1
  IF(ISWICH.EQ.1)ICAT=ICAT-1
ELSE
  IF(ISWICH.EQ.0)ICAT=ICAT+2
  IF(ISWICH.EQ.1)ICAT=ICAT-2
ENDIF

```

```

IF(ISWICH.EQ.0)THEN
  IF(ICAT.LT.3)GO TO 5020
ELSE
  IF(ICAT.EQ.1.OR.ICAT.EQ.0)GO TO 5020
ENDIF
161  CONTINUE
IF(ISWICH.EQ.0)ICAT=0
IF(ISWICH.EQ.1)ICAT=2
IF(ISWICH.EQ.0)THEN
  ISWICH=1
ELSE
  ISWICH=0
ENDIF
444  CONTINUE
C
C-----Double sweep has been completed
C
C-----Test for convergence
C
E=0.0
NPOINT=0.0

ICAT=0
KA=IL+1
KB=IM
KC=JB+1
KD=IN-1
132  IF(ICAT.EQ.1)THEN
  KA=IM+1
  KB=IR-1
  KC=JB+1
  KD=JT-1
ENDIF
IF(ICAT.EQ.2)THEN
  KA=IL+1
  KB=IM
  KC=IN+1
  KD=JT-1
ENDIF
131  DO I=KA,KI
      DO J=KC,KD
        DO K=KS+1,KT-1
          IF(ILET.EQ.1.OR.ILET.EQ.3)THEN

```

```

        IF(J.EQ.IN)GO TO 10
      ENDIF
      IF(ILET.EQ.2.OR.ILET.EQ.3)THEN
        IF(I.EQ.IM)GO TO 10
      ENDIF
      T=AP(I,J,K)*X(I,J,K)-AE(I,J,K)*X(I+1,J,K)-AW(I,J,K)*
        X(I-1,J,K)
      IF(ILET.EQ.2.OR.ILET.EQ.3)THEN
        IF(I.EQ.IM-1)T=AP(I,J,K)*X(I,J,K)-AE(I,J,K)*
          X(IM+1,J,K)-AW(I,J,K)*X(I-1,J,K)
        IF(I.EQ.IM+1)T=AP(I,J,K)*X(I,J,K)-AE(I,J,K)*
          X(I+1,J,K)-AW(I,J,K)*X(IM-1,J,K)
      ENDIF
      IF(ILET.EQ.2)THEN
        T=T-AN(I,J,K)*X(I,J+1,K)-AS(I,J,K)*X(I,J-1,K)
      ENDIF
      IF(ILET.EQ.1.OR.ILET.EQ.3)THEN
        IF(J.LT.IN-1.OR.J.GT.IN+1)T=T-AN(I,J,K)*
          X(I,J+1,K)-AS(I,J,K)*X(I,J-1,K)
        IF(J.EQ.IN-1)T=T-AN(I,J,K)*X(I,IN+1,K)-
          AS(I,J,K)*X(I,J-1,K)
        IF(J.EQ.IN+1)T=T-AN(I,J,K)*X(I,J+1,K)-
          AS(I,J,K)*X(I,IN-1,K)
      ENDIF
      T=T-AT(I,J,K)*X(I,J,K+1)-AB(I,J,K)*X(I,J,K-1)-S(I,J,K)
      E=E+ABS(T)
      NPOINT=NPOINT+1.0
10   END DO
      END DO
      END DO
      ICAT=ICAT+1
      IF(ICAT.LT.3)GO TO 132
      E=E/NPOINT
      IF(E.LT.TO)GO TO 999
      8 FORMAT(2F11.4)
      333 CONTINUE
      WRITE(6,*)"NOT CONVERGED IN SUB TDMA"
      999 CONTINUE
C
      WRITE(6,*)"NPOINT = ",NPOINT
      WRITE(6,*)"NO OF DOUBLE SWEEPS IN SUB TDMA = ",ITER
      WRITE(6,*)"RESIDUE IN SUB TDMA = ",E
      RETURN
      END

```

```

SUBROUTINE COEFFU(M,N,KM,RENOL,H,RELAX,DU,AP,AE,AW,AN,
' AS,AT,AB,S,IM,IN,THC)
IMPLICIT REAL (A-H,O-Z)
PARAMETER(ID = 50,JD = 50,LD = 30)
COMMON/VEL/U(ID,JD,LD),V(ID,JD,LD),W(ID,JD,LD),
' P(ID,JD,LD)
DIMENSION AP(ID,JD,LD),AE(ID,JD,LD),AW(ID,JD,LD),
' AN(ID,JD,LD),AS(ID,JD,LD),AT(ID,JD,LD),AB(ID,JD,LD)
DIMENSION DU(ID,JD,LD),S(ID,JD,LD)
COMMON/XINDEX/X(ID),XU(ID),XDIF(ID),XCV(ID)
COMMON/RINDEX/R(JD),RV(JD),RDIF(JD),RCV(JD)
COMMON/TINDEX/TH(JD),TV(JD),TDIF(JD),TCV(JD)

```

C

```

ICAT=0
KA=3
KB=IM
KC=2
KD=IN-1
122 IF(ICAT.EQ.2)THEN
    KA=3
    KB=IM
    KC=IN+1
    KD=N-1
ENDIF
IF(ICAT.EQ.1)THEN
    KA=IM+1
    KB=M-2
    KC=2
    KD=N-1
ENDIF
DO I=KA,KB
    DO J=KC,KD
        DO K=2,KM-1
            IF(ICAT.EQ.1)THEN
                IF(J.EQ.IN)GO TO 19
            ENDIF
            RE=R(J)
            RW=R(J)
            RT=R(J)
            RB=R(J)
            DELT=TCV(K)
            DELTT=TDIF(K+1)
            DELTB=TDIF(K)
            IF(I.LT.IM)THEN

```

```

DELX = XDIF(I)
DELXE = XCV(I)
DELXW = XCV(I-1)
ENDIF
IF(I.EQ.IM)THEN
  DELX = X(IM + 1)-X(IM-1)
  DELXE = XCV(I)
  DELXW = XCV(I-1)
ENDIF
IF(I.GT.IM)THEN
  DELX = XDIF(I + 1)
  DELXE = XCV(I)
  DELXW = XCV(I-1)
ENDIF
RN = RV(J + 1)
RS = RV(J)
IF(J.GT.IN)THEN
  RN = RV(J)
  RS = RV(J-1)
ENDIF
IF(J.LT.IN)THEN
  DELR = RCV(J)
  DELRN = RDIF(J + 1)
  DELRS = RDIF(J)
ENDIF
IF(J.GT.IN)THEN
  DELR = RCV(J-1)
  DELRN = RDIF(J + 1)
  DELRS = RDIF(J)
ENDIF
IF(J.EQ.2)DELRS = DELR
IF(J.EQ.N-1)DELRN = DELR
IF(I.GT.IM)THEN
  IF(J.EQ.IN-1)DELRN = R(IN + 1)-R(IN-1)
  IF(J.EQ.IN + 1)DELRS = R(IN + 1)-R(IN-1)
ENDIF
IF(I.LT.IM + 1)THEN
  IF(J.EQ.IN-1)DELRN = DELR
  IF(J.EQ.IN + 1)DELRS = DELR
ENDIF
UE = (U(I,J,K) + U(I + 1,J,K))*0.5
UW = (U(I,J,K) + U(I-1,J,K))*0.5
IF(J.LT.IN)THEN
  IF(I.LT.IM)THEN

```

```

        CALL AINTP(XCV(I-1),XCV(I),V(I-1,J+1,K),
        V(I,J+1,K),VN)
        CALL AINTP(XCV(I-1),XCV(I),V(I-1,J,K),
        V(I,J,K),VS)
    ENDIF
    IF(I.EQ.IM)THEN
        CALL AINTP(XCV(I-1),XCV(I),V(I-1,J+1,K),
        V(I+1,J+1,K),VN)
        CALL AINTP(XCV(I-1),XCV(I),V(I-1,J,K),
        V(I+1,J,K),VS)
    ENDIF
    IF(I.GT.IM)THEN
        CALL AINTP(XCV(I-1),XCV(I),V(I,J+1,K),
        V(I+1,J+1,K),VN)
        CALL AINTP(XCV(I-1),XCV(I),V(I,J,K),
        V(I+1,J,K),VS)
    ENDIF
    ENDIF

    IF(J.GT.IN)THEN
        IF(I.LT.IM)THEN
            CALL AINTP(XCV(I-1),XCV(I),V(I-1,J,K),
            V(I,J,K),VN)
            CALL AINTP(XCV(I-1),XCV(I),V(I-1,J-1,K),
            V(I,J-1,K),VS)
        ENDIF
        IF(I.EQ.IM)THEN
            CALL AINTP(XCV(I-1),XCV(I),V(I-1,J,K),
            V(I+1,J,K),VN)
            CALL AINTP(XCV(I-1),XCV(I),V(I-1,J-1,K),
            V(I+1,J-1,K),VS)
        ENDIF
        IF(I.GT.IM)THEN
            CALL AINTP(XCV(I-1),XCV(I),V(I,J,K),
            V(I+1,J,K),VN)
            CALL AINTP(XCV(I-1),XCV(I),V(I,J-1,K),
            V(I+1,J-1,K),VS)
        ENDIF
    ENDIF
    IF(I.LT.IM)THEN
        CALL AINTP(XCV(I-1),XCV(I),W(I-1,J,K+1),
        W(I,J,K+1),WT)
        CALL AINTP(XCV(I-1),XCV(I),W(I-1,J,K),
        W(I,J,K),WB)
    ENDIF

```

```

ENDIF
IF(I.EQ.IM)THEN
    CALL AINTP(XCV(I-1),XCV(I),W(I-1,J,K+1),
    W(I+1,J,K+1),WT)
    CALL AINTP(XCV(I-1),XCV(I),W(I-1,J,K),
    W(I+1,J,K),WB)
ENDIF
IF(I.GT.IM)THEN
    CALL AINTP(XCV(I-1),XCV(I),W(I,J,K+1),
    W(I+1,J,K+1),WT)
    CALL AINTP(XCV(I-1),XCV(I),W(I,J,K),
    W(I+1,J,K),WB)
ENDIF
IF(K.EQ.2)DELTB = DELT
IF(K.EQ.KM-1)DELT = DELT

FN = VN*RN*RN*DELX*DELT
FS = VS*RS*RS*DELX*DELT
FE = UE*RE*RE*DELR*DELT
FW = UW*RW*RW*DELR*DELT
FT = RT*WT*DELX*DELR
FB = RB*WB*DELX*DELR

DN = 4.0*H*RN*RN*DELT*DELX/(RENOL*DELRN)
DS = 4.0*H*RS*RS*DELT*DELX/(RENOL*DELRS)
DE = RE*RE*DELT*DELR/(RENOL*H*DELXE)
DW = RW*RW*DELT*DELR/(RENOL*H*DELXW)
DT = 4.0*H*DELX*DELR/(RENOL*THC*THC*DELT)
DB = 4.0*H*DELX*DELR/(RENOL*THC*THC*DELTB)

CALL POWER(FN,DN,ACOF)
AN(I,J,K) = ACOF + AMAX1(0.0,-FN)
CALL POWER(FS,DS,ACOF)
AS(I,J,K) = ACOF + AMAX1(0.0,FS)
CALL POWER(FE,DE,ACOF)
AE(I,J,K) = ACOF + AMAX1(0.0,-FE)
CALL POWER(FW,DW,ACOF)
AW(I,J,K) = ACOF + AMAX1(0.0,FW)
CALL POWER(FT,DT,ACOF)
AT(I,J,K) = ACOF + AMAX1(0.0,-FT)
CALL POWER(FB,DB,ACOF)
AB(I,J,K) = ACOF + AMAX1(0.0,FB)

USUM = AE(I,J,K) + AW(I,J,K) + AN(I,J,K) +

```

```

      AT(I,J,K) + AB(I,J,K)
      AP(I,J,K) = (1.0/RELAX)*USUM
      S(I,J,K) = AP(I,J,K)*(1.0-RELAX)*U(I,J,K)
      IF(I.LT.IM)S(I,J,K) = S(I,J,K) + (P(I-1,J,K)-P(I,J,K))*RE*RE*DELT*DELR
      IF(I.EQ.IM)S(I,J,K) = S(I,J,K) + (P(I-1,J,K)-P(I+1,J,K))*RE*RE*DELT*DELR
      IF(I.GT.IM)S(I,J,K) = S(I,J,K) + (P(I,J,K)-P(I+1,J,K))*RE*RE*DELT*DELR
      DU(I,J,K) = (RE*RE*DELT*DELR)/(AP(I,J,K)-USUM)
19   END DO
      END DO
      END DO
      ICAT=ICAT+1
      IF(ICAT.LT.3)GO TO 122
C
      RETURN
      END

```

SUBROUTINE COEFFV(M,N,KM,RENOL,H,RELAX,DV,AP,AE,AW,AN,
 AS,AT,AB,S,IM,IN,THC)

```

IMPLICIT REAL (A-H,O-Z)
PARAMETER(ID = 50,JD = 50,LD = 30)
COMMON/VEL/U(ID,JD,LD),V(ID,JD,LD),W(ID,JD,LD),
' P(ID,JD,LD)
DIMENSION AP(ID,JD,LD),AE(ID,JD,LD),AW(ID,JD,LD),
' AN(ID,JD,LD),AS(ID,JD,LD),AT(ID,JD,LD),AB(ID,JD,LD)
DIMENSION DV(ID,JD,LD),S(ID,JD,LD)
COMMON/XINDEX/X(ID),XU(ID),XDIF(ID),XCV(ID)
COMMON/RINDEX/R(JD),RV(JD),RDIF(JD),RCV(JD)
COMMON/TINDEX/TH(JD),TV(JD),TDIF(JD),TCV(JD)

```

```

C
      ICAT=0
      KA=2
      KB=IM
      KC=3
      KD=IN-1
133 IF(ICAT.EQ.1)THEN
      KA=IM+1
      KB=M-1
      KC=3
      KD=N-2
      ENDIF

```

```

IF(ICAT.EQ.2)THEN
  KA = 2
  KB = IM
  KC = IN + 1
  KD = N-2
ENDIF
DO I=KA,KB
  DO J=KC,KD
    DO K=2,KM-1
      IF(I.EQ.IM)GO TO 9
      RE = RV(J)
      RW = RE
      RT = RE
      RB = RE
      DELT = TCV(K)
      DELTT = TDIF(K + 1)
      DELTB = TDIF(K)
      IF(I.LT.IM)THEN
        DELX = XCV(I)
        DELXE = XDIF(I + 1)
        DELXW = XDIF(I)
      ENDIF
      IF(I.GT.IM)THEN
        DELX = XCV(I-1)
        DELXE = XDIF(I + 1)
        DELXW = XDIF(I)
      ENDIF
      IF(I.EQ.IM-1)DELXE = X(IM + 1)-X(IM-1)
      IF(I.EQ.IM + 1)DELXW = X(IM + 1)-X(IM-1)
      IF(I.EQ.2)DELXW = DELX
      IF(I.EQ.M-1)DELXE = DELX
      RN = R(J)
      RS = R(J-1)
      IF(J.LT.IN)THEN
        DELRN = RCV(J)
        DELRS = RCV(J-1)
        DELR = RDIF(J)
      ENDIF
      IF(J.EQ.IN)THEN
        DELR = R(IN + 1)-R(IN-1)
        DELRN = RCV(J)
        DELRS = RCV(J-1)
      ENDIF
      IF(J.GT.IN)THEN

```

```

DELR = RDIF(J + 1)
DELRN = RCV(J)
DELRS = RCV(J - 1)
ENDIF
IF(J.EQ.IN)THEN
  RN = R(J + 1)
  RS = R(J - 1)
ENDIF
IF(J.GT.IN)THEN
  RN = R(J + 1)
  RS = R(J)
ENDIF
IF(I.LT.IM)THEN
  IF(J.LT.IN)THEN
    CALL AINTP(RCV(J-1),RCV(J),U(I+1,J-1,K),
               U(I+1,J,K),UE)
    CALL AINTP(RCV(J-1),RCV(J),U(I,J-1,K),
               U(I,J,K),UW)
  ENDIF
  IF(J.EQ.IN)THEN
    CALL AINTP(RCV(J-1),RCV(J),U(I+1,J-1,K),
               U(I+1,J+1,K),UE)
    CALL AINTP(RCV(J-1),RCV(J),U(I,J-1,K),
               U(I,J+1,K),UW)
  ENDIF
  IF(J.GT.IN)THEN
    CALL AINTP(RCV(J-1),RCV(J),U(I+1,J,K),
               U(I+1,J+1,K),UE)
    CALL AINTP(RCV(J-1),RCV(J),U(I,J,K),
               U(I,J+1,K),UW)
  ENDIF
ENDIF
IF(I.GT.IM)THEN
  IF(J.LT.IN)THEN
    CALL AINTP(RCV(J-1),RCV(J),U(I,J-1,K),
               U(I,J,K),UE)
    CALL AINTP(RCV(J-1),RCV(J),U(I-1,J-1,K),
               U(I-1,J,K),UW)
  ENDIF
  IF(J.EQ.IN)THEN
    CALL AINTP(RCV(J-1),RCV(J),U(I,J-1,K),
               U(I,J+1,K),UE)
    CALL AINTP(RCV(J-1),RCV(J),U(I-1,J-1,K),
               U(I-1,J+1,K),UW)
  ENDIF
ENDIF

```

```

ENDIF
IF(J.GT.IN)THEN
    CALL AINTP(RCV(J-1),RCV(J),U(I,J,K),
    U(I,J+1,K),UE)
    CALL AINTP(RCV(J-1),RCV(J),U(I-1,J,K),
    U(I-1,J+1,K),UW)
ENDIF
ENDIF
IF(J.LT.IN)THEN
    CALL AINTP(RCV(J-1),RCV(J),W(I,J-1,K+1),
    W(I,J,K+1),WT)
    CALL AINTP(RCV(J-1),RCV(J),W(I,J-1,K),
    W(I,J,K),WB)
ENDIF

IF(J.EQ.IN)THEN
    CALL AINTP(RCV(J-1),RCV(J),W(I,J-1,K+1),
    W(I,J+1,K+1),WT)
    CALL AINTP(RCV(J-1),RCV(J),W(I,J-1,K),
    W(I,J+1,K),WB)
ENDIF
IF(J.GT.IN)THEN
    CALL AINTP(RCV(J-1),RCV(J),W(I,J,K+1),
    W(I,J+1,K+1),WT)
    CALL AINTP(RCV(J-1),RCV(J),W(I,J,K),
    W(I,J+1,K),WB)
ENDIF
CALL AINTP(TDIF(K),TDIF(K+1),WB,WT,WC)
IF(K.EQ.2)DELTB=DELT
IF(K.EQ.KM-1)DELT=DELT

VN=(V(I,J,K)+V(I,J+1,K))*0.5
VS=(V(I,J,K)+V(I,J-1,K))*0.5

FN=VN*RN*RN*DELX*DELT
FS=VS*RS*RS*DELX*DELT
FE=UE*RE*RE*DELR*DELT
FW=UW*RW*RW*DELR*DELT
FT=RT*WT*DELX*DELR
FB=RB*WB*DELX*DELR

DN=4.0*H*RN*RN*DELT*DELX/(RENOL*DELRN)
DS=4.0*H*RS*RS*DELT*DELX/(RENOL*DELRS)
DE=RE*RE*DELT*DELR/(RENOL*H*DELXE)

```

```

DW = RW*RW*DELT*DELR/(RENOL*H*DELXW)
DT = 4.0*H*DELX*DELR/(RENOL*THC*THC*DELT)
DB = 4.0*H*DELX*DELR/(RENOL*THC*THC*DELTB)

CALL POWER(FN,DN,ACOF)
AN(I,J,K)=ACOF+AMAX1(0.0,-FN)
CALL POWER(FS,DS,ACOF)
AS(I,J,K)=ACOF+AMAX1(0.0,FS)
CALL POWER(FE,DE,ACOF)
AE(I,J,K)=ACOF+AMAX1(0.0,-FE)
CALL POWER(FW,DW,ACOF)
AW(I,J,K)=ACOF+AMAX1(0.0,FW)
CALL POWER(FT,DT,ACOF)
AT(I,J,K)=ACOF+AMAX1(0.0,-FT)
CALL POWER(FB,DB,ACOF)
AB(I,J,K)=ACOF+AMAX1(0.0,FB)

VSUM=AE(I,J,K)+AW(I,J,K)+AN(I,J,K)+AS(I,J,K)+  

AT(I,J,K)+AB(I,J,K)
AP(I,J,K)=(1.0/RELAX)*(VSUM+(4.0*H*DELR*  

DELX*DELT/RENOL))
S(I,J,K)=(1.0-RELAX)*AP(I,J,K)*V(I,J,K)
IF(J.LT.IN)S(I,J,K)=S(I,J,K)+(P(I,J-1,K)-P(I,J,K))*  

RE*RE*4.0*H*H*DELX*DELT
IF(J.EQ.IN)S(I,J,K)=S(I,J,K)+(P(I,J-1,K)-P(I,J+1,K))*  

RE*RE*4.0*H*H*DELX*DELT
IF(J.GT.IN)S(I,J,K)=S(I,J,K)+(P(I,J,K)-P(I,J+1,K))*  

RE*RE*4.0*H*H*DELX*DELT
S(I,J,K)=S(I,J,K)+8.0*H*DELX*DELR*(WB-WT)/RENOL
S(I,J,K)=S(I,J,K)+THC*THC*DELX*DELR*  

DELT*WC*WC*RE
DV(I,J,K)=(RE*RE*DELT*DELX)/(AP(I,J,K)-VSUM)
9    END DO
      END DO
      END DO

ICAT=ICAT+1
IF(ICAT.LT.3)GO TO 133

RETURN
END

SUBROUTINE COEFFW(M,N,KM,RENOL,H,RELAX,DWA,AP,AE,AW,AN,  

' AS,AT,AB,S,IM,IN,THC)

```

```

IMPLICIT REAL (A-H,O-Z)
PARAMETER(ID = 50,JD = 50,LD = 30)
COMMON/VEL/U(ID,JD,LD),V(ID,JD,LD),W(ID,JD,LD),
' P(ID,JD,LD)
DIMENSION AP(ID,JD,LD),AE(ID,JD,LD),AW(ID,JD,LD),
' AN(ID,JD,LD),AS(ID,JD,LD),AT(ID,JD,LD),AB(ID,JD,LD)
DIMENSION S(ID,JD,LD),DWA(ID,JD,LD)
COMMON/XINDEX/X(ID),XU(ID),XDIF(ID),XCV(ID)
COMMON/RINDEX/R(JD),RV(JD),RDIF(JD),RCV(JD)
COMMON/TINDEX/TH(JD),TV(JD),TDIF(JD),TCV(JD)

C
ICAT=0
KA=2
KB=IM
KC=2
KD=IN-1
122 IF(ICAT.EQ.2)THEN
    KA=2
    KB=IM
    KC=IN+1
    KD=N-1
ENDIF
IF(ICAT.EQ.1)THEN
    KA=IM+1
    KB=M-1
    KC=2
    KD=N-1
ENDIF
DO I=KA,KB
    DO J=KC,KD
        DO K=3,KM-1
            IF(ICAT.EQ.1)THEN
                IF(J.EQ.IN)GO TO 19
            ENDIF
            IF(I.EQ.IM)GO TO 19

            RE=R(J)
            RW=R(J)
            RT=R(J)
            RB=R(J)

            DELT=TDIF(K)
            DELTT=TCV(K)
            DELTB=TCV(K-1)

```

```

IF(I.LT.IM)THEN
  DELX = XCV(I)
  DELXE = XDIF(I + 1)
  DELXW = XDIF(I)
ENDIF
IF(I.GT.IM)THEN
  DELX = XCV(I-1)
  DELXE = XDIF(I + 1)
  DELXW = XDIF(I)
ENDIF
IF(I.EQ.IM-1)DELXE = X(IM + 1)-X(IM-1)
IF(I.EQ.IM + 1)DELXW = X(IM + 1)-X(IM-1)

IF(I.EQ.2)DELXW = DELX
IF(I.EQ.M-1)DELXE = DELX

RN = RV(J + 1)
RS = RV(J)

IF(J.GT.IN)THEN
  RN = RV(J)
  RS = RV(J-1)
ENDIF

IF(J.LT.IN)THEN
  DELR = RCV(J)
  DELRN = RDIF(J + 1)
  DELRS = RDIF(J)
ENDIF
IF(J.GT.IN)THEN
  DELR = RCV(J-1)
  DELRN = RDIF(J + 1)
  DELRS = RDIF(J)
ENDIF

IF(J.EQ.2)DELRS = DELR
IF(J.EQ.N-1)DELRN = DELR
IF(I.GT.IM)THEN
  IF(J.EQ.IN-1)DELRN = R(IN + 1)-R(IN-1)
  IF(J.EQ.IN + 1)DELRS = R(IN + 1)-R(IN-1)
ENDIF
IF(I.LT.IM + 1)THEN
  IF(J.EQ.IN-1)DELRN = DELR
  IF(J.EQ.IN + 1)DELRS = DELR

```

```

ENDIF
IF(K.EQ.3)DELTB=DELT
IF(K.EQ.KM-1)DELTT=DELT

WT=(W(I,J,K)+W(I,J,K+1))*0.5
WB=(W(I,J,K)+W(I,J,K-1))*0.5

IF(J.LT.IN)THEN
    CALL AINTP(TCV(K-1),TCV(K),V(I,J+1,K-1),
    V(I,J+1,K),VN)
    CALL AINTP(TCV(K-1),TCV(K),V(I,J,K-1),
    V(I,J,K),VS)
ENDIF
IF(J.EQ.IN)THEN
    CALL AINTP(TCV(K-1),TCV(K),V(I,J+1,K-1),
    V(I,J+1,K),VN)
    CALL AINTP(TCV(K-1),TCV(K),V(I,J-1,K-1),
    V(I,J-1,K),VS)
ENDIF
IF(J.GT.IN)THEN
    CALL AINTP(TCV(K-1),TCV(K),V(I,J,K-1),
    V(I,J,K),VN)
    CALL AINTP(TCV(K-1),TCV(K),V(I,J-1,K-1),
    V(I,J-1,K),VS)
ENDIF
IF(I.LT.IM)THEN
    CALL AINTP(TCV(K-1),TCV(K),U(I+1,J,K-1),
    U(I+1,J,K),UE)
    CALL AINTP(TCV(K-1),TCV(K),U(I,J,K-1),
    U(I,J,K),UW)
ENDIF
IF(I.EQ.IM)THEN
    CALL AINTP(TCV(K-1),TCV(K),U(I+1,J,K-1),
    U(I+1,J,K),UE)
    CALL AINTP(TCV(K-1),TCV(K),U(I-1,J,K-1),
    U(I-1,J,K),UW)
ENDIF
IF(I.GT.IM)THEN
    CALL AINTP(TCV(K-1),TCV(K),U(I,J,K-1),
    U(I,J,K),UE)
    CALL AINTP(TCV(K-1),TCV(K),U(I-1,J,K-1),
    U(I-1,J,K),UW)
ENDIF
IF(J.LT.IN)THEN

```

```

        CALL AINTP(RDIF(J),RDIF(J+1),V(I,J,K),
        V(I,J+1,K),VT)
        CALL AINTP(RDIF(J),RDIF(J+1),V(I,J,K-1),
        V(I,J+1,K-1),VB)
    ENDIF
    IF(J.EQ.IN)THEN
        CALL AINTP(RDIF(J),RDIF(J+1),V(I,IN-1,K),
        V(I,IN+1,K),VT)
        CALL AINTP(RDIF(J),RDIF(J+1),V(I,IN-1,K-1),
        V(I,IN+1,K-1),VB)
    ENDIF
    IF(J.GT.IN)THEN
        CALL AINTP(RDIF(J),RDIF(J+1),V(I,J-1,K),
        V(I,J,K),VT)
        CALL AINTP(RDIF(J),RDIF(J+1),V(I,J-1,K-1),
        V(I,J,K-1),VB)
    ENDIF
    CALL AINTP(RDIF(J),RDIF(J+1),VS,VN,VC)

29   FN = VN*RN*RN*DELX*DELT
      FS = VS*RS*RS*DELX*DELT
      FE = UE*RE*RE*DELR*DELT
      FW = UW*RW*RW*DELR*DELT
      FT = RT*WT*DELX*DELR
      FB = RB*WB*DELX*DELR

      DN = 4.0*H*RN*RN*DELT*DELX/(RENOL*DELRN)
      DS = 4.0*H*RS*RS*DELT*DELX/(RENOL*DELRS)
      DE = RE*RE*DELT*DELR/(RENOL*H*DELXE)
      DW = RW*RW*DELT*DELR/(RENOL*H*DELXW)
      DT = 4.0*H*DELX*DELR/(RENOL*THC*THC*DELT)
      DB = 4.0*H*DELX*DELR/(RENOL*THC*THC*DELTB)

      CALL POWER(FN,DN,ACOF)
      AN(I,J,K)=ACOF+AMAX1(0.0,-FN)
      CALL POWER(FS,DS,ACOF)
      AS(I,J,K)=ACOF+AMAX1(0.0,FS)
      CALL POWER(FE,DE,ACOF)
      AE(I,J,K)=ACOF+AMAX1(0.0,-FE)
      CALL POWER(FW,DW,ACOF)
      AW(I,J,K)=ACOF+AMAX1(0.0,FW)
      CALL POWER(FT,DT,ACOF)
      AT(I,J,K)=ACOF+AMAX1(0.0,-FT)
      CALL POWER(FB,DB,ACOF)

```

```

AB(I,J,K) = ACOF + AMAX1(0.0,FB)

WSUM = AE(I,J,K) + AW(I,J,K) + AN(I,J,K) + AS(I,J,K) +
      AT(I,J,K) + AB(I,J,K)

AP(I,J,K) = (1.0/RELAX)*(WSUM + DELX*DELT*DELR*
      (4.0*H/RENOL) + VC*RE*DELX*DELT*DELR)

S(I,J,K) = AP(I,J,K)*(1.0-RELAX)*W(I,J,K)
S(I,J,K) = S(I,J,K) + ((P(I,J,K-1)-P(I,J,K))*4.0*RE*DELR*
      H*H*DELX/(THC*THC))

S(I,J,K) = S(I,J,K) + 8.0*H*DELX*DELR*
      (VT-VB)/(RENOL*THC*THC)

DWA(I,J,K) = RT*(DELX*DELR)/(AP(I,J,K)-WSUM)

19    END DO
      END DO
      ENDDO
      ICAT=ICAT+1
      IF(ICAT.LT.3)GO TO 122

      RETURN
      END

SUBROUTINE POWER(F,D,ACOF)
IMPLICIT REAL(A-H,O-Z)
C      REAL*8 ACOF,TEMPO,D
      ACOF=D
      IF(F.EQ.0.0) GO TO 11
      TEMPO=D-ABS(F)*0.1
      ACOF=0.0
      IF(TEMPO.LE.0.0) GO TO 11
      TEMPO=TEMPO/D
      ACOF=D*TEMPO*TEMPO*TEMPO*TEMPO*TEMPO

11    RETURN
      END

SUBROUTINE AINTP(DBS,DFS,VBS,VFS,VALUE)

      VALUE=(DBS*VFS+DFS*VBS)/(DBS+DFS)

```

```

RETURN
END

SUBROUTINE CRIT(G,GSTR,IL,IR,JB,JT,KB,KT,E,IM,IN,KM,ILET)
IMPLICIT REAL(A-H,O-Z)
PARAMETER(ID = 50,JD = 50,LD = 30)
DIMENSION G(ID,JD,LD),GSTR(ID,JD,LD)

NPOINT=0.0
E=0.0
ICAT=0.0
IA=IL+1
IB=IM
IC=JB+1
IK=IN-1
661 IF(ICAT.EQ.1)THEN
  IA=IM+1
  IB=IR-1
  IC=JB+1
  IK=JT-1
ENDIF
IF(ICAT.EQ.2)THEN
  IA=IL+1
  IB=IM
  IC=IN+1
  IK=JT-1
ENDIF

DO 10 I=IA,IB
  DO 10 J=IC,IK
    DO 10 K=KB+1,KT-1
      IF(ILET.EQ.1.OR.ILET.EQ.3)THEN
        IF(J.EQ.IN)GO TO 10
      ENDIF
      IF(ILET.EQ.2.OR.ILET.EQ.3)THEN
        IF(I.EQ.IM)GO TO 10
      ENDIF
      DIFF=GSTR(I,J,K)-G(I,J,K)
      IF(GSTR(I,J,K).EQ.0.0)GO TO 10
      DIFF=(DIFF*DIFF)/(GSTR(I,J,K)*GSTR(I,J,K))
      E=E+DIFF
      NPOINT=NPOINT+1.0
10 CONTINUE

```

```
ICAT=ICAT+1
IF(ICAT.LT.3)GO TO 661
E=SQRT(E)
E=E/NPOINT
```

```
RETURN
END
```